



Nonlinear optical properties of glass

MARC DUSSAUZE

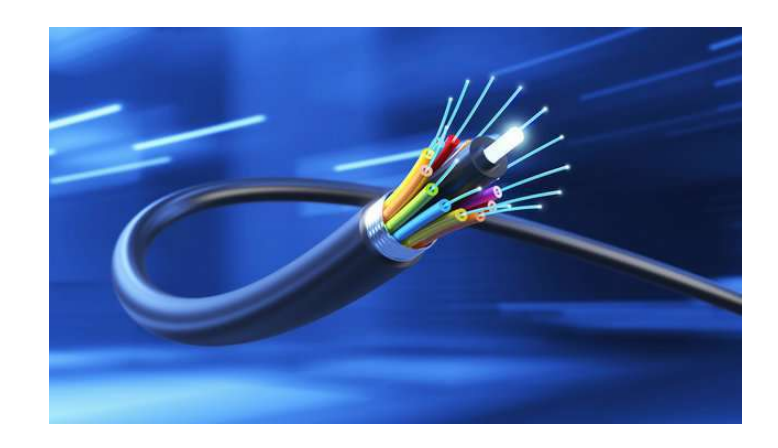
CNRS

Institut des Sciences Moléculaires, Université de Bordeaux

ECOLE VERRE ET OPTIQUE – OCTOBRE 2025

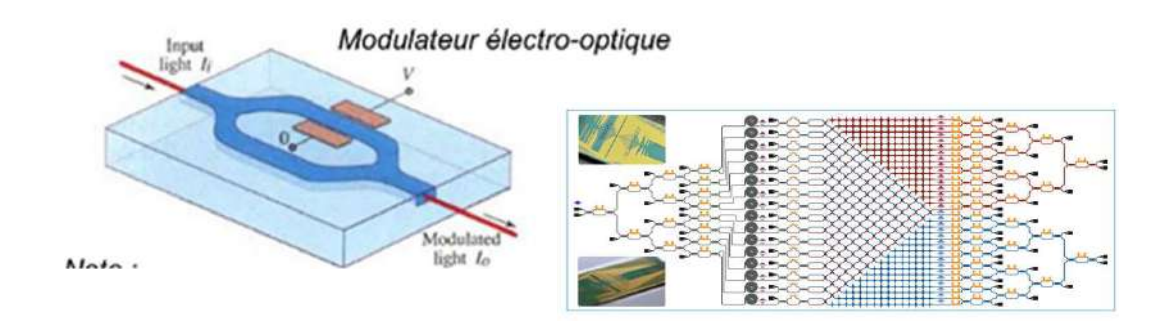




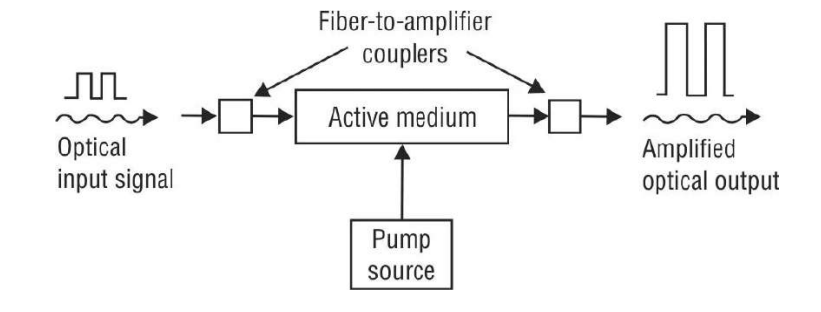


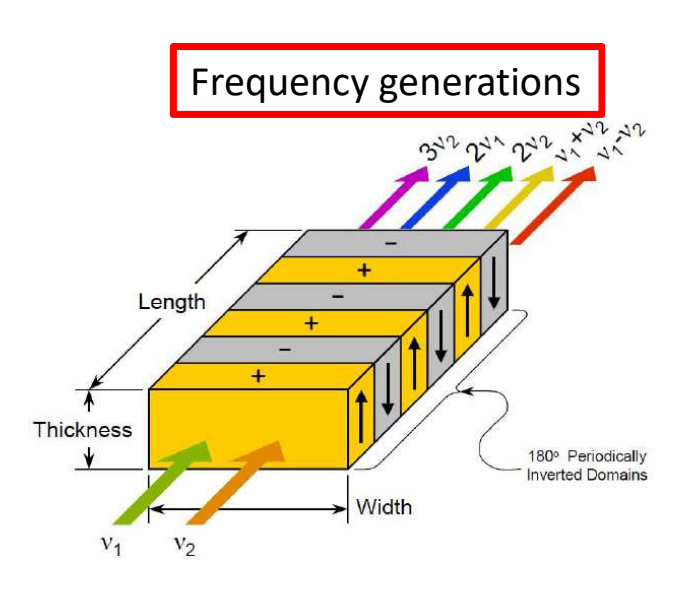
NLO properties -> Active Optical functionalities!

Phase and Amplitude (electro) optical modulation



Signal amplification





Nonlinear optical properties of glass

- Introduction non linear optics
- Third order optical response and glass chemistry
- Second order optical response in glass

1st Linear optic

$$E(r,t) = E_0(e^{(ik.r-i\omega t)})$$

induced microscopic/molecular dipole moment µ

$$\mu_i(\omega) = \alpha(\omega)E(\omega)$$

induced macroscopic polarization

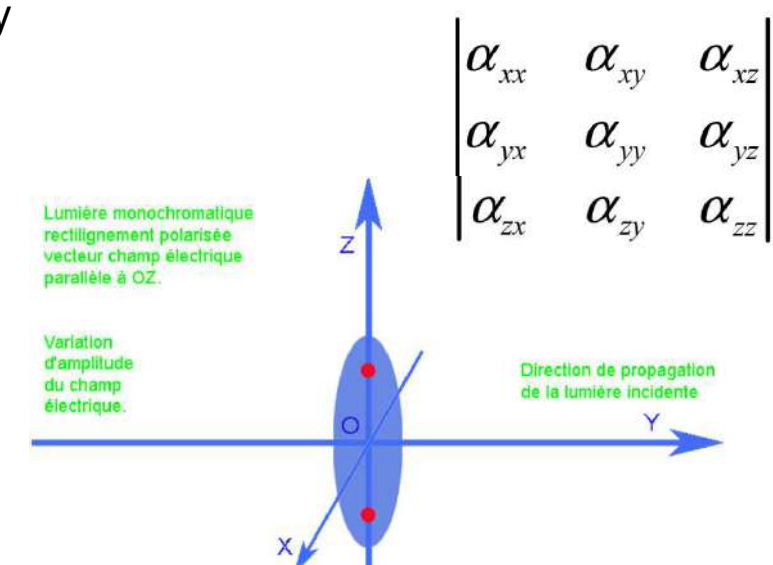
$$P(\omega) = N f_{\omega} \alpha(\omega) E(\omega) = \chi^{(1)}(\omega) E(\omega)$$

N the number density and f a local field factor $\chi^{\text{\tiny (1)}}$ the linear susceptibility

$$(n^2 = 1 + 4\pi\chi^{(1)})$$

With ω being the pulsation of the electromagnetic field also equals to $2\pi\nu$ (ν being the frequency), ω .t a time-dependent phase term and k.r a space-dependent phase term. k is the wave vector that indicates the direction of light propagation, it is equal to $2\pi n/\lambda$ (n being the refractive index, λ being the wavelength).

α the molecular first order polarizability or linear polarizability



Non Linear optical response

At the microscopic/molecular level

$$\mu_i = \mu^{(1)} + \mu^{(2)} + \mu^{(3)} + \dots = \alpha E + \beta E E + \gamma E E E + \dots$$

At the macroscopic level

$$P = P^{(1)} + P^{(2)} + P^{(3)} + \dots = \chi^{(1)}E + \chi^{(2)}EE + \chi^{(3)}EEE + \dots$$

Example of second order polarizability and susceptibility tensor

$$P_{i}^{(2)} = \sum_{j,k} \chi_{ijk}^{(2)} E_{j} E_{k} \qquad \begin{bmatrix} P_{x}^{(2)} \\ P_{y}^{(2)} \\ P_{z}^{(2)} \end{bmatrix} = \begin{bmatrix} \chi_{xxx}^{(2)} & \chi_{xyy}^{(2)} & \chi_{xzz}^{(2)} & \chi_{xyz}^{(2)} & \chi_{xzx}^{(2)} & \chi_{xxx}^{(2)} & \chi_{xxy}^{(2)} & \chi_{xxy}^{(2)} & \chi_{xxz}^{(2)} & \chi_{xxy}^{(2)} & \chi_{xxy}^{(2)} & \chi_{xxx}^{(2)} & \chi_{xxx}^{($$

$$P_i^{(2)} = \sum_{j,k} \chi_{ijk}^{(2)} E_j E_k$$

$$\begin{bmatrix} P_{x}^{(2)} \\ P_{y}^{(2)} \\ P_{z}^{(2)} \end{bmatrix} = \begin{bmatrix} \chi_{xxx}^{(2)} & \chi_{xyy}^{(2)} & \chi_{xzz}^{(2)} & \chi_{xyz}^{(2)} & \chi_{xzx}^{(2)} & \chi_{xzx}^{(2)} & \chi_{xxx}^{(2)} & \chi_{xyx}^{(2)} & \chi_{xxy}^{(2)} & \chi_{yxx}^{(2)} & \chi_{yxx}^{(2)} & \chi_{yxx}^{(2)} & \chi_{yxx}^{(2)} & \chi_{yxx}^{(2)} & \chi_{yxx}^{(2)} & \chi_{xxy}^{(2)} & \chi_{xxx}^{(2)} & \chi_{xxx}^{(2)$$

For SHG
$$E_j = E_k$$

$$\begin{bmatrix} P_x^{(2)} \\ P_y^{(2)} \\ P_z^{(2)} \end{bmatrix} = \begin{bmatrix} \chi_{xxx}^{(2)} & \chi_{xyy}^{(2)} & \chi_{xzz}^{(2)} & \chi_{xyz}^{(2)} & \chi_{xxx}^{(2)} & \chi_{xxy}^{(2)} \\ \chi_{yxx}^{(2)} & \chi_{yyy}^{(2)} & \chi_{yzz}^{(2)} & \chi_{yyz}^{(2)} & \chi_{yxy}^{(2)} & \chi_{yxy}^{(2)} \\ \chi_{zxx}^{(2)} & \chi_{zyy}^{(2)} & \chi_{zzz}^{(2)} & \chi_{zyz}^{(2)} & \chi_{zxx}^{(2)} & \chi_{zxy}^{(2)} \end{bmatrix} \begin{bmatrix} E_x \\ E_y \\ E_z \\ 2E_y E_z \\ 2E_z E_z \end{bmatrix}$$

$$\chi_{ijk}^{(2)} \longrightarrow 2^* d_{il}$$
 $i = 1,2,3$

	xx	уу	ZZ	yz = zy	xz = zx	xy = yx
l =	1	2	3	4	5	6

$$\begin{bmatrix} P_x^{(2)}(2\omega) \\ P_y^{(2)}(2\omega) \\ P_z^{(2)}(2\omega) \end{bmatrix} = \begin{bmatrix} d_{11} & d_{12} & d_{13} & d_{14} & d_{15} & d_{16} \\ d_{21} & d_{22} & d_{23} & d_{24} & d_{25} & d_{26} \\ d_{31} & d_{32} & d_{33} & d_{34} & d_{35} & d_{36} \end{bmatrix} \begin{bmatrix} E_x^2(\omega) \\ E_y^2(\omega) \\ E_z^2(\omega) \\ 2(E_y(\omega)E_z(\omega)) \\ 2(E_x(\omega)E_z(\omega)) \\ 2(E_x(\omega)E_y(\omega)) \end{bmatrix}$$

2nd and 3rd order optical responses ... effect of the material symmetry

Quartz: D3 symmetry
$$\rightarrow \begin{bmatrix} d_{11} & -d_{11} & 0 & d_{14} & 0 & 0 \\ 0 & 0 & 0 & 0 & -d_{14} & d_{11} \\ 0 & 0 & 0 & 0 & 0 & 0 \end{bmatrix}$$

$$\text{Poled glass/polymer: $C_{\infty v}$ symmetry} \rightarrow \begin{bmatrix} 0 & 0 & 0 & 0 & d_{31} & 0 \\ 0 & 0 & 0 & d_{31} & 0 & 0 \\ d_{31} & d_{31} & d_{33} & 0 & 0 & 0 \end{bmatrix}$$

2nd and 3rd order optical responses ... effect of the material symmetry

For a centro symmetric material, there is a center of inversion. This symmetry implies that:

$$E \to -E$$

$$P \to -P$$

Neumanns Principle: a symmetry operation must leave the sign and intensity of a physical property unchanged

$$\chi^{(2)} \to \chi^{(2)}$$

So combining all we obtain:

For a centro symmetric material

$$P^{(2)} = \chi^{(2)}EE \rightarrow -P^{(2)} = \chi^{(2)}(-E)(-E) \longrightarrow \chi^{(2)}=0$$

$$P = P^{(1)} + P^{(2)} + P^{(3)} + \dots = \chi^{(1)}E + \chi^{(2)}EE + \chi^{(3)}EEE + \dots$$

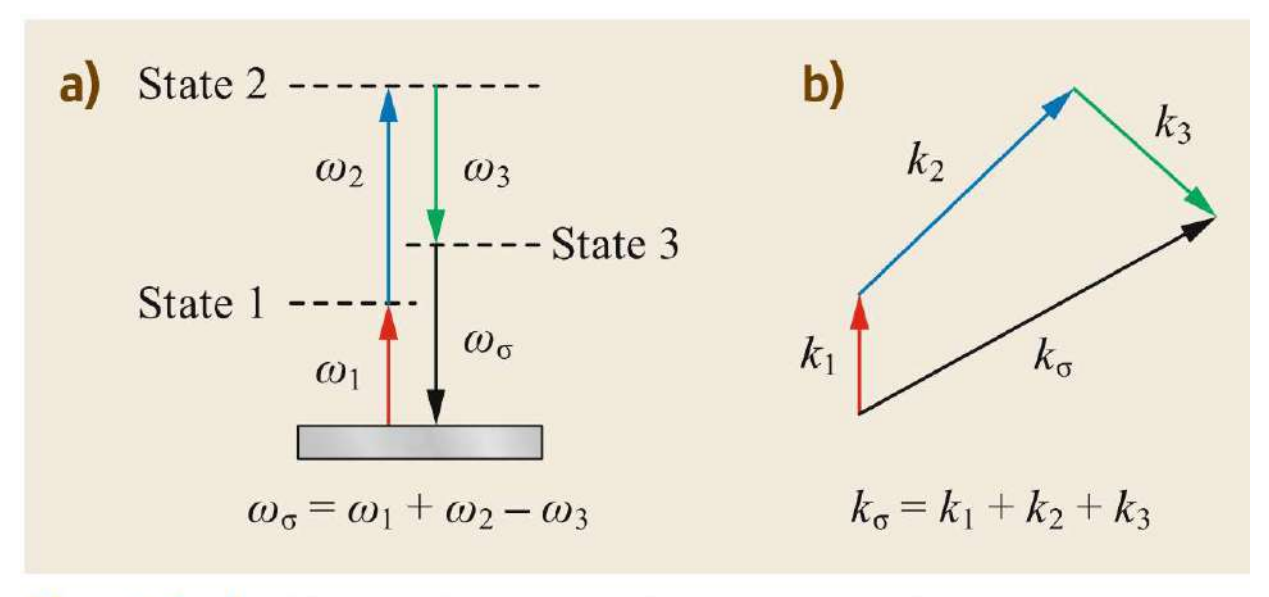
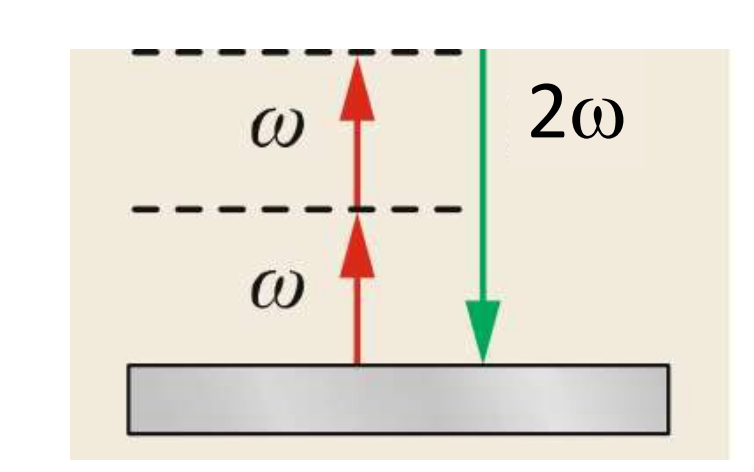


Fig. 6.1a,b General case of four-wave mixing: preservation of energy (a) and momentum (b)

Order	Tensor	Effect	Description
2	$\chi^{(2)}(-\omega;\omega,0)$	Linear electro optical effect (Pockels effect)	Under an electric field there is a change of refractive index in the NLO medium.
2	$\chi^{(2)}(0;\omega,-\omega)$	Optical rectification	A static electric field occurs in the NLO medium under illumination.
2	$\chi^{(2)}(-2\omega;\omega,\omega)$	Second harmonic generation	The emission of light with double frequency happens under illumination of the NLO medium.
2	$\chi^{(2)}(-\omega_3;\omega_2,\omega_1)$	Generation of light with frequency equal to the sum of frequencies of incident radiations, $\omega_3 = (\omega_2 + \omega_1)$	It is observed at illumination of the NLO medium by two light sources with different frequency. The frequency of emission equals the sum of the two excitation source frequencies.
3	$\chi^{(3)}(-\omega;\omega,-0,0)$	Kerr effect	Under the action of two electric fields there is a change of refractive index in the NLO medium.
3	$\chi^{(3)}(-\omega;\omega,-\omega,\omega)$	Nonlinear refractive index also called Kerr effect, self phase modulation.	The refractive index of the medium changes with intensity according to the formula: $n = n_0 + n_2I$. Self-focusing and self-defocusing of a laser beam are special cases.
3	$\chi^{(3)}(-3\omega,\omega,\omega,\omega)$	Third harmonic generation.	There is an emission of light with triple frequency under illumination of the medium.
3	$\chi^{(3)}(-\omega_4;\omega_1,\omega_2,\omega_3)$	Multiwave mixing.	When illuminated with three light sources with different frequencies a generation of light occurs whose frequency equals the sum of the three excitation frequencies.

Second Harmonic Generation

$$E(r,t) = E_0(e^{(ik.r-i\omega t)}) \qquad \chi^{(2)}(-2\omega;\omega,\omega)$$



$$P^{(2)} = \chi^{(2)} E E = \chi^{(2)} E_0 \left(e^{ik.r - i\omega t} + cc \right) E_0 \left(e^{ik.r - i\omega t} + cc \right)$$
$$= 2\chi^{(2)} E_0^2 + \chi^{(2)} E_0^2 \left(e^{i2k.r - i2\omega t} + cc \right)$$

SHG
SFG (Sum Frequency Generation
DFG (Difference Frequency Generation)

$$E_{0,1}(e^{ik_1.r-i\omega_1t}+cc) \quad E_2(r,t) = E_{0,2}(e^{ik_2.r-i\omega_2t}+cc)$$

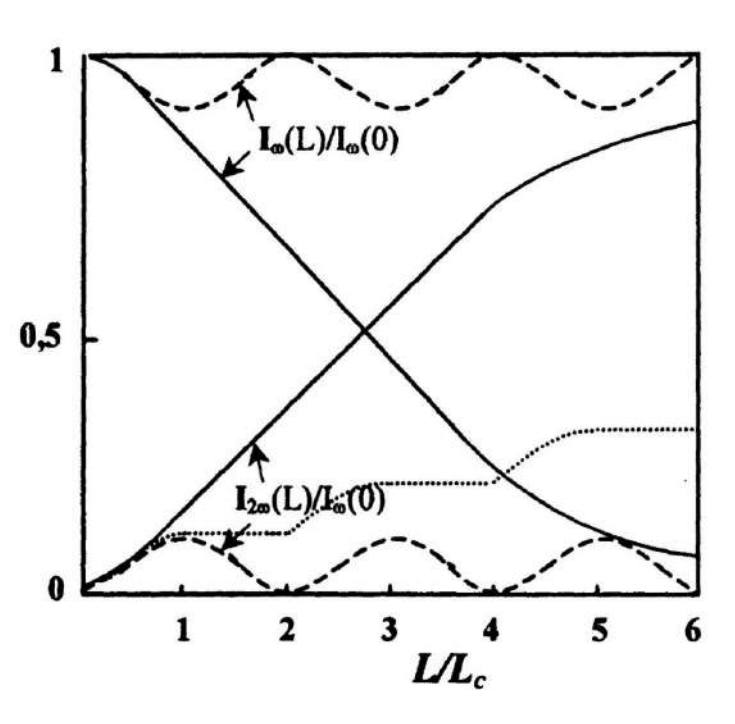
$$\chi^{(2)}(-\omega_3;\omega_1,\omega_2)$$

$$P^{(2)} = 2\chi^{(2)}E_{0,1}^{2} + 2\chi^{(2)}E_{0,2}^{2} + (I-\chi^{(2)}E_{0,1}^{2})^{2}(e^{i2k_{1}\cdot r - i2\omega_{1}t} + cc) + \chi^{(2)}E_{0,2}^{2}(e^{i2k_{2}\cdot r - i2\omega_{2}t} + cc) + (I-\chi^{(2)}E_{0,1}^{2})^{2}(e^{i2k_{1}\cdot r - i2\omega_{1}t} + cc) + \chi^{(2)}E_{0,2}^{2}(e^{i2k_{2}\cdot r - i2\omega_{2}t} + cc) + (I-\chi^{(2)}E_{0,1}^{2})^{2}(e^{i2k_{1}\cdot r - i2\omega_{1}t} + cc) + \chi^{(2)}E_{0,1}^{2}(e^{i2k_{1}\cdot r - i2\omega_{1}t} + cc) + 2\chi^{(2)}E_{0,1}E_{0,2}(e^{i(k_{1}-k_{2})\cdot r - i(\omega_{1}-\omega_{2})t} + cc) + (I-\chi^{(2)}E_{0,1}^{2})^{2}(e^{i2k_{1}\cdot r - i2\omega_{1}t} + cc) + \chi^{(2)}E_{0,1}E_{0,2}(e^{i(k_{1}-k_{2})\cdot r - i(\omega_{1}-\omega_{2})t} + cc) + (I-\chi^{(2)}E_{0,1}E_{0,2}^{2}(e^{i2k_{1}\cdot r - i2\omega_{2}t} + cc) + \chi^{(2)}E_{0,1}E_{0,2}(e^{i(k_{1}-k_{2})\cdot r - i(\omega_{1}-\omega_{2})t} + cc) + \chi^{(2)}E_{0,1}E_{0,2}(e^{i(k_{1}-k_{2})\cdot r - i(\omega_{1}-$$

Characterization method: Second order optical susceptibility $\chi^{(2)}$ The Maker fringes technique

Second Harmonic Generation $\chi^{(2)}(-2\omega;\omega,\omega)$

$$I_{2\omega}(L) = \frac{(2\omega)^2}{8\varepsilon_0 c^3} \frac{\left|\chi^{(2)}(-2\omega;\omega,\omega)\right|^2}{n^2_{\omega} n_{2\omega}} .I_{\omega}^2 L^2 .\sin c^2 ((2k - k_2).L/2)$$

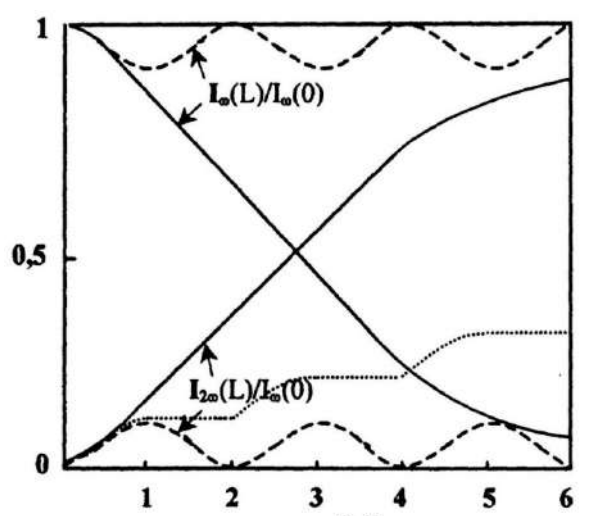


$$\Delta k=0, n_{\omega}=n_{2\omega}$$
 $\Delta k\neq 0, n_{\omega}\neq n_{2\omega}$

$$\Delta k = 2k - k_2 = \frac{2\omega(n_\omega - n_{2\omega})}{c}$$

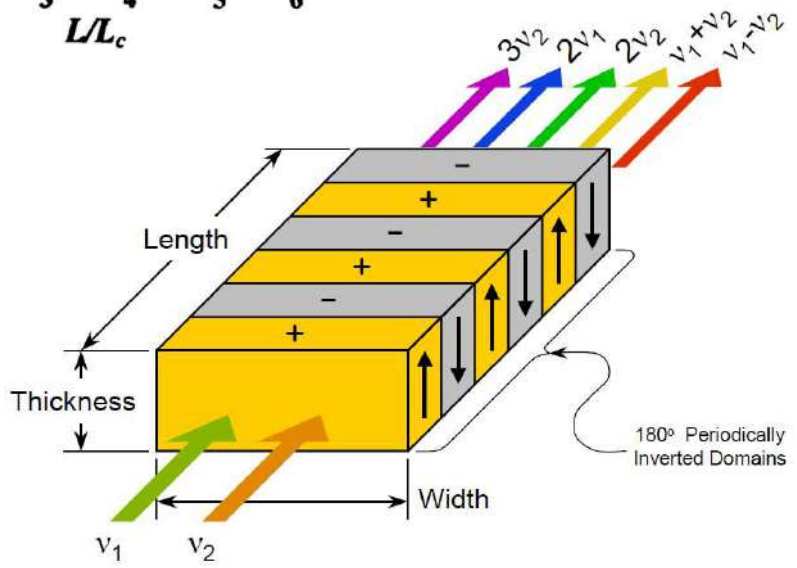
$$L_C = \left| \frac{\pi}{\Delta k} \right|$$

Needs for Harmonic Generation applications

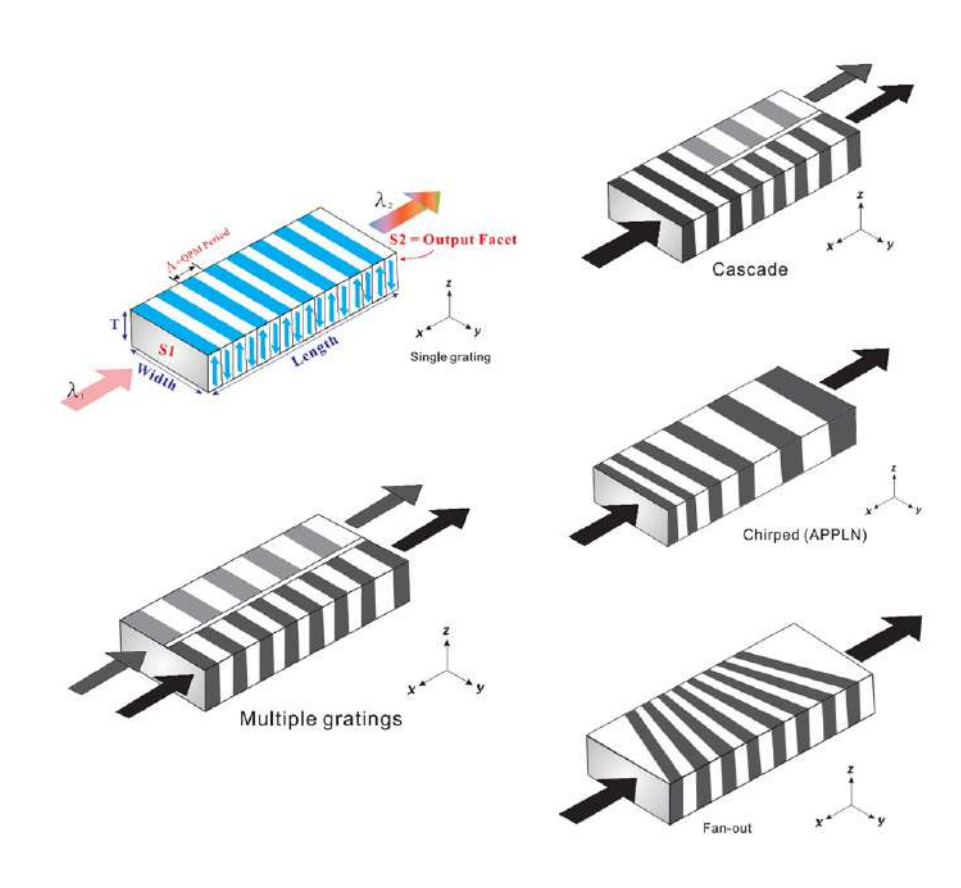


$$\Delta k = 2k - k_2 = \frac{2\omega(n_\omega - n_{2\omega})}{c}$$

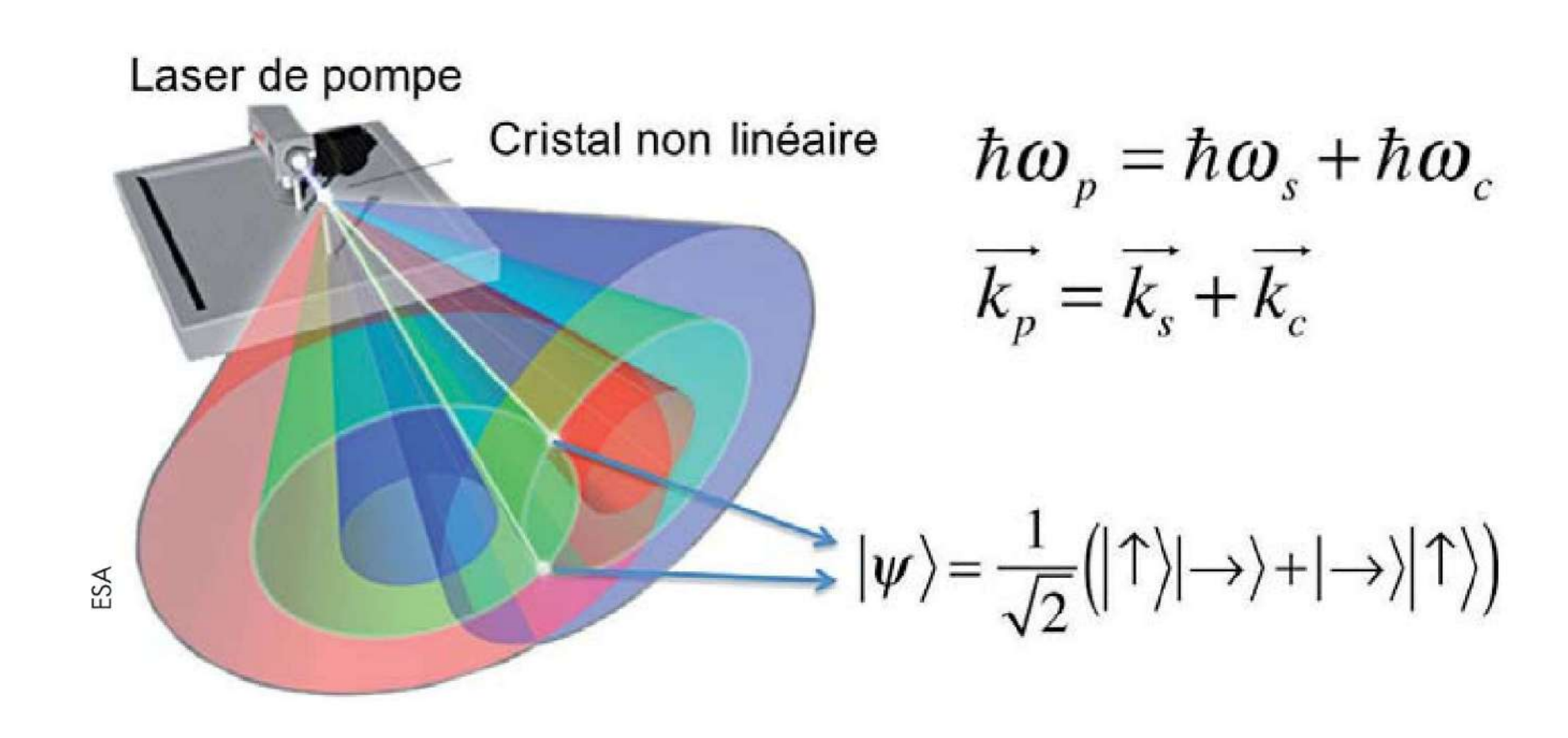
$$L_C = \left| \frac{\pi}{\Delta k} \right|$$



Examples of PPLN systems: Periodically Poled LiNbO₃



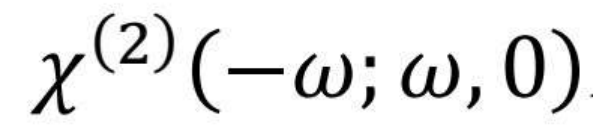
NLO→ Source of intricate photons!

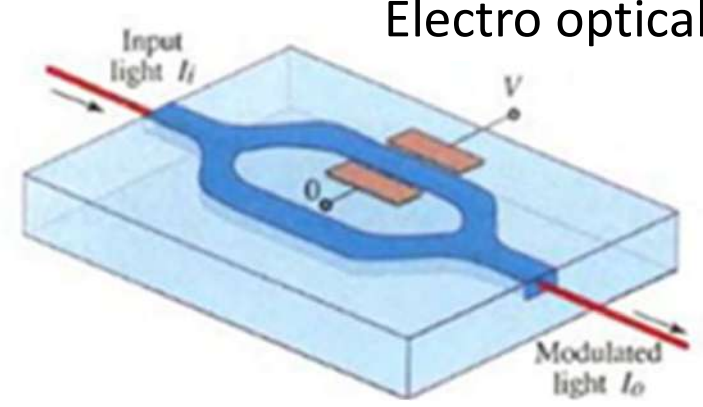


Order	Tensor	Effect	Description
2	$\chi^{(2)}(-\omega;\omega,0)$	Linear electro optical effect (Pockels effect)	Under an electric field there is a change of refractive index in the NLO medium.
2	$\chi^{(2)}(0;\omega,-\omega)$	Optical rectification	A static electric field occurs in the NLO medium under illumination.
2	$\chi^{(2)}(-2\omega;\omega,\omega)$	Second harmonic generation	The emission of light with double frequency happens under illumination of the NLO medium.
2	$\chi^{(2)}(-\omega_3;\omega_2,\omega_1)$	Generation of light with frequency equal to the sum of frequencies of incident radiations. $\omega_3 = (\omega_2 + \omega_1)$	It is observed at illumination of the NLO medium by two light sources with different frequency. The frequency of emission equals the sum of the two excitation source frequencies.
3	$\chi^{(3)}(-\omega;\omega,-0,0)$	Kerr effect	Under the action of two electric fields there is a change of refractive index in the NLO medium.
3	$\chi^{(3)}(-\omega;\omega,-\omega,\omega)$	Nonlinear refractive index also called Kerr effect, self phase modulation.	The refractive index of the medium changes with intensity according to the formula: $n = n_0 + n_2I$. Self-focusing and self-defocusing of a laser beam are special cases.
3	$\chi^{(3)}(-3\omega,\omega,\omega,\omega)$	Third harmonic generation.	There is an emission of light with triple frequency under illumination of the medium.
3	$\chi^{(3)}(-\omega_4;\omega_1,\omega_2,\omega_3)$	Multiwave mixing.	When illuminated with three light sources with different frequencies a generation of light occurs whose frequency equals the sum of the three excitation frequencies.

Electro optical effect / Pockels effect

Electro optical modulator



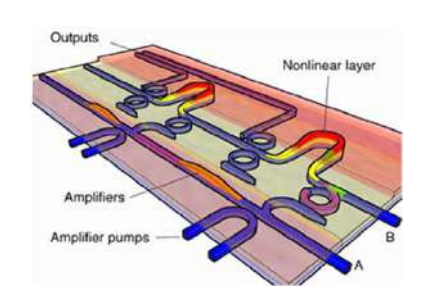


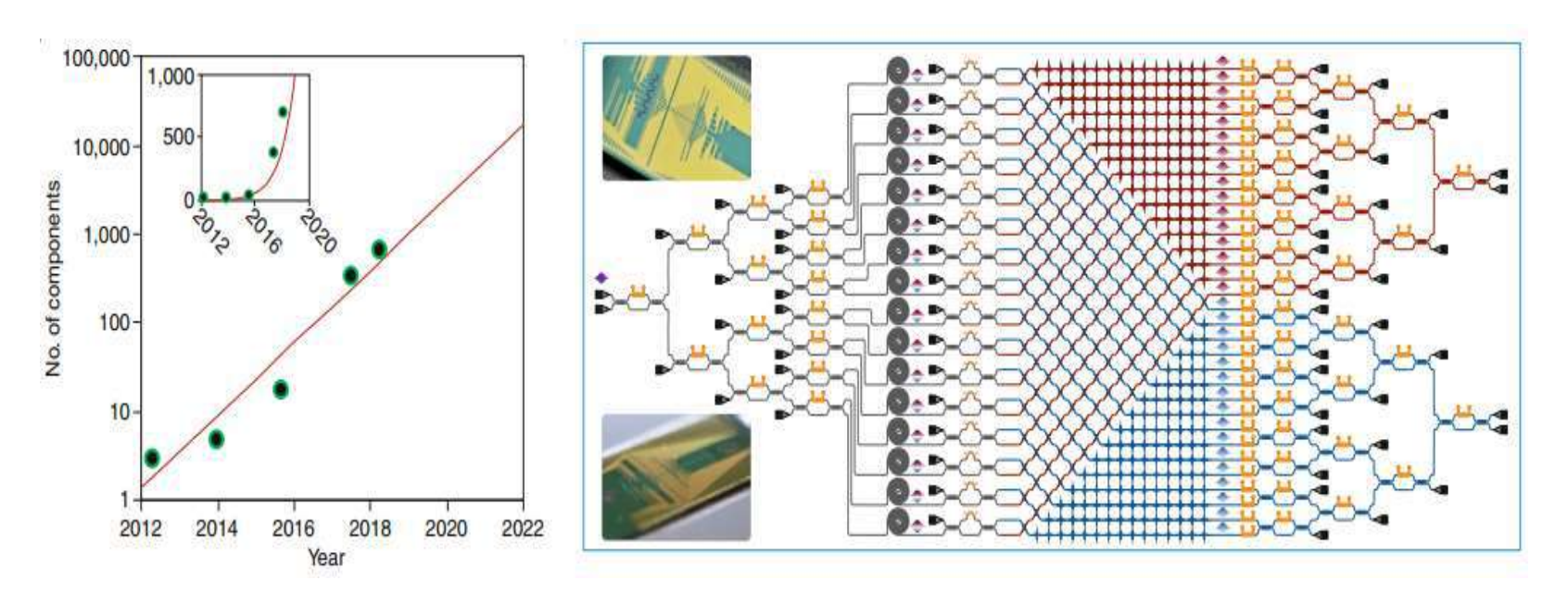
$$P^{(2)}(\omega) = \chi^{(2)}(-\omega; \omega, 0)E(0)E_0(e^{ik.r-i\omega t} + cc)$$

$$P(\omega) = \chi^{(1)} E(\omega) + \chi^{(2)} E(0) E(\omega) = \left(\chi^{(1)} + \chi^{(2)} E(0)\right) E(\omega) = \chi_{eff} E(\omega)$$

Pour rappel:
$$(n^2 = 1 + 4\pi\chi^{(1)})$$

Integrated photonics





Example of a photonic circuit for quantum computation

Nature photonics 2019

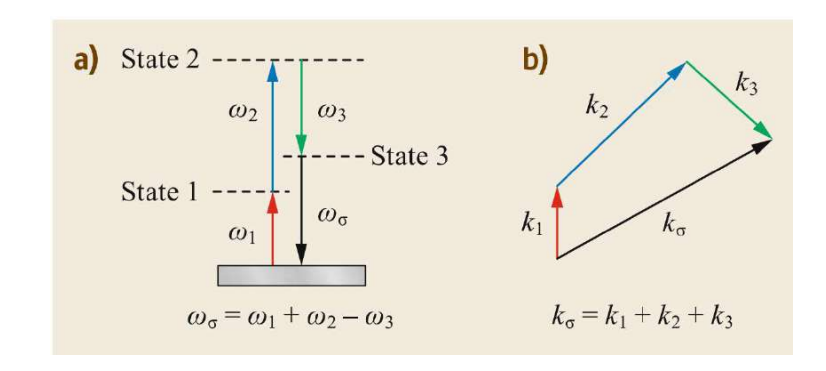
Order	Tensor	Effect	Description
2	$\chi^{(2)}(-\omega;\omega,0)$	Linear electro optical effect (Pockels effect)	Under an electric field there is a change of refractive index in the NLO medium.
2	$\chi^{(2)}(0;\omega,-\omega)$	Optical rectification	A static electric field occurs in the NLO medium under illumination.
2	$\chi^{(2)}(-2\omega;\omega,\omega)$	Second harmonic generation	The emission of light with double frequency happens under illumination of the NLO medium.
2	$\chi^{(2)}(-\omega_3;\omega_2,\omega_1)$	Generation of light with frequency equal to the sum of frequencies of incident radiations. $\omega_3 = (\omega_2 + \omega_1)$	It is observed at illumination of the NLO medium by two light sources with different frequency. The frequency of emission equals the sum of the two excitation source frequencies.
3	$\chi^{(3)}(-\omega;\omega,-0,0)$	Kerr effect	Under the action of two electric fields there is a change of refractive index in the NLO medium.
3	$\chi^{(3)}(-\omega;\omega,-\omega,\omega)$	Nonlinear refractive index also called Kerr effect, self phase modulation.	The refractive index of the medium changes with intensity according to the formula: $n = n_0 + n_2I$. Self-focusing and self-defocusing of a laser beam are special cases.
3	$\chi^{(3)}(-3\omega,\omega,\omega,\omega)$	Third harmonic generation.	There is an emission of light with triple frequency under illumination of the medium.
3	$\chi^{(3)}(-\omega_4;\omega_1,\omega_2,\omega_3)$	Multiwave mixing.	When illuminated with three light sources with different frequencies a generation of light occurs whose frequency equals the sum of the three excitation frequencies.

Optical Kerr effect / non linear optical index

$$\chi^{(3)}(-\omega; \omega, -\omega, \omega)$$

 $\mathsf{P}^{(3)}\#\ \chi^{(3)}(-\omega;\omega,-\omega,\ \omega).\mathsf{E}_0\mathsf{e}^{\mathsf{i}\mathsf{k}\mathsf{r}\mathsf{-}\mathsf{i}\omega\mathsf{t}}\mathsf{E}_0\mathsf{e}^{\mathsf{-}\mathsf{i}\mathsf{k}\mathsf{r}\mathsf{+}\mathsf{i}\omega\mathsf{t}}\mathsf{E}_0\mathsf{e}^{\mathsf{i}\mathsf{k}\mathsf{r}\mathsf{-}\mathsf{i}\omega\mathsf{t}}$

$$P^{(3)} \# (\chi^{(3)}(-\omega;\omega,-\omega,\omega).E_0^2)E_0e^{ikr-i\omega t}$$



$$\mathbf{P} \simeq arepsilon_0 \left(\chi^{(1)} + rac{3}{4}\chi^{(3)}|\mathsf{E}_0|^2
ight) \mathsf{E}_0 \mathsf{e}^{\mathsf{i}\mathsf{k}\mathsf{r} ext{-}\mathsf{i}\omega\mathsf{t}}$$

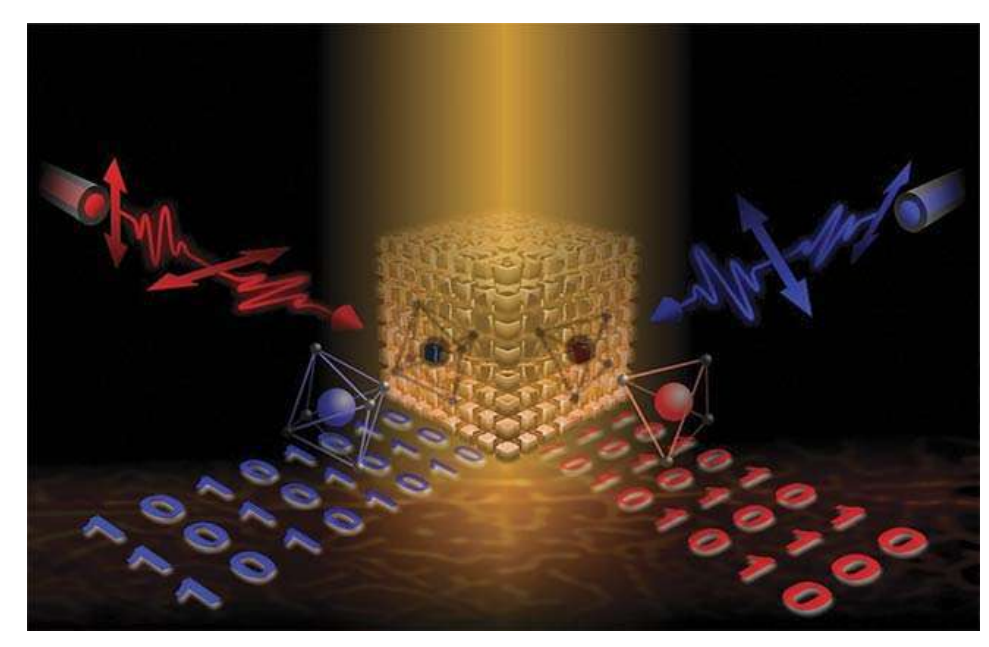
$$n = (1+\chi)^{1/2} = (1+\chi_{
m LIN}+\chi_{
m NL})^{1/2} \simeq n_0 \left(1+rac{1}{2{n_0}^2}\chi_{
m NL}
ight)$$

$$n=n_0+rac{3\chi^{(3)}}{8n_0}|{f E}_{\omega}|^2=n_0+n_2I$$

All-Optical Switching and Logic

An optical beam can control the phase or amplitude of another.

Applications: optical logic gates, all-optical switches, optical multiplexers.



Michael Eisenstein, Photonics Spectra 2020

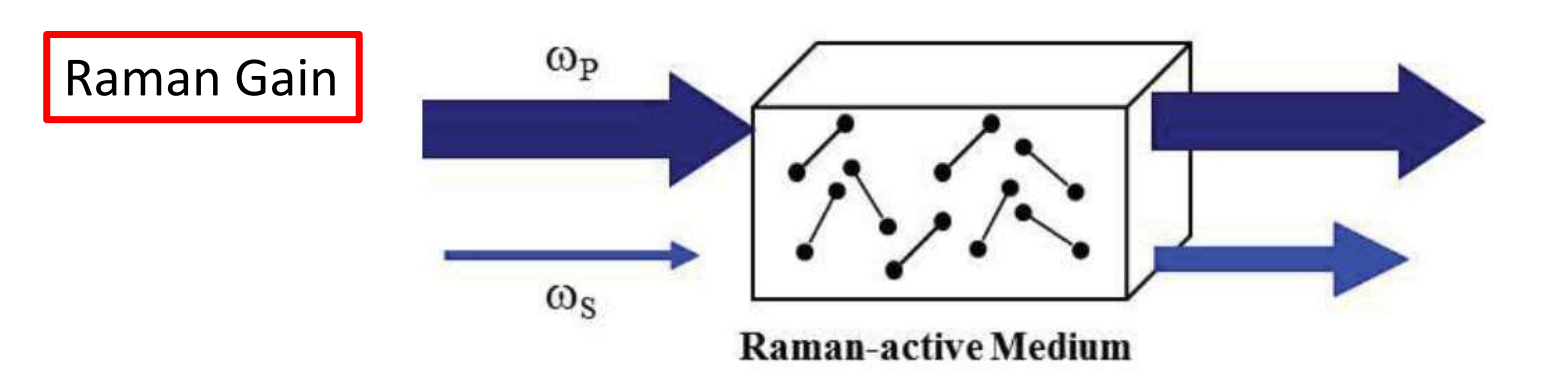
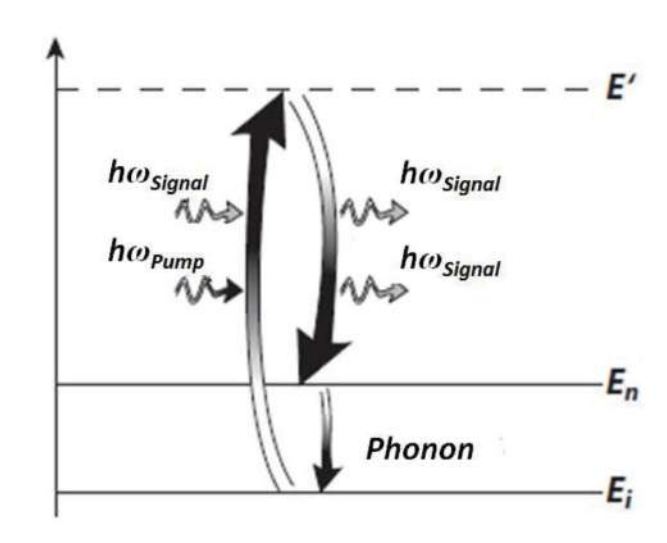


Figure 4.1 Schematic representation of the Raman gain process

$$\chi^{(3)}(-\omega_s,\omega_p,-\omega_s,\omega_p)$$



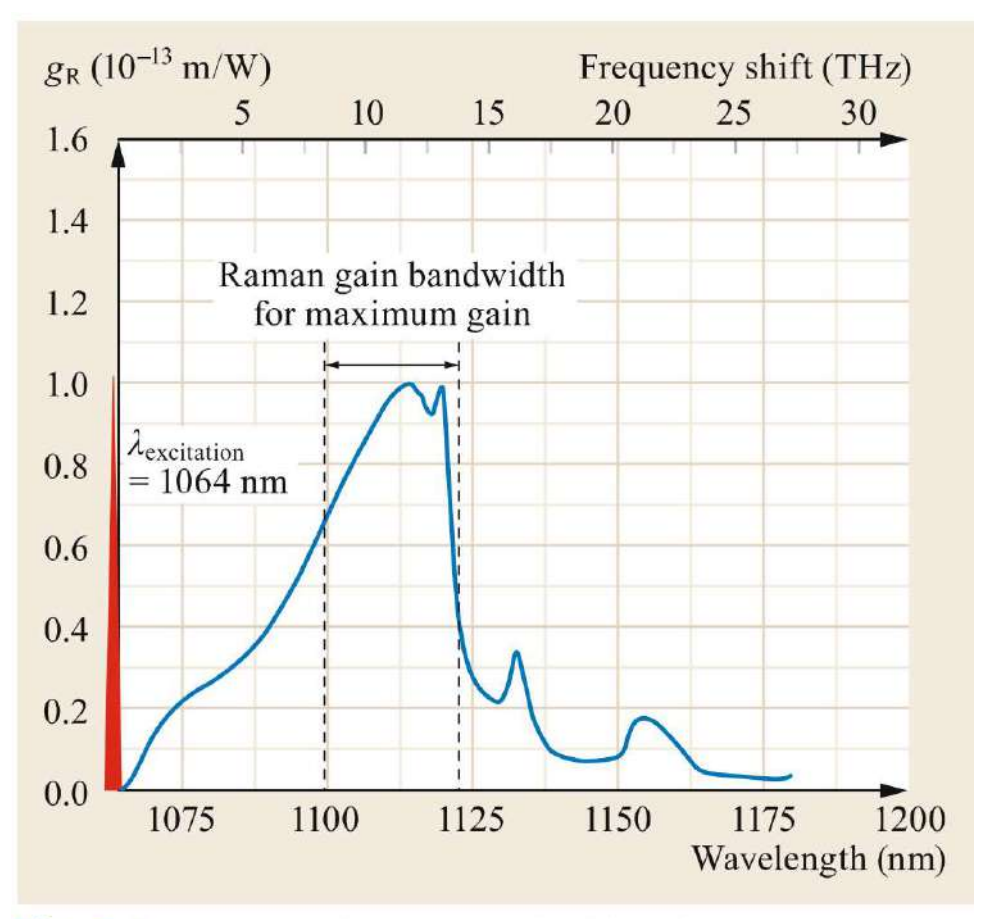
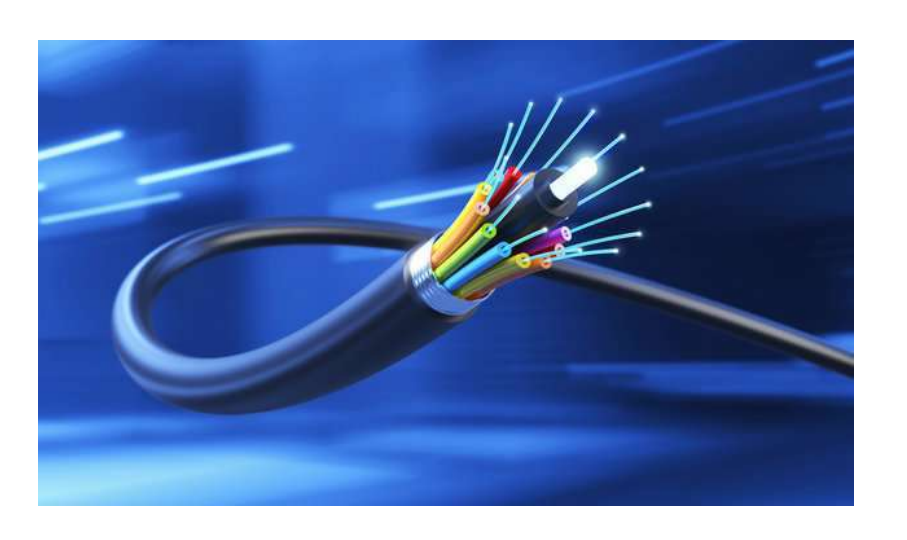
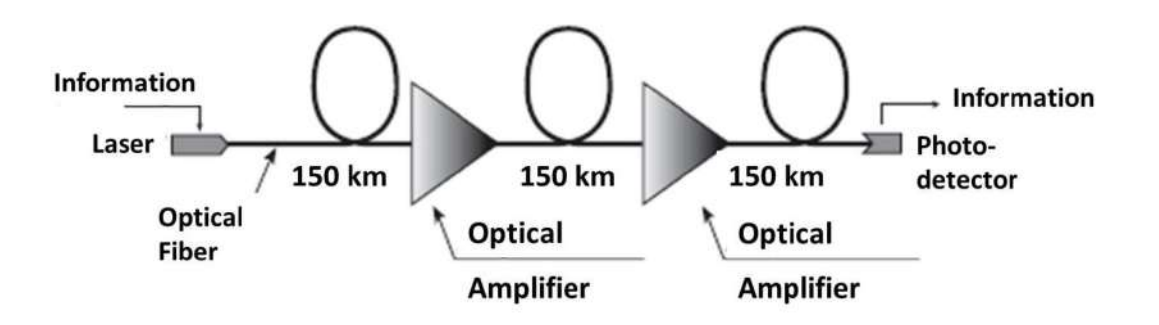
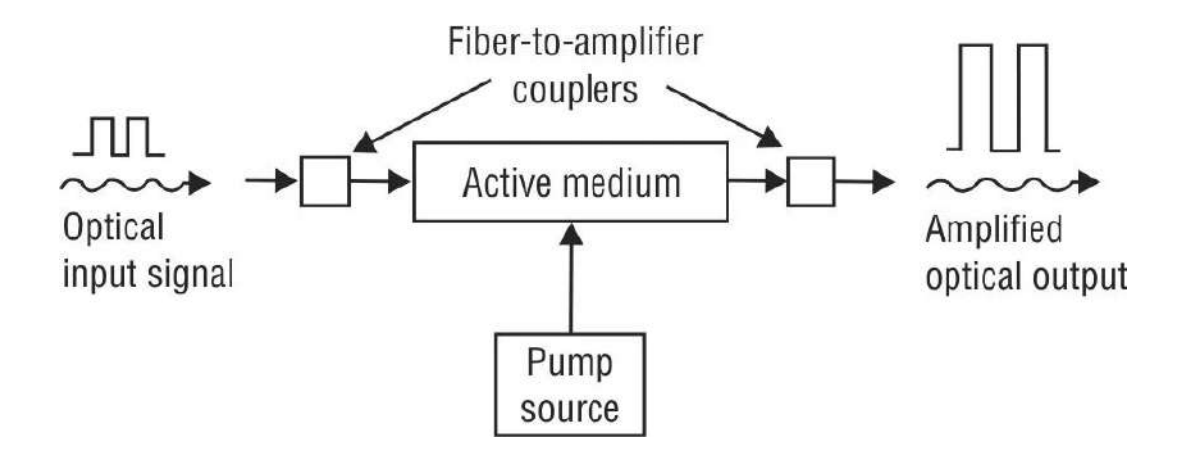


Fig. 6.8 Raman gain spectra of silica glass with a pump laser at 1064 nm. Here, the gain bandwidth is defined by the full width at half maximum (FWHM)

Communication

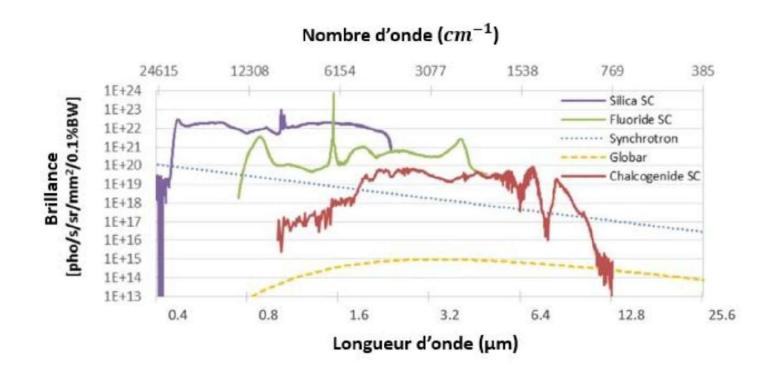






SuperContinuum Generation

the generation of a supercontinuum is an interesting infrared source because of its properties in terms of brightness, tunability and coherence. Supercontinuum is the spectral broadening obtained as a result of the non-linear propagation of an optical wave in a medium.



Origin of the spectral broadening:

In the case of short pulses, SCG in the normal dispersion regime is based **on phase** self-modulation (SPM), four-wave mixing (FWM) and Raman scattering (RS).

Optical Kerr effect:

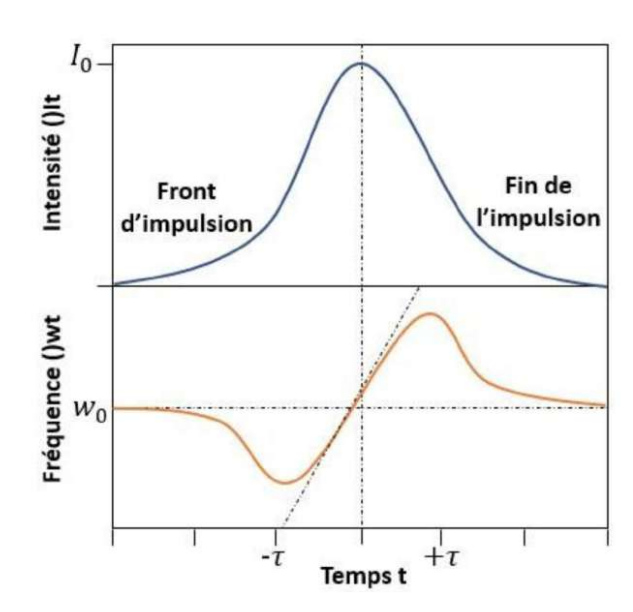
$$n(I) = n_0 + n_2 \cdot I$$

Induce a variation of the Phase of the propagating wave:

$$\phi(t) = \omega_0 t - \frac{2\pi}{\lambda_0} \cdot n(I)L$$

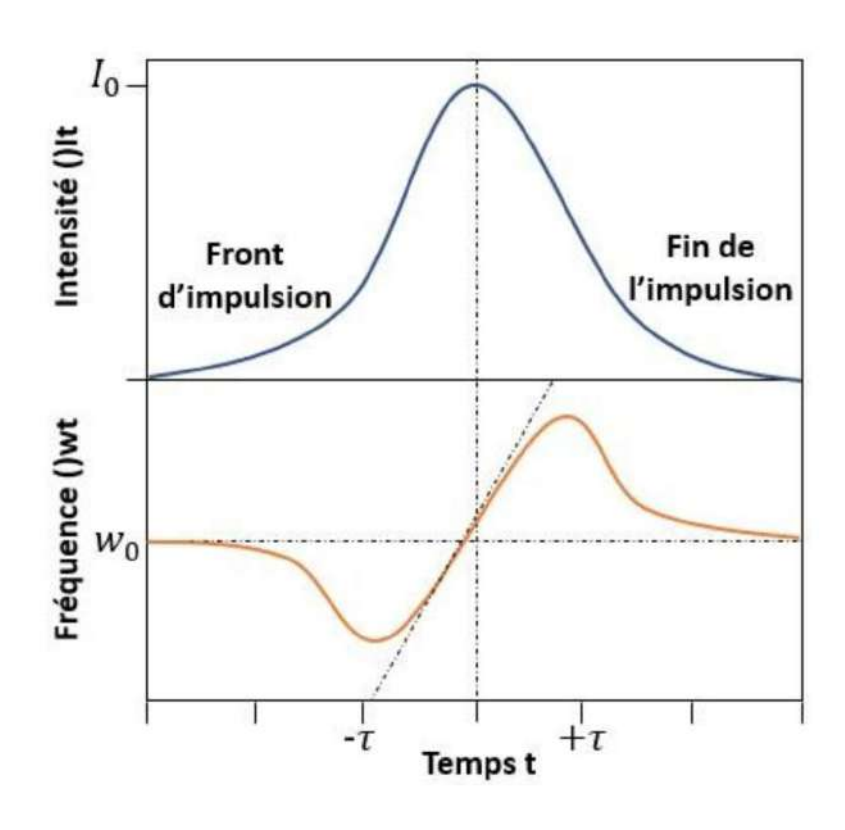
And thus modify the frequency (or Wavelenght) of the propagating wave:

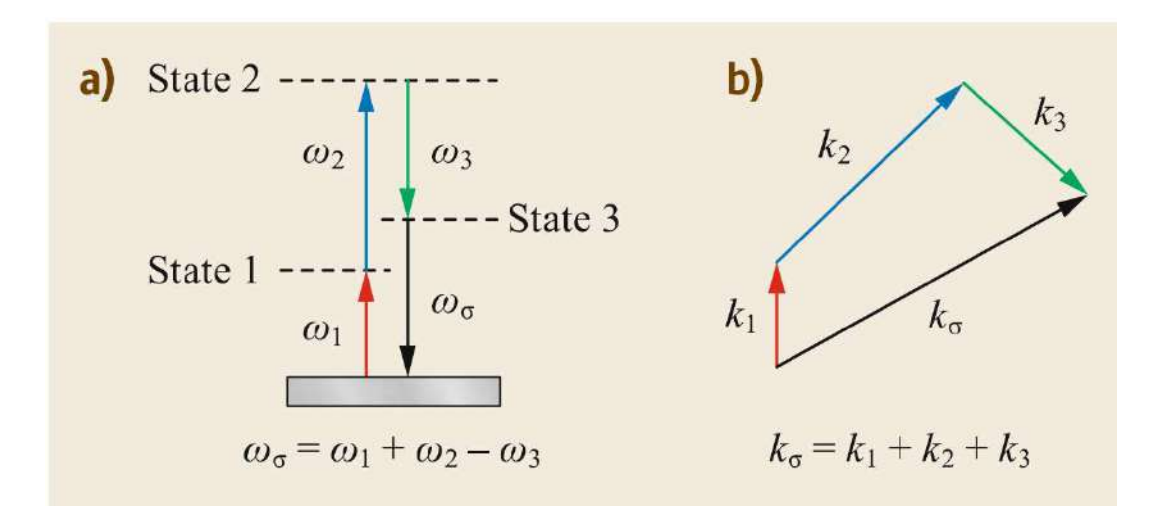
$$\omega(t) = \frac{d\phi(t)}{dt} = \omega_0 - \frac{2\pi L}{\lambda_0} \frac{dn(I)}{dt}.$$



Origin of the spectral broadening:

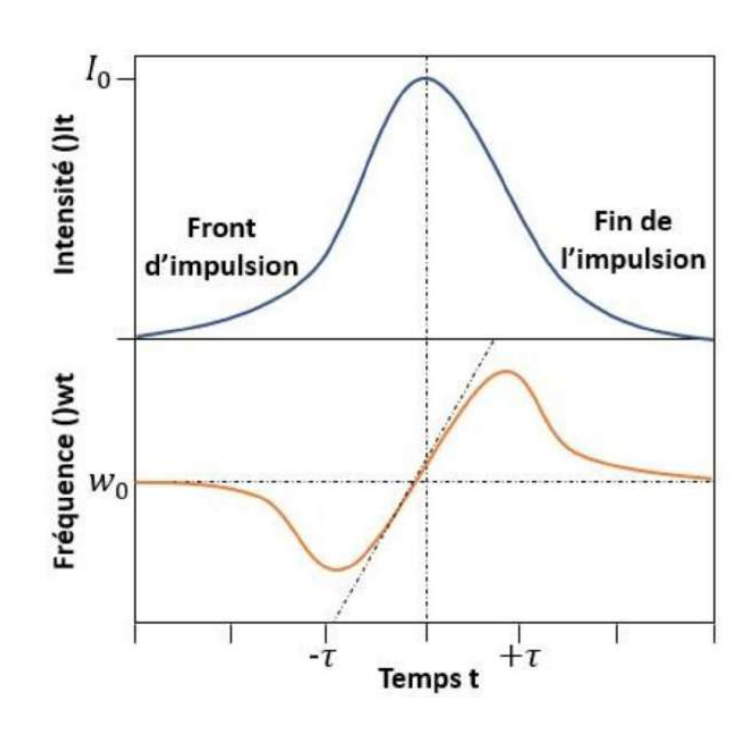
In the case of short pulses, SCG in the normal dispersion regime is based **on phase** self-modulation (SPM), four-wave mixing (FWM) and Raman scattering (RS).

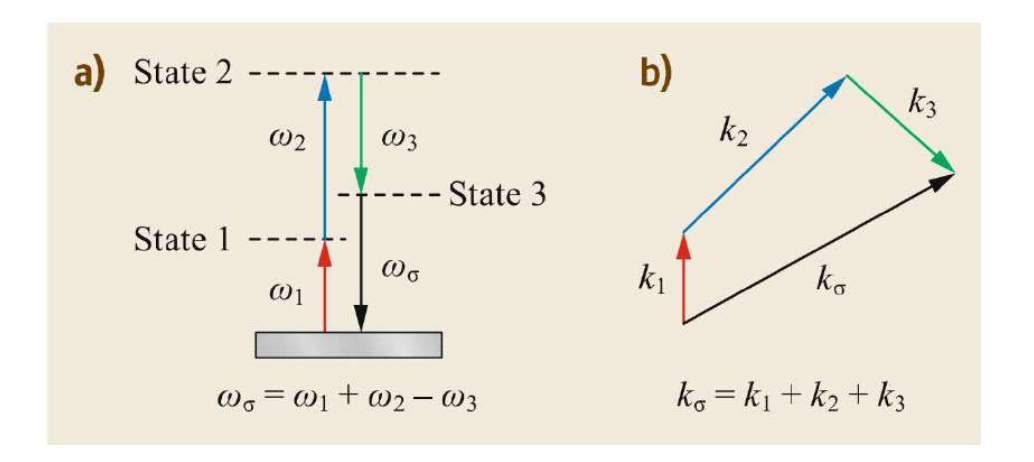


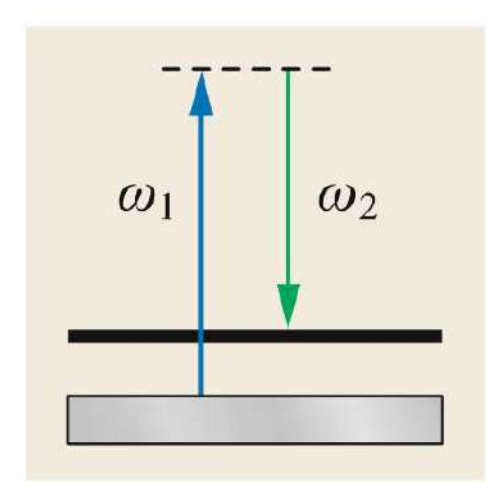


Origin of the spectral broadening:

In the case of short pulses, SCG in the normal dispersion regime is based **on phase self-modulation (SPM)**, four-wave mixing (FWM) and Raman scattering (RS).

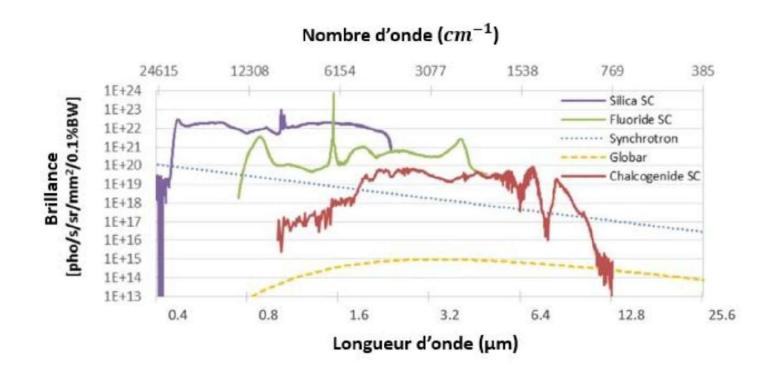






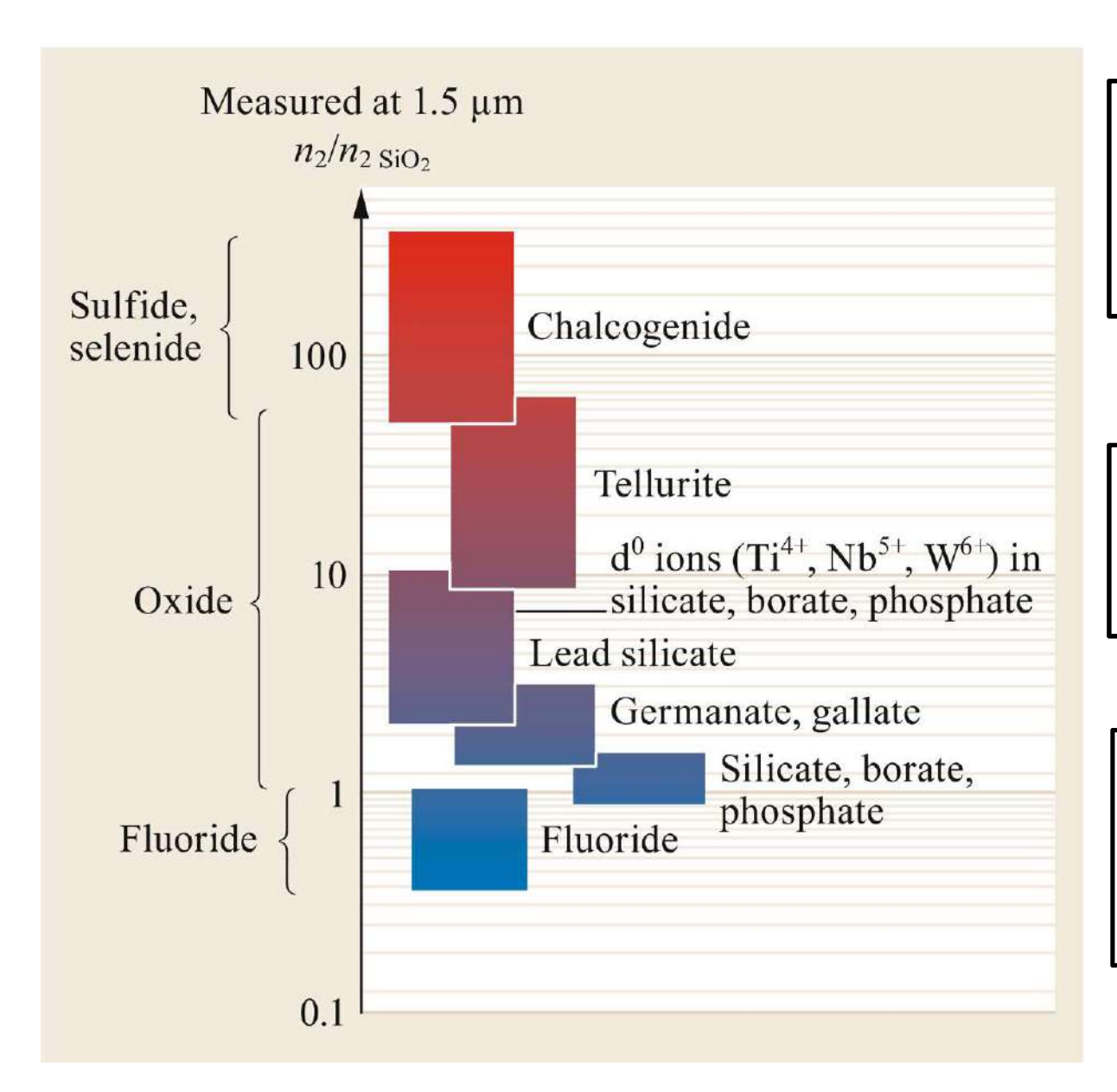
SuperContinuum Generation

the generation of a supercontinuum is an interesting infrared source because of its properties in terms of brightness, tunability and coherence. Supercontinuum is the spectral broadening obtained as a result of the non-linear propagation of an optical wave in a medium.



Nonlinear optical properties of glass

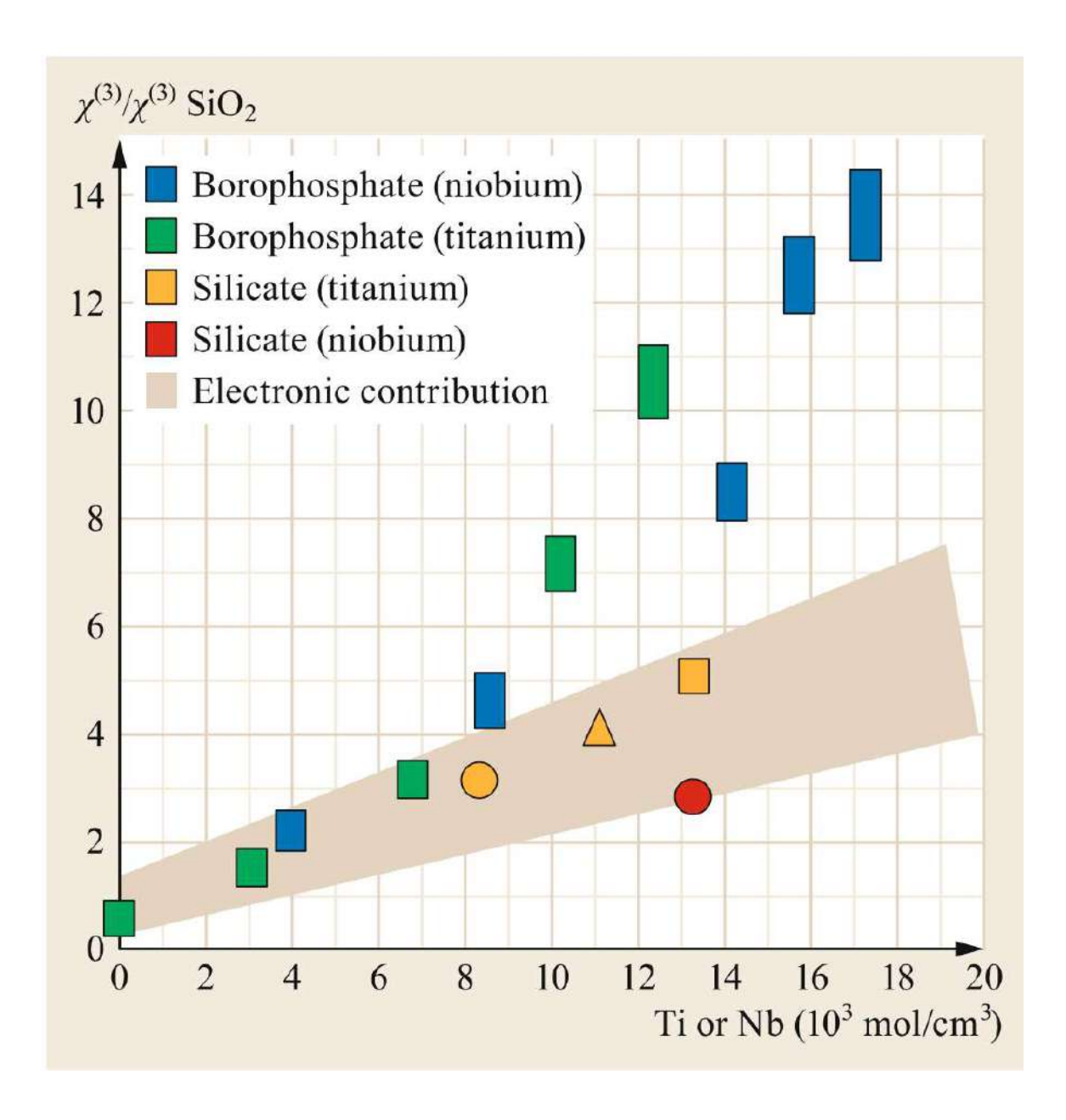
- Introduction non linear optics
- Characterization methods
- Third order optical response and glass chemistry
 - Two important third order optical process for applications:
 - Raman Gain
 - Supercontinuum generation
- Second order optical response in glass

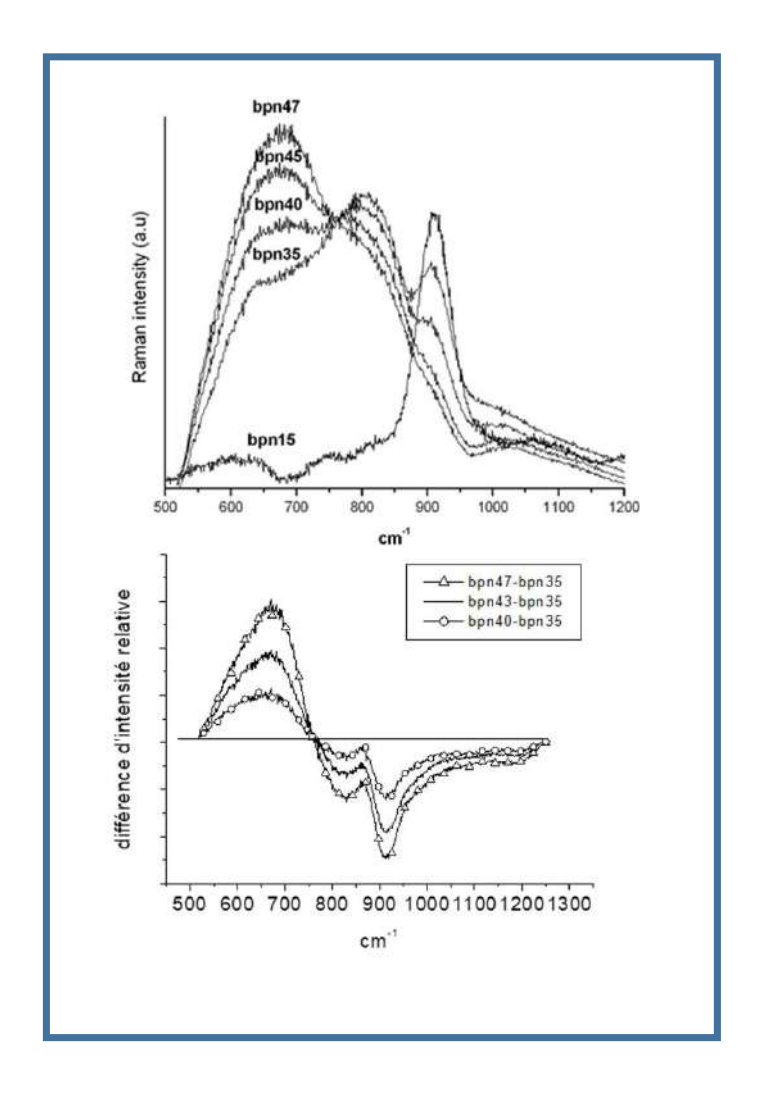


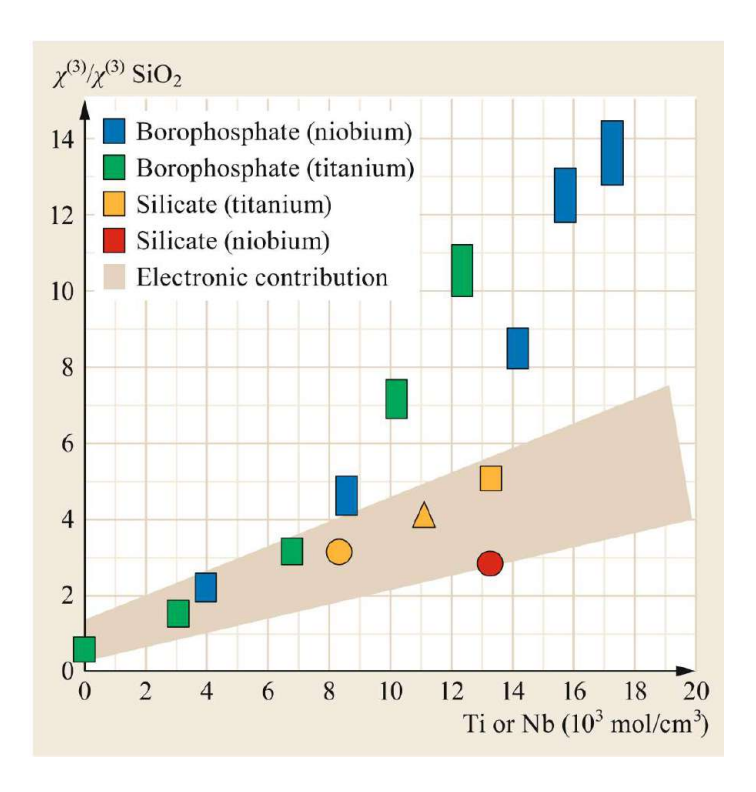
It has been established that the fast response time Kerr effect (1 picosecond) out of resonance is, in a first approximation, following the evolution the glass polarizability and more precisely the polarizability of the anions (F-<O²⁻<S²⁻<Se²⁻)

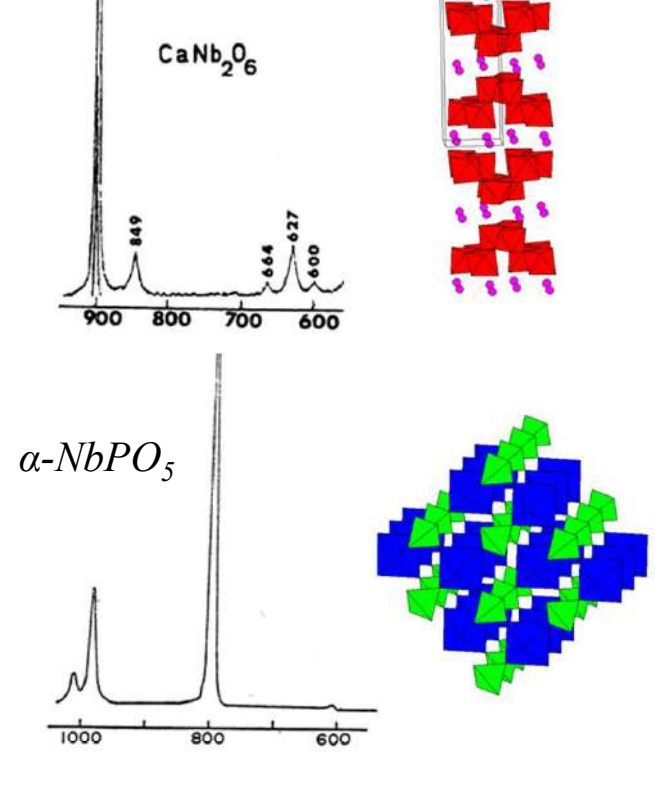
Considering a specific glass family, it appears that the evolution is complex and the impact of the glass structure and composition has a huge impact on the nonlinear optical responses of the material

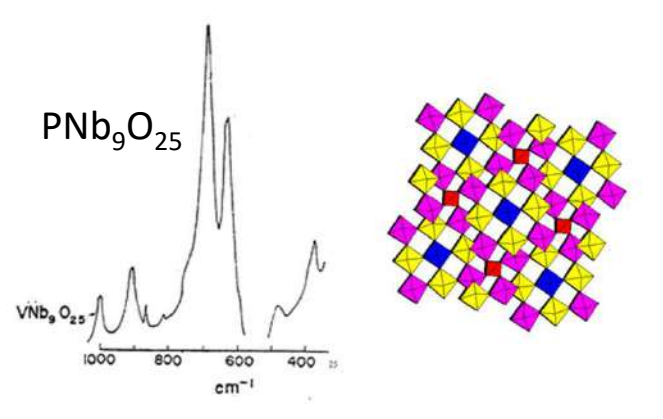
Regarding oxides, silicates, phosphates and borates, the introduction of alkali and alkaline earth ions by forming non-bridging oxygen between the glass formers increases the linear and the nonlinear indices

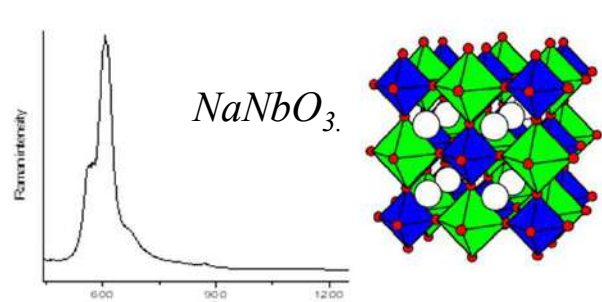




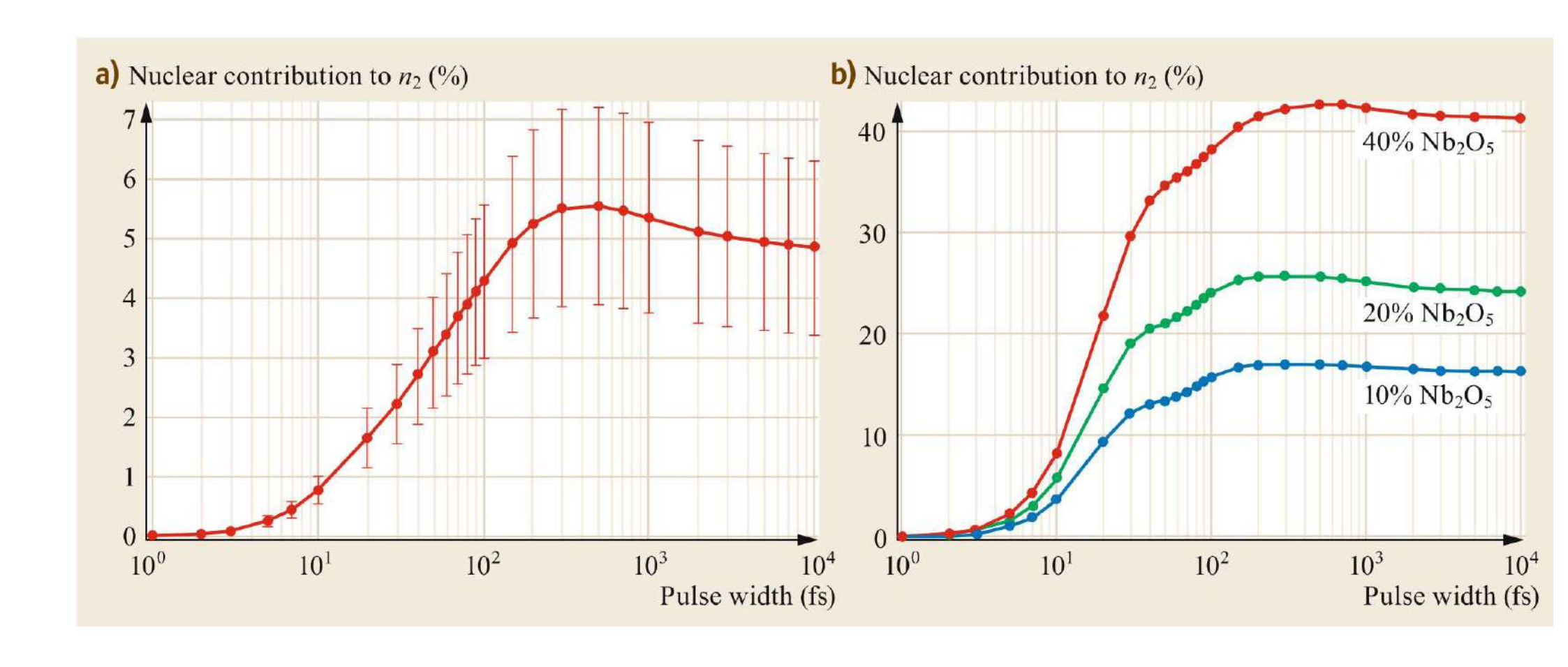


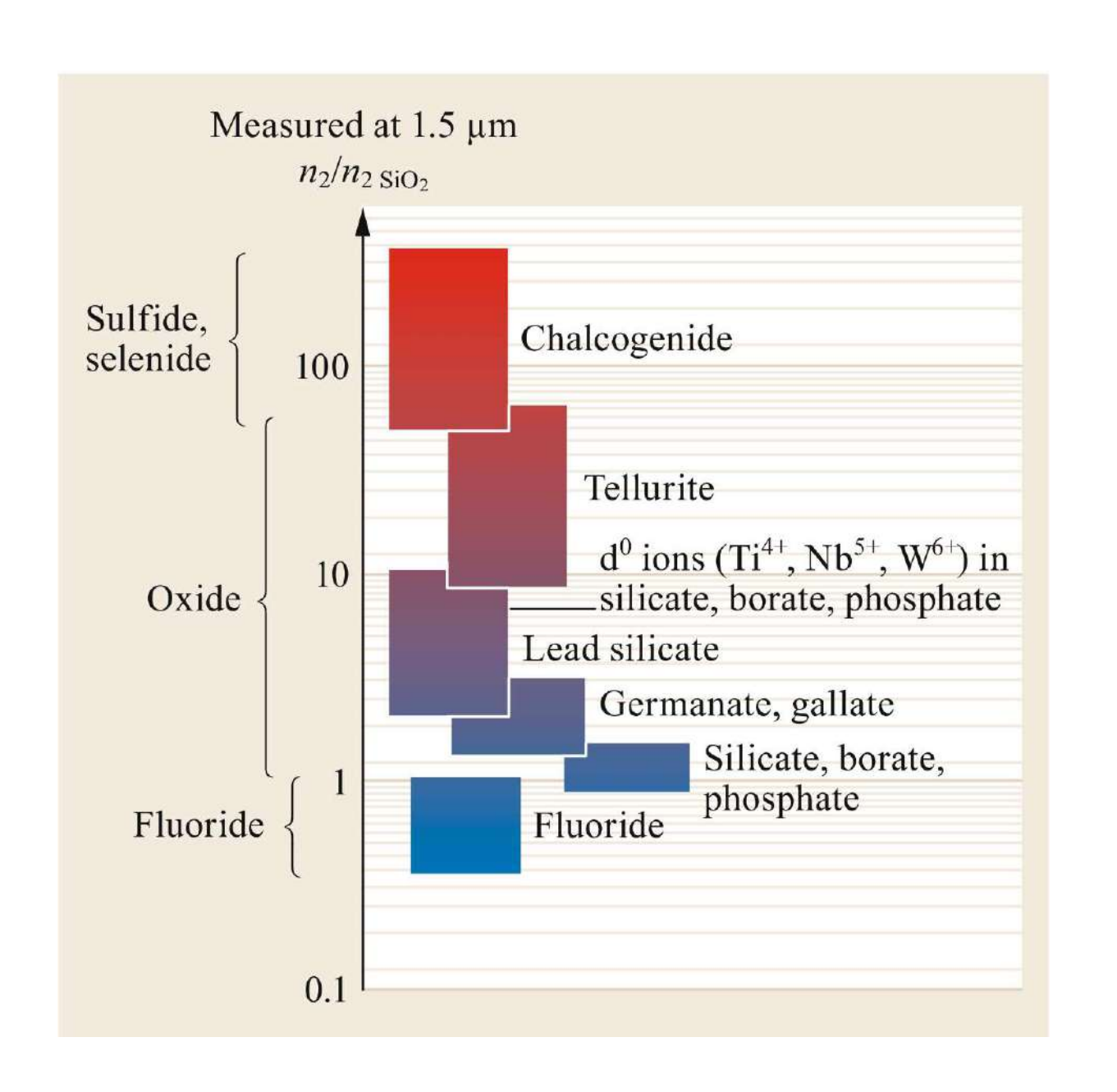


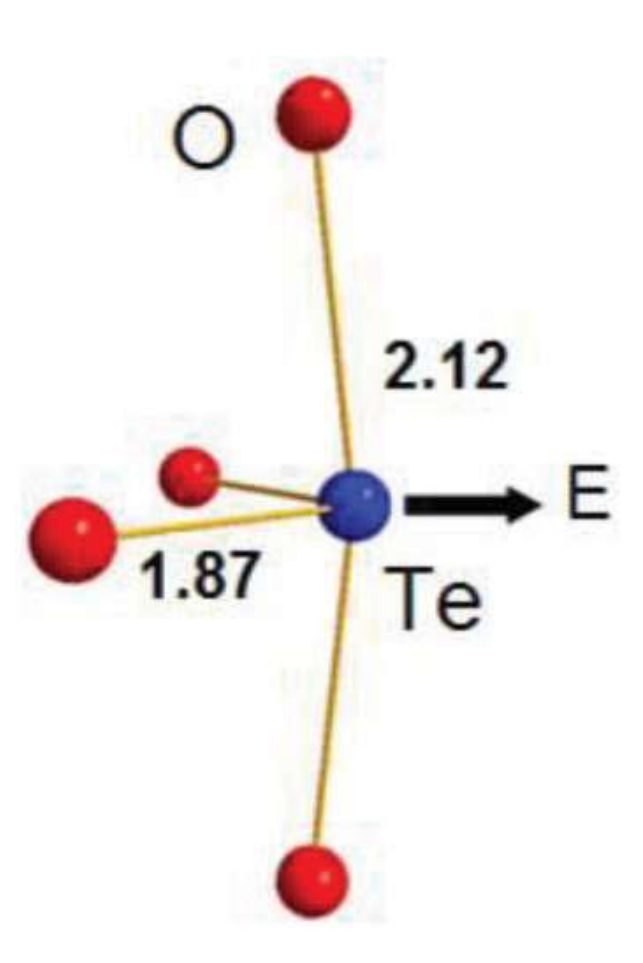




$$n_2 = n_2^{electronic} + n_2^{nuclear} + n_2^{electrostrictive} + n_2^{thermal}$$







Nonlinear optical properties more than 10 times silica can be obtained in **lone pairs of electron ns² oxide based compounds**. It is the case for instance of tellurite glass composition in which the tellurium oxide amount can reach 99% of TeO₂. The Te⁴⁺ ion occupies a TeO₄ disphenoid site where the tellurium ion is at the center of a trigonal bipyramid TeO₄E in which the electronic doublet E form the third equatorial corner.

Glass composition (Mol%)	Third order susceptibility $\chi^{(3)}$ (10 ⁻²³ SI) ± 20%
90TeO ₂ -10Tl ₂ O	141
90TeO ₂ -10Nb ₂ O ₅	115
90TeO ₂ -10WO ₃	97
90TeO ₂ -10Al ₂ O ₃	78
90TeO ₂ -10Ga ₂ O ₃	72
90TeO ₂ -10Sb ₂ O ₄	58
SF59 (lead silicate)	57

The highest nonlinear indices observed in tellurite glass have been obtained when the TeO₂ is combined with other ions also having a ns2 lone pair of electrons such as Tl⁺, Pb²⁺ or Bi³⁺.

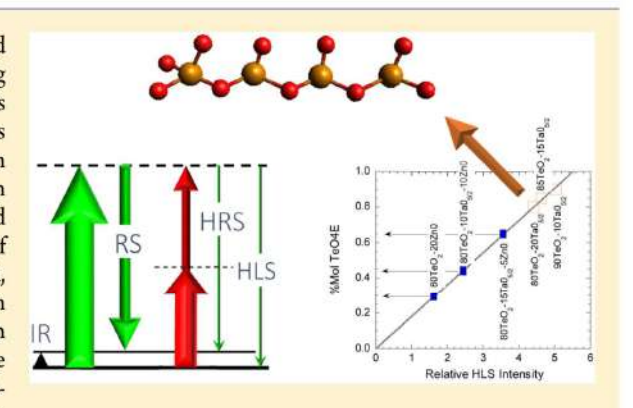


Raman Gain in Tellurite Glass: How Combination of IR, Raman, Hyper-Raman and Hyper-Rayleigh Brings New Understandings

Vincent Rodriguez,**,† Guillaume Guery,†,‡,§ Marc Dussauze,† Frederic Adamietz,† Thierry Cardinal,‡ and Kathleen Richardson^{§,||}

Supporting Information

ABSTRACT: A new multimodal approach that combines linear and nonlinear vibrational spectroscopies and hyper-Rayleigh scattering has been applied in the TeO_2 – $TaO_{5/2}$ –ZnO glass system to assess and quantify the relation between Raman gain and optical responses within the glass' network arrangement. The level of polymerization of the TeO_4 chain-like structure in a TeO_2 glass system has been identified to be the main parameter for reaching high linear and nonlinear optical constant. We have observed that replacement of $TaO_{5/2}$ by ZnO strongly modifies the optical properties and, primarily, the Raman and hyper-Raman spectra of the glasses. In particular, we clearly demonstrate a linear relationship between Raman gain and the linear and second-order optical response of the glass, which is directly related to the number density of TeO_4 chain-like units. Assuming that only TeO_4 chain-like units contribute



significantly to the glass' polarizability, we have found that about 30% of the Te atoms contribute to the hyperpolarizability of the binary system 80TeO₂-20ZnO in very good accordance with neutron diffraction results.

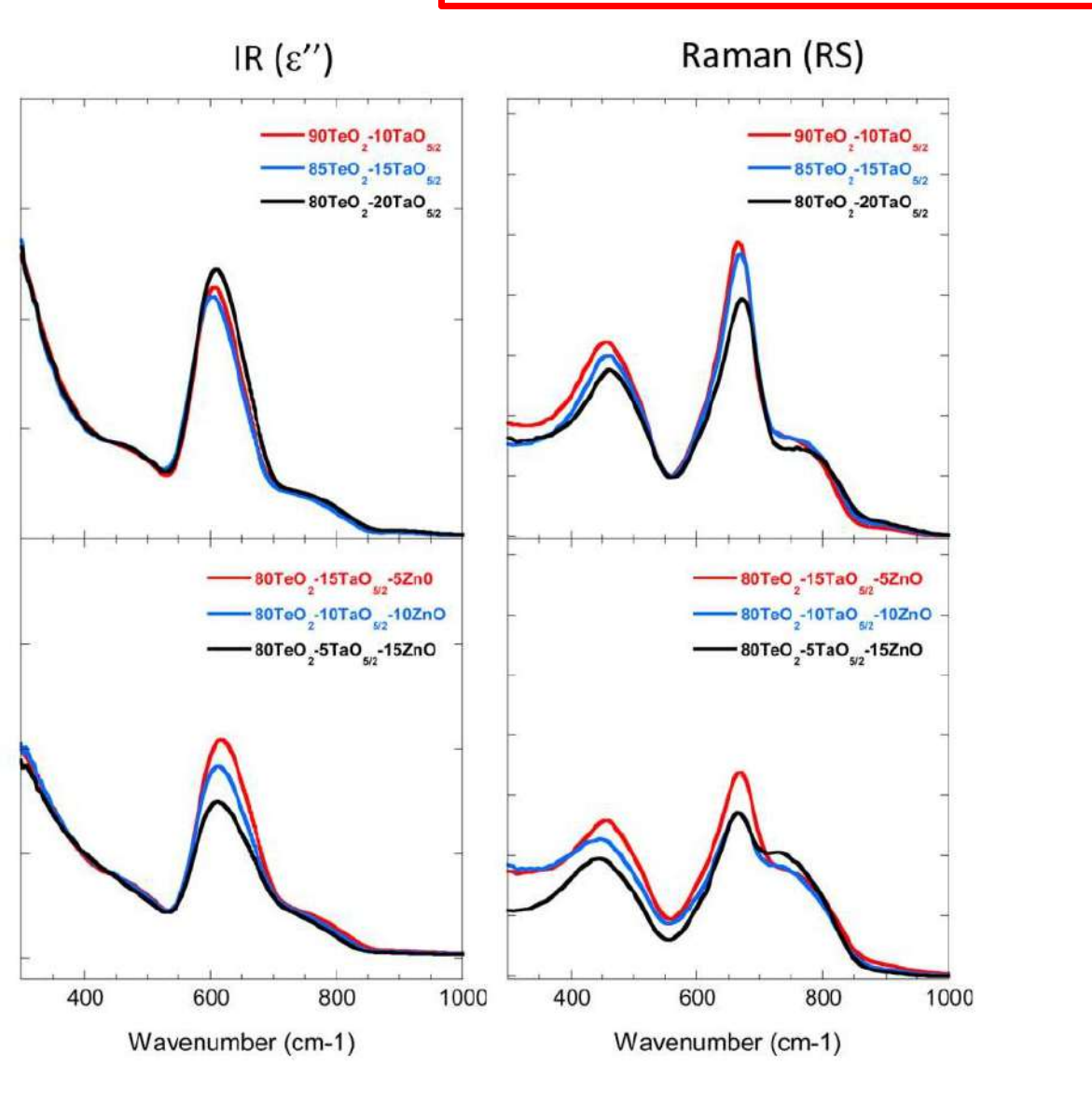
[†]Université de Bordeaux, Institut des Sciences Moléculaires, CNRS UMR 5255, 351 cours de la Libération, 33405 Talence Cedex, France

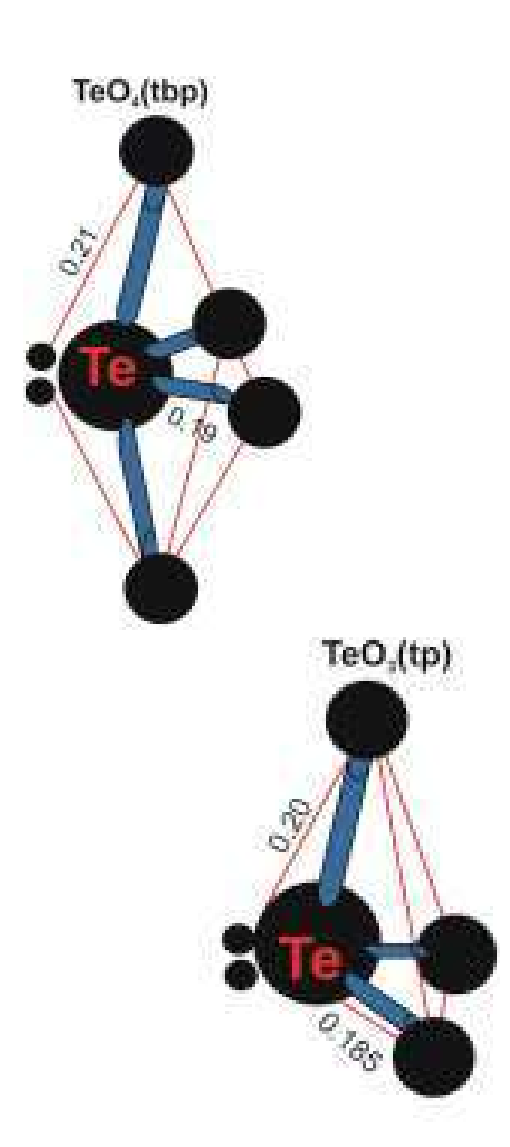
[‡]CNRS, Université de Bordeaux, ICMCB UPR 9048, 87 av. Schweitzer, 33608 Pessac Cedex, France

[§]COMSET, School of Materials Science and Engineering, Clemson University, Clemson, South Carolina 29634, United States

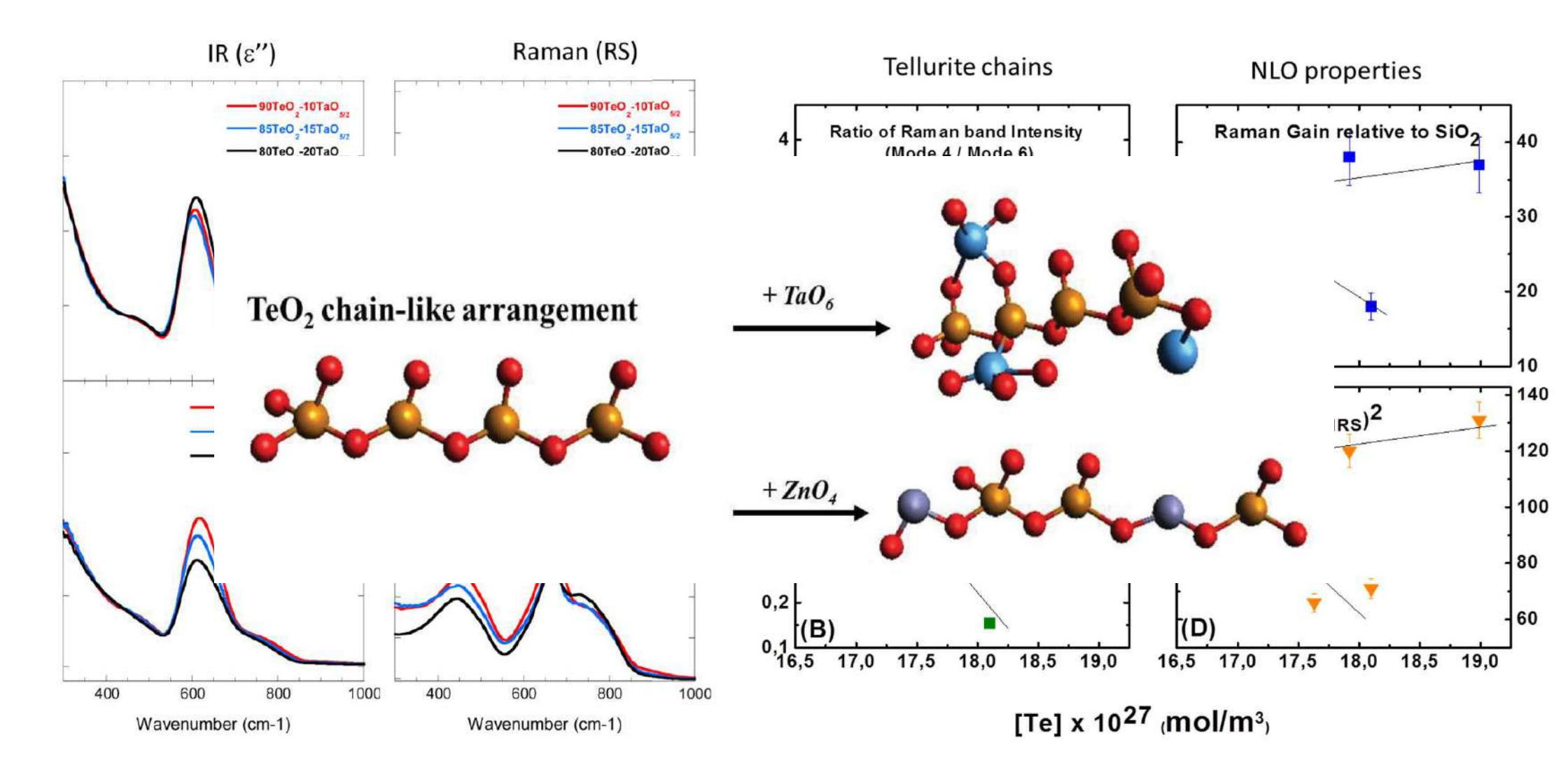
CREOL, College of Optics and Photonics, Department of Materials Science and Engineering, University of Central Florida, Orlando, Florida 32816, United States

$(100 - x)\text{TeO}_2 - (x - y)\text{TaO}_{5/2} - y\text{ZnO}$

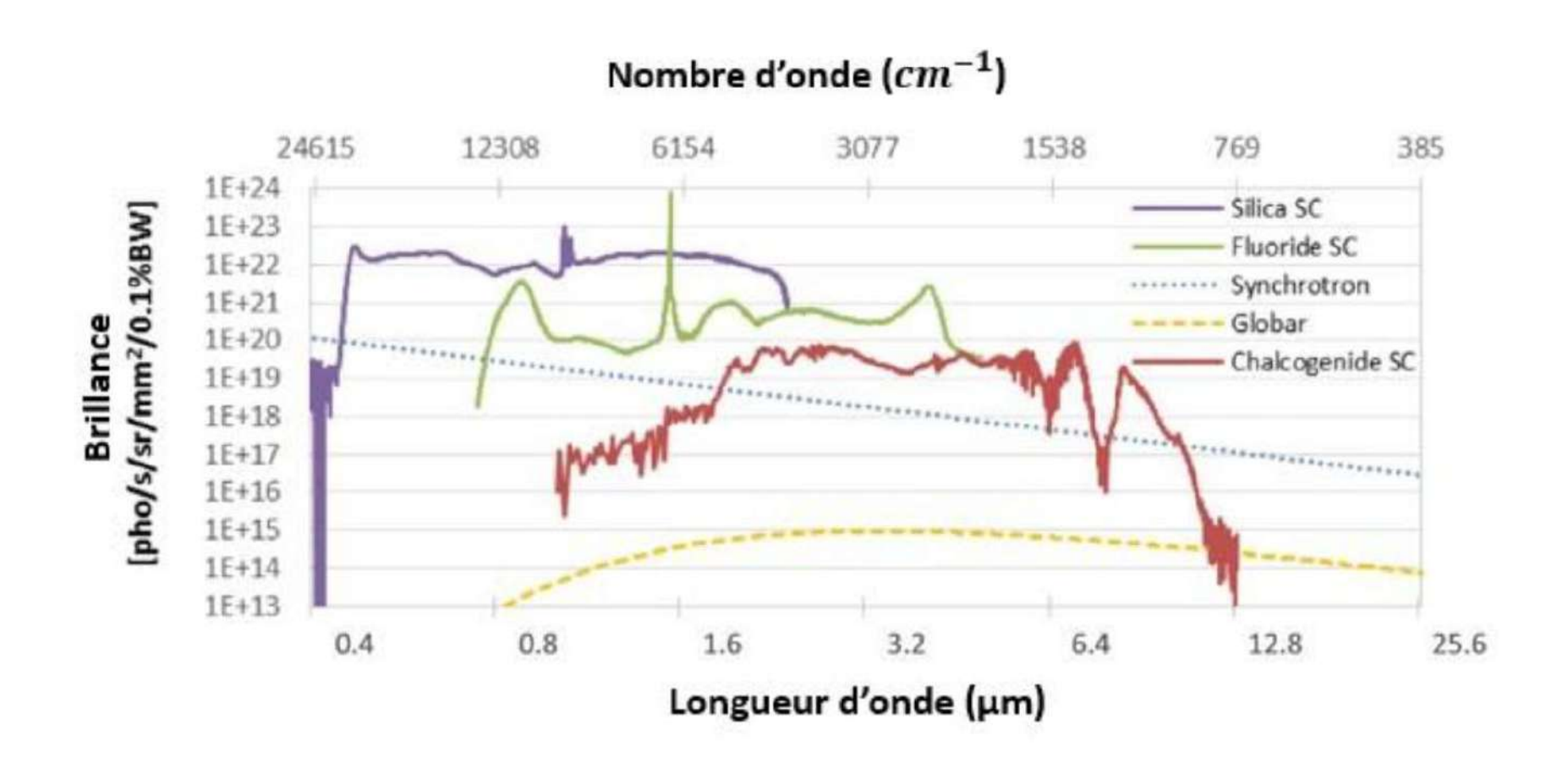




$$(100 - x)\text{TeO}_2 - (x - y)\text{TaO}_{5/2} - y\text{ZnO}$$



Pour terminer avec l'ordre 3!



Nonlinear optical properties of glass

- Introduction non linear optics
- Characterization methods
- Third order optical response and glass chemistry
 - Second order optical response in glass
 - Glass ceramic
 - Optical poling
 - Thermal poling

2nd and 3rd order optical responses ... effect of the material symmetry

For a centro symmetric material, there is a center of inversion. This symmetry implies that:

$$E \to -E$$

$$P \to -P$$

Neumanns Principle: a symmetry operation must leave the sign and intensity of a physical property unchanged

$$\chi^{(2)} \to \chi^{(2)}$$

So combining all we obtain:

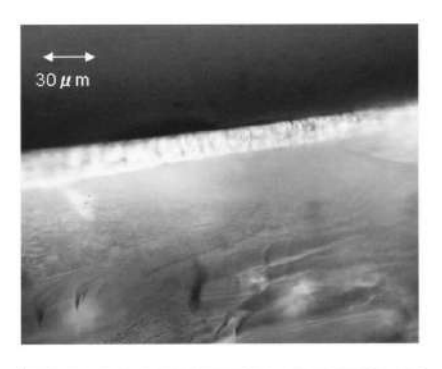
For a centro symmetric material

$$P^{(2)} = \chi^{(2)}EE \rightarrow -P^{(2)} = \chi^{(2)}(-E)(-E) \longrightarrow \chi^{(2)}=0$$

Second harmonic generation in transparent surface crystallized glasses with stillwellite-type ${\tt LaBGeO_5}$

Y. Takahashi, Y. Benino, T. Fujiwara, and T. Komatsu^{a)}
Department of Chemistry, Nagaoka University of Technology, Kamitomioka-cho, Nagaoka 940-2188, Japan
(Received 24 July 2000; accepted for publication 6 February 2001)

Transparent optical nonlinear crystallized glasses with the composition of $25\text{La}_2\text{O}_3$ $25\text{B}_2\text{O}_3$ 50GeO_2 , stoichiometric to ferroelectric stillwellite-type LaBGeO₅ crystalline phase, have been prepared by a two-step heat-treatment (first heat treatment: $T_1 = 670\,^{\circ}\text{C}$, $t_1 = 10\,\text{h}$, second heat-treatment: T_2 , t_2), and their second harmonic (SH) intensities have been examined using the Maker fringe method. The samples obtained by heat treatments at $T_2 = 720 \sim 725\,^{\circ}\text{C}$ for $t_2 = 3\,\text{h}$ show only surface crystallization and exhibit clear and fine (narrow) fringe patterns. The samples heat treated at $T_2 = 740\,$ and $750\,^{\circ}\text{C}$ exhibit relatively strong SH intensities, but the fringe patterns in such samples proad. It is proposed that SH waves generated from surface LaBGeO₅ crystalline layers scatter at LaBGeO₅ crystals formed in the interior of glass, causing the disappearance of fine fringe patterns. © $2001\,$ American Institute of Physics. [DOI: 10.1063/1.1360699]



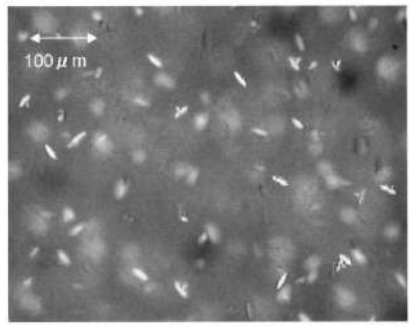


FIG. 7. Polarization micrographs for transparent LBGO surface crystallized glass obtained by heat treatment at $T_2 = 750$ °C for $t_2 = 5$ h.

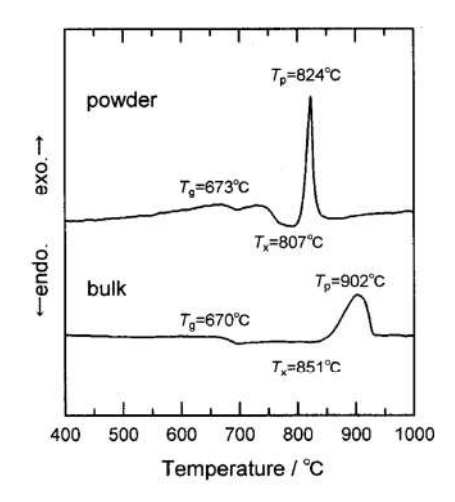


FIG. 1. DTA curves for bulk and powdered glasses of $25La_2O_3$ $25B_2O_3$ $50GeO_2$. Heating rate was 10 K min^{-1} .

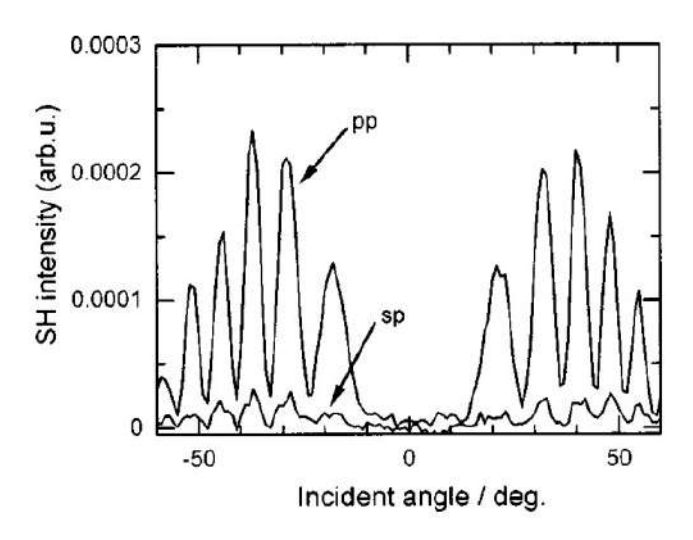
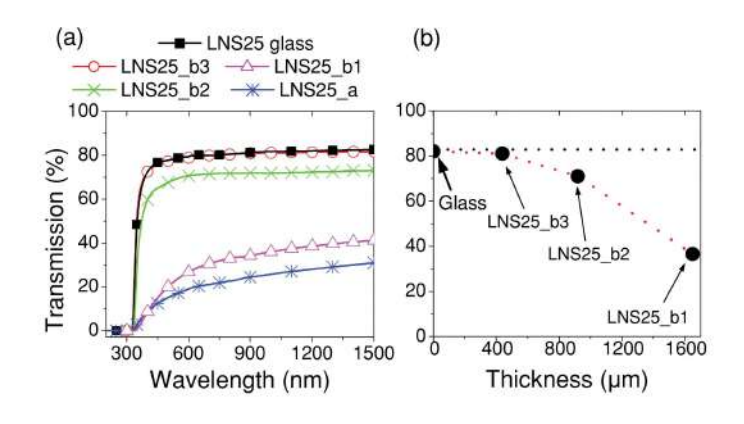


FIG. 6. Maker fringe patterns for transparent LBGO surface crystallized glasses obtained by heat treatment at $T_2 = 725$ °C for $t_2 = 3$ h. SH intensity was measured pp- and sp-polarization modes.

Synthesis and Multiscale Evaluation of LiNbO₃-Containing Silicate Glass-Ceramics with Efficient Isotropic SHG Response

Hélène Vigouroux, Evelyne Fargin,* Sonia Gomez, Bruno Le Garrec, Grigoris Mountrichas, Efstratios Kamitsos, Frédéric Adamietz, Marc Dussauze, and Vincent Rodriguez*

Sample	Treatment <i>nucleation</i> / growth	Initial thickness [μm]	Final thickness for optical characterizations [µm]
LNS25_a	620 °C 1 h/690 °C 75 min	850	760
LNS25_b1	580 °C 2 h/670 °C 17 min	1650	1650
LNS25_b2	580 °C 2 h/670 °C 17 min	1700	900
LNS25_b3	580 °C 2 h/670 °C 17 min	1650	440



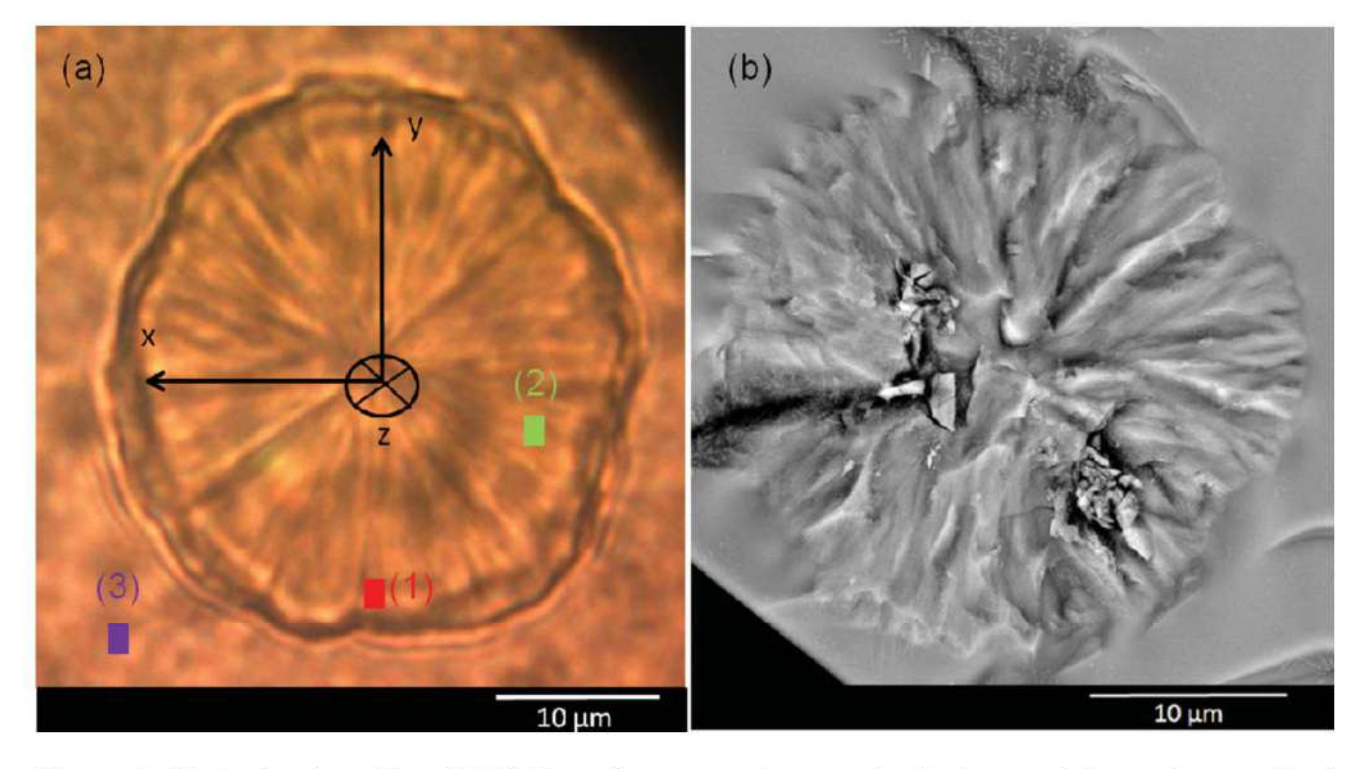
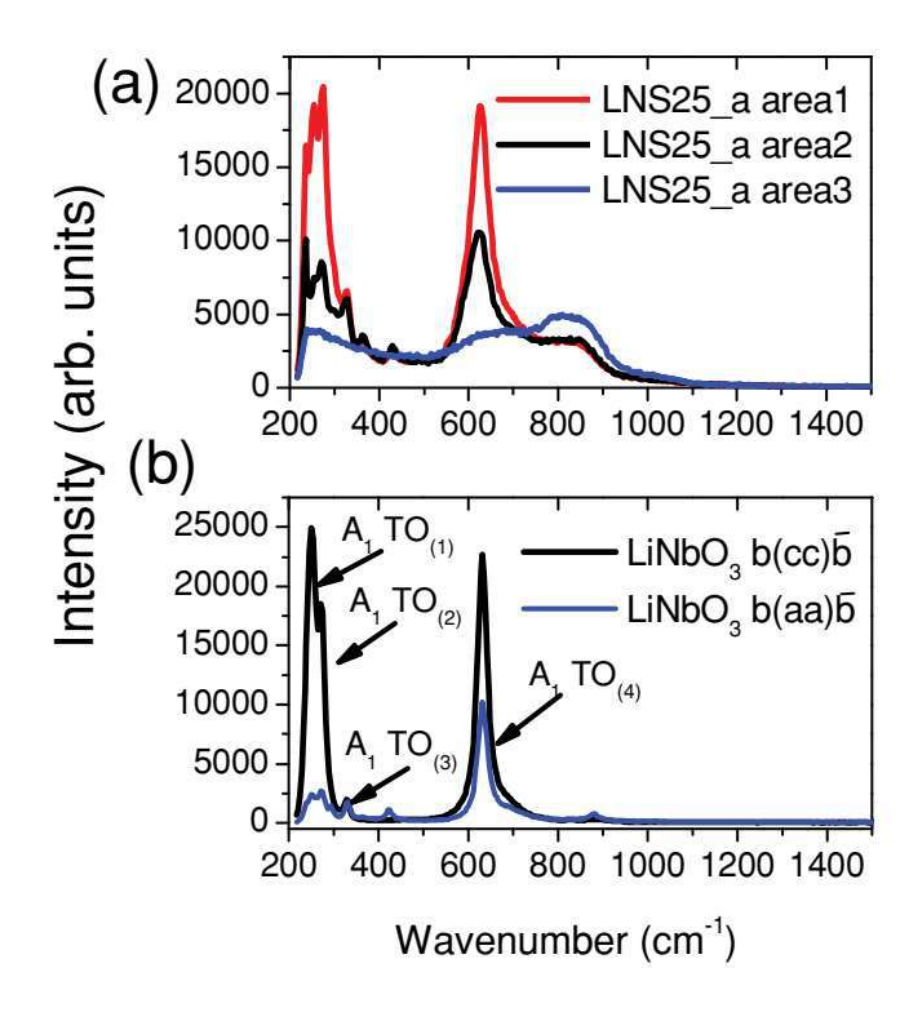


Figure 2. Typical spherulite of LNS25_a glass-ceramic sample a) observed through an optical microscope in the transmission mode and b) a high-resolution environmental SEM. The xyz axes represent the arbitrary orthogonal lab-framework. Points 1, 2, and 3 symbolize different areas where further analyses were carried out.



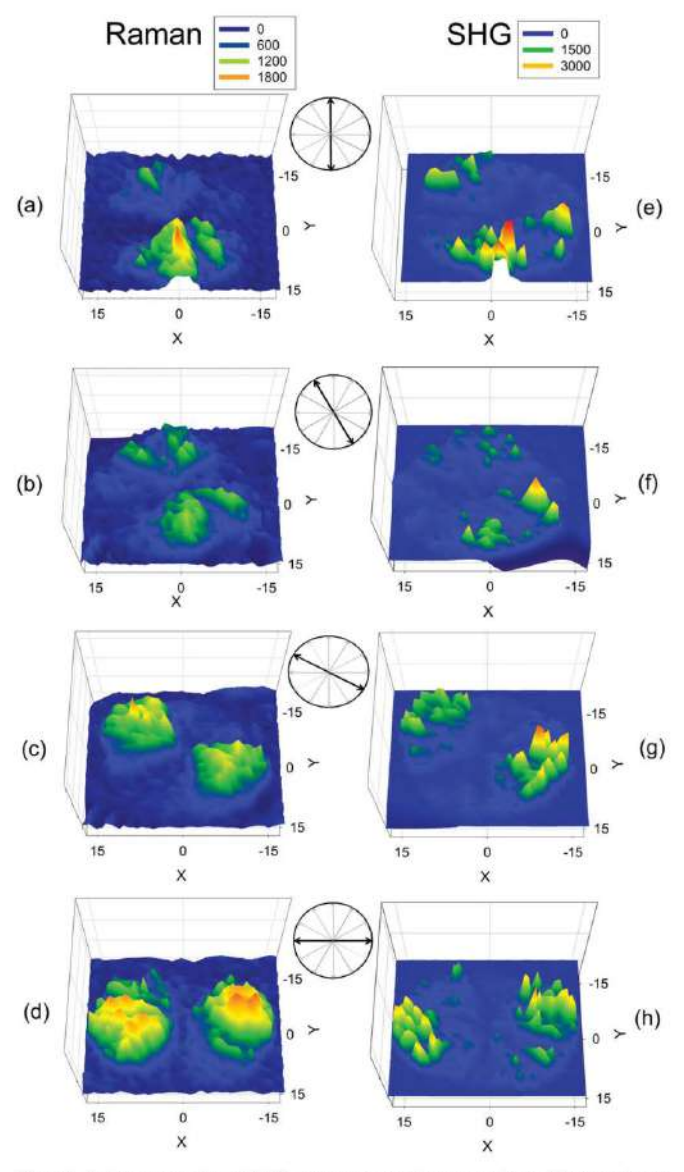
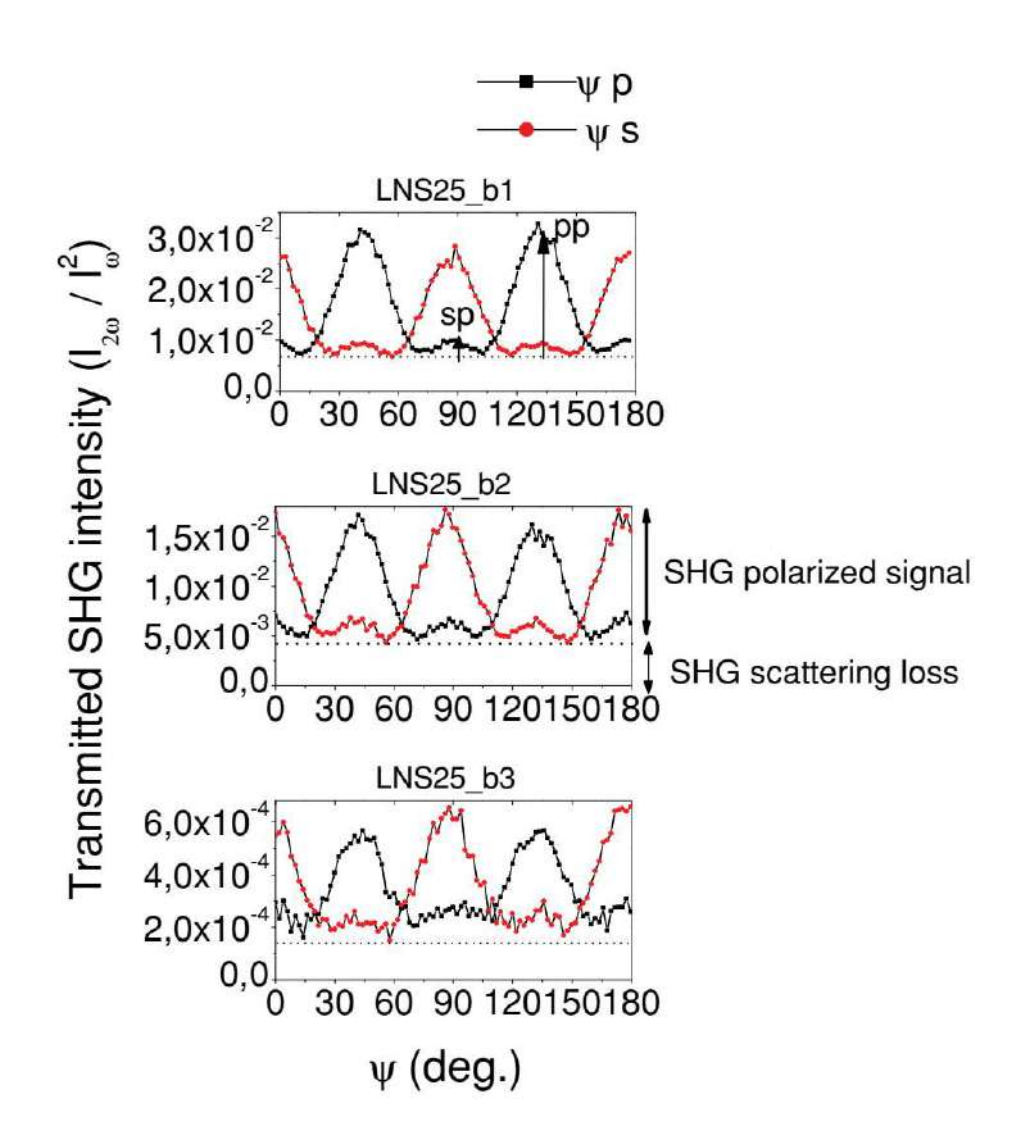


Figure 4. Probing a spherulite of LNS25_a glass ceramic: Raman mapping at different angles of polarization (0, 30, 60, 90°) (left) and micro-SHG mapping at the same angle of polarizations (right). Both mapping scales are expressed in μ m along X and Y directions.



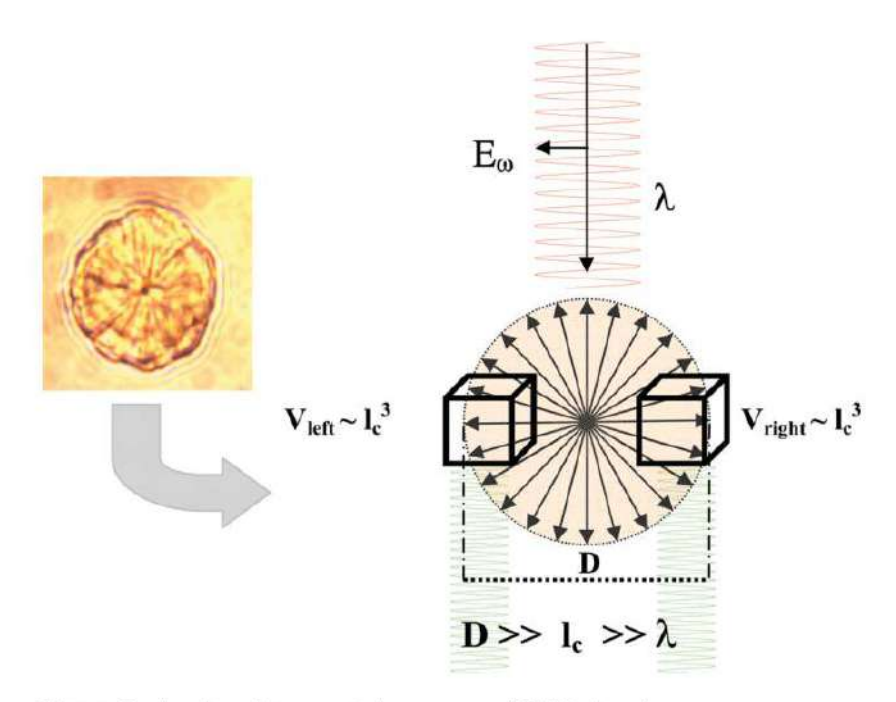


Figure 8. A spherulite as a twin source of SHG signal.

Nonlinear optical crystal-line writing in glass by yttrium aluminum garnet laser irradiation

Tsuyoshi Honma, Yasuhiko Benino, Takumi Fujiwara, and Takayuki Komatsu^{a)} Department of Chemistry, Nagaoka University of Technology, Nagaoka 940-2188, Japan

Ryuji Sato

Department of Materials Engineering, Tsuruoka National College of Technology, Tsuruoka 997-8511, Japan

(Received 5 November 2002; accepted 16 December 2002)

Crystal lines with second-order optical nonlinearity have been successfully fabricated at the surface of $10\mathrm{Sm_2O_3}.35\mathrm{Bi_2O_3}.55\mathrm{B_2O_3}$ glass by continuous irradiation of Nd:YAG laser. The laser-induced crystalline phase was confirmed to be $\mathrm{Bi_{0.7}Sm_{0.3}BO_3}$ by x-ray diffraction measurements, and second-harmonic generation (SHG) from the phase was clearly observed. An array structure of crystal lines was fabricated by laser writing under automatic computer control, and Maker fringe patterns of SHG were observed, indicating that the direction of polarization in the structure with a crystal line array was parallel to the sample surface. In addition, we measured polarization optical microphotographs, and found uniform phase retardation for a whole length of crystal lines. It is strongly suggested from these results that crystal lines by laser irradiation are formed in single-domain crystalline phase (single crystal) with second-order nonlinearity. © 2003 American Institute of Physics. [DOI: 10.1063/1.1544059]

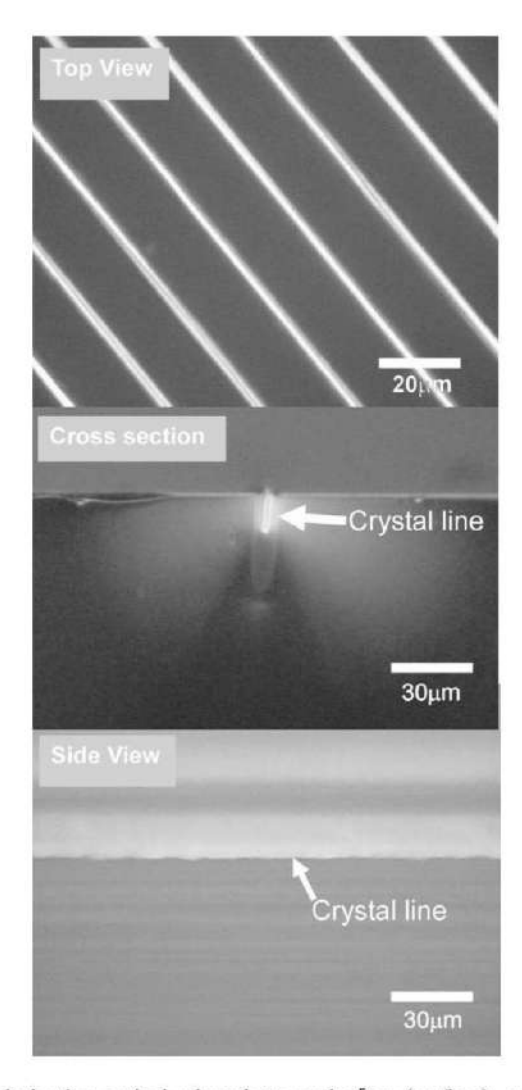


FIG. 1. Polarization optical microphotographs [top (surface), cross-section, side views] for the sample obtained by YAG laser irradiation (power: 0.66 W, scanning speed: $10 \, \mu \mathrm{m \, s^{-1}}$).

Direct laser-writing of ferroelectric single-crystal waveguide architectures in glass for 3D integrated optics

Adam Stone¹, Himanshu Jain¹, Volkmar Dierolf², Masaaki Sakakura³, Yasuhiko Shimotsuma⁴, Kiyotaka Miura⁴, Kazuyuki Hirao⁴, Jerome Lapointe⁵ & Raman Kashyap^{5,6}

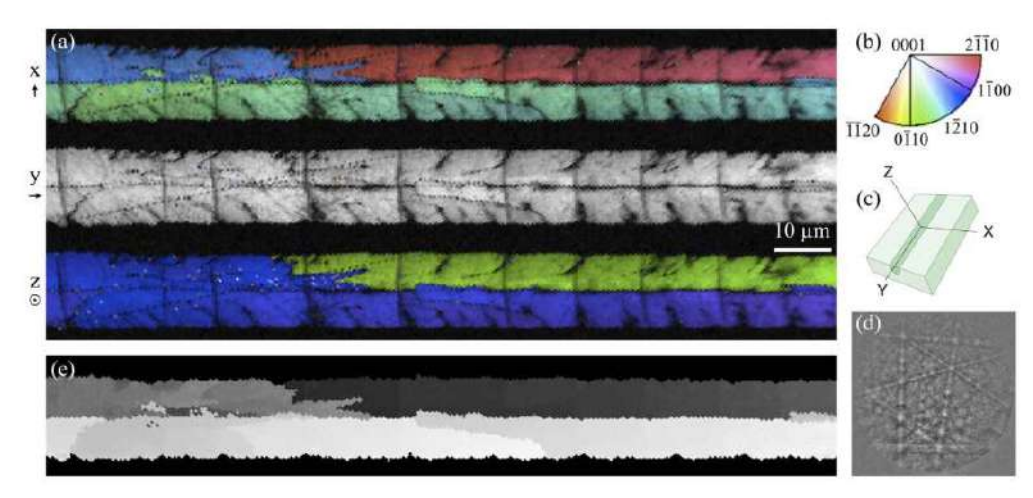


Figure 1. EBSD results for a polycrystal line grown at $25\,\mu\text{m/s}$ scan speed and $500\,\text{mW}$ average power, with no aberration correction. Crystal orientation IPF maps overlaid with grayscale image quality masks are given in (a) with respect to the three orthogonal axes indicated to the left of each map. The color correspondence of crystal orientation parallel to each reference axis is given in (b), and a schematic of the reference coordinate system relative to the sample geometry is given in (c). Inversion averaging was disabled in the OIM software in order to highlight the 180° twin (red region in the x-map). An example diffraction pattern is included in (d), and (e) shows the low-angle grain structure in the x-oriented IPF map, converted to grayscale and contrast-enhanced.

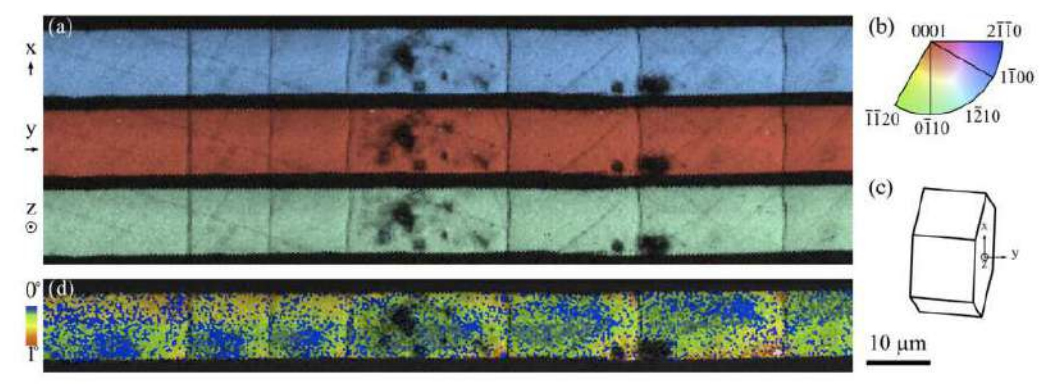


Figure 2. EBSD results for a single-crystal line grown at $42\mu m/s$ scan speed and $300\,mW$ average power, with aberration correction applied. Crystal orientation IPF maps overlaid with grayscale image quality masks are given in (a) with respect to the same reference axis defined in Fig. 1. The color correspondence of crystal orientation parallel to each reference axis is given in (b), and an illustration of the lattice orientation (represented by a hexagonal cell) is given in (c). The angular deviations from the average orientation are mapped in (d) to confirm the absence of low-angle grain boundaries.

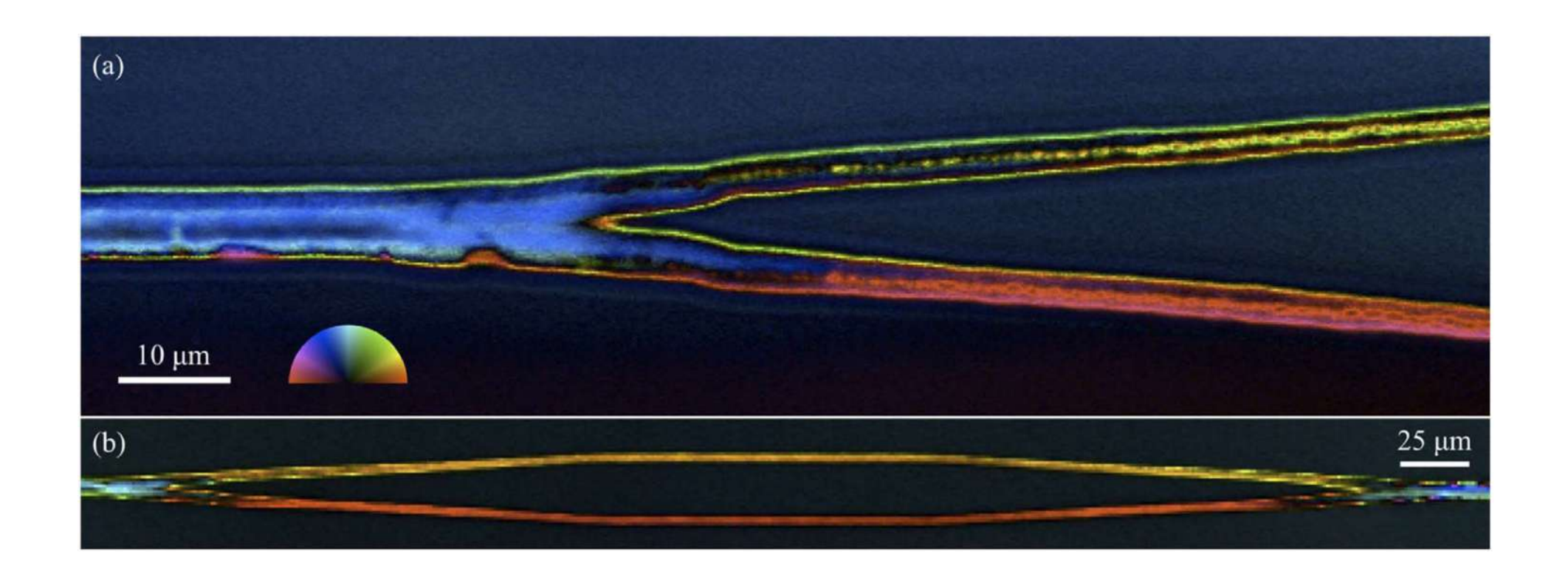


Figure 17: birefringence micrographs of crystal junctions written inside a LaBGeO₅ glass by femtosecond laser showing a) independent lattice orientations developed in each branch, b)the merging of the two branches back to a single line. The angle of either the fast or slow axis of birefringence is indicated by the color wheel. [98]

Nonlinear optical properties of glass

- Introduction non linear optics
- Characterization methods
- Third order optical response and glass chemistry
 - Two important third order optical process for applications:
 - Raman Gain
 - Supercontinuum generation
- Second order optical response in glass
 - Glass ceramic
 - Optical poling

$$\chi^{(2)}(-2\omega; \omega, \omega) = 3\chi^{(3)}(-2\omega; \omega, \omega, 0). E_{DC}$$

Thermal poling

T. J. Driscoll and N. M. Lawandy

Vol. 11, No. 2/February 1994/J. Opt. Soc. Am. B 355

Optically encoded second-harmonic generation in bulk silica-based glasses

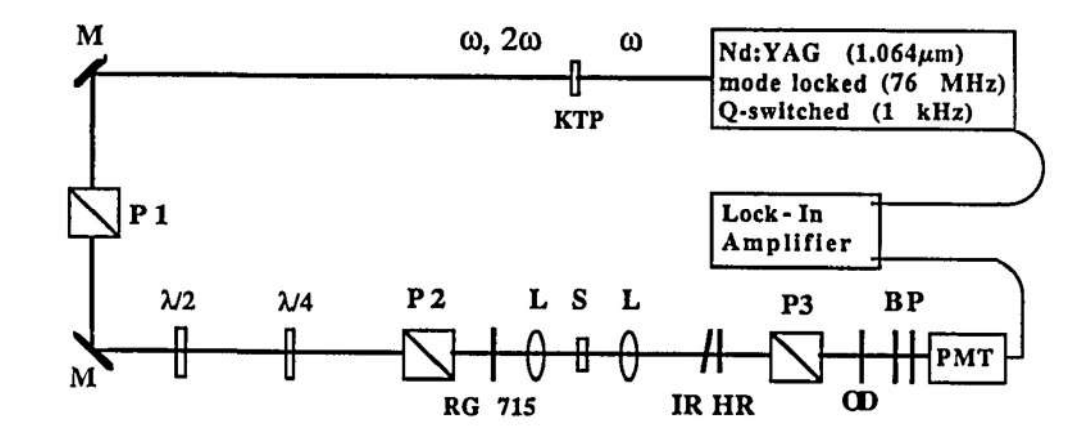
T. J. Driscoll

Department of Physics, Brown University, Providence, Rhode Island 02912

N. M. Lawandy

Division of Engineering and Department of Physics, Brown University, Providence, Rhode Island 02912

Received January 15, 1993; revised manuscript received May 20, 1993



... a free-space second-harmonic mode whose symmetry and tensor components were more consistent with an internal electric field ...

 $2 \qquad \chi^{(2)}(0;\omega,-\omega)$

Optical rectification

A static electric field occurs in the NLO medium under illumination.

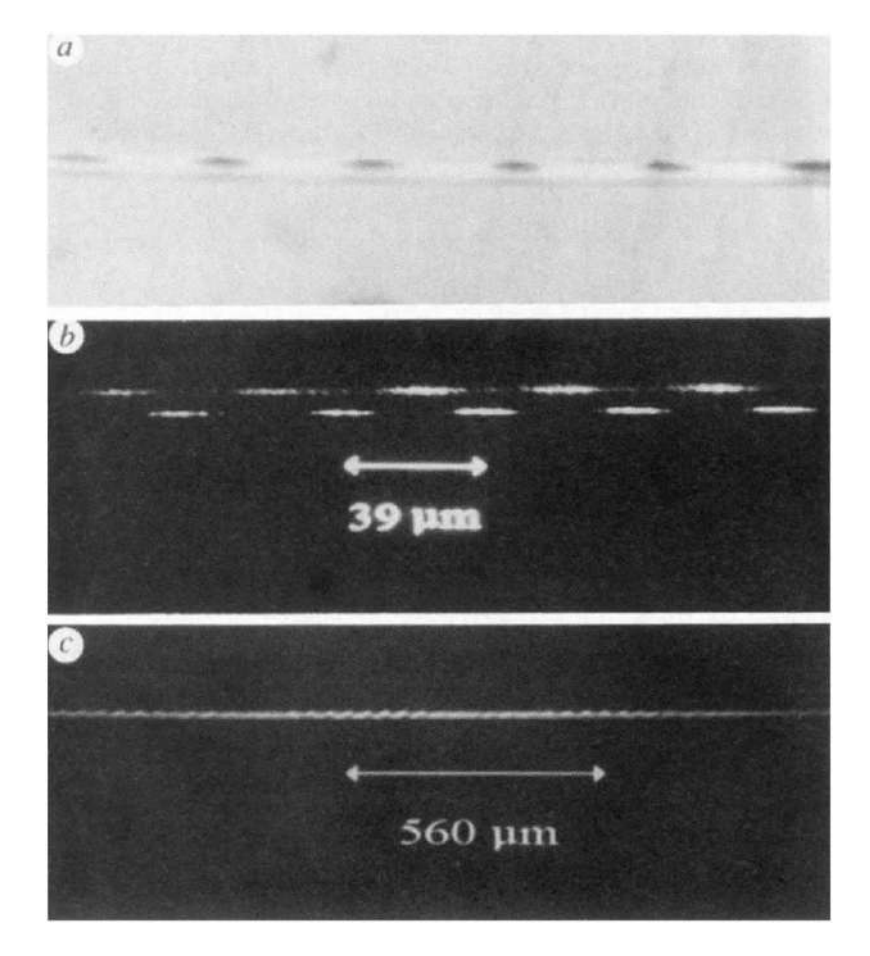
$$\chi^{(2)}(-2\omega; \, \omega, \, \omega) = 3\chi^{(3)}(-2\,\omega; \omega, \omega, 0).\, E_{DC}$$

Imaging the nonlinear grating in frequency-doubling fibres

W. Margulis*, F. Laurell* & B. Lesche‡

* Physics Department, Pontificia Universidade Católica do Rio de Janeiro, Rio de Janeiro, 22453–900, Brazil
† Physics II Department, Royal Institute of Technology, Stockholm, S10044, Sweden
‡ Physics Institute, Federal University of Rio de Janeiro, Rio de Janeiro, 21945–970, Brazil

NATURE · VOL 378 · 14 DECEMBER 1995

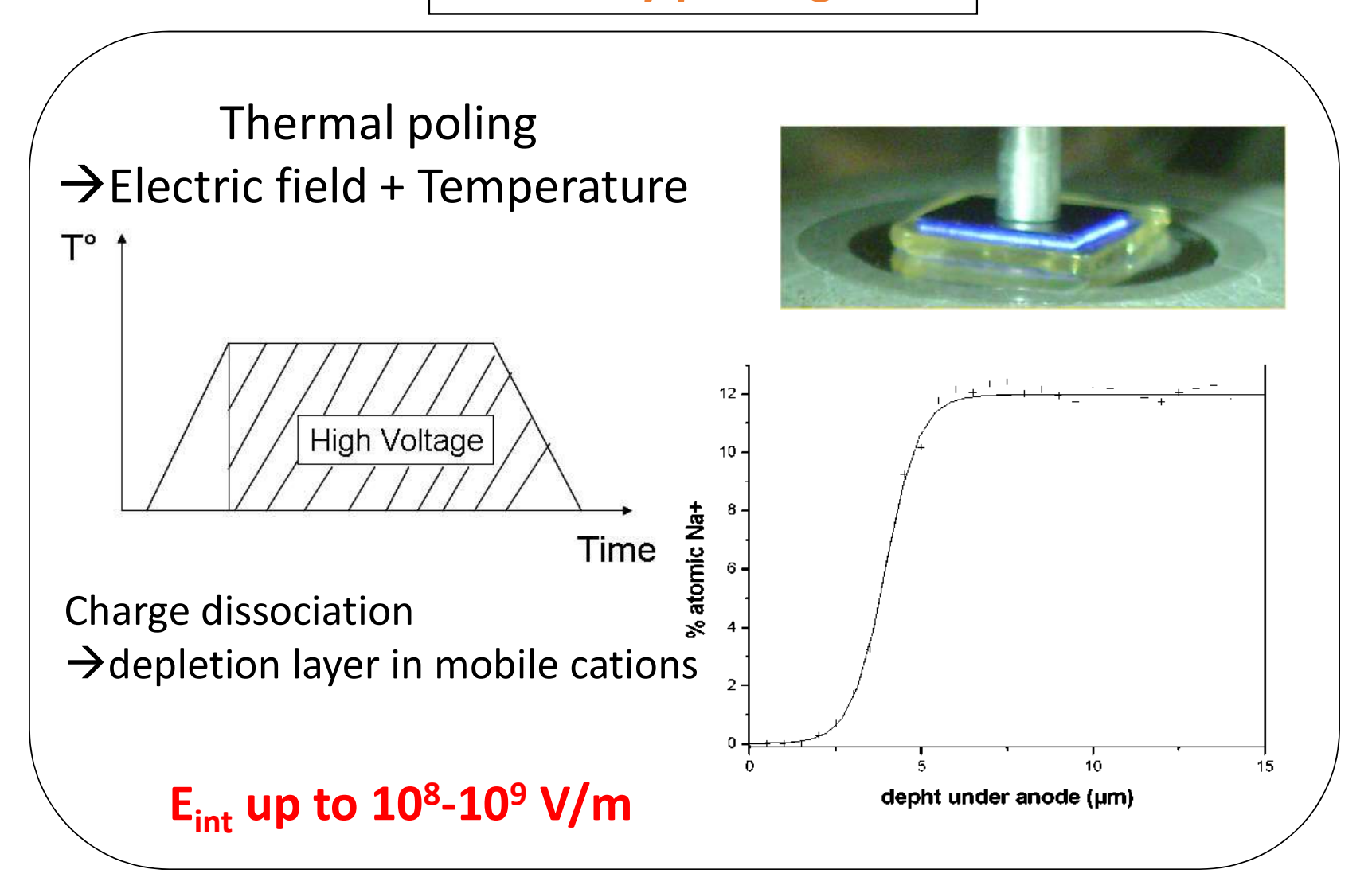


Second-order nonlinear gratings in frequency-doubling fibers revealed by chemical attack and observed using a phase-contrast microscope [94]

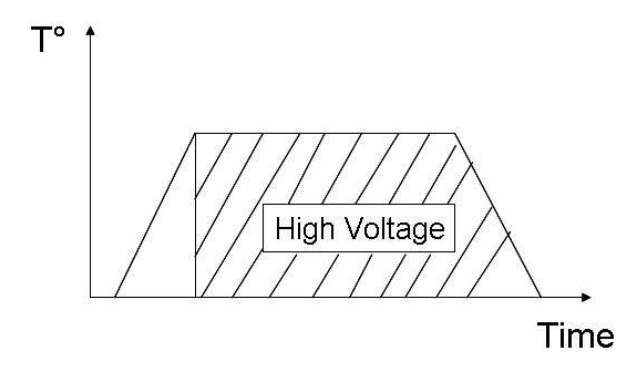
Nonlinear optical properties of glass

- Introduction non linear optics
- Characterization methods
- Third order optical response and glass chemistry
 - Two important third order optical process for applications:
 - Raman Gain
 - Supercontinuum generation
- Second order optical response in glass
 - Glass ceramic
 - Optical poling
 - Thermal poling

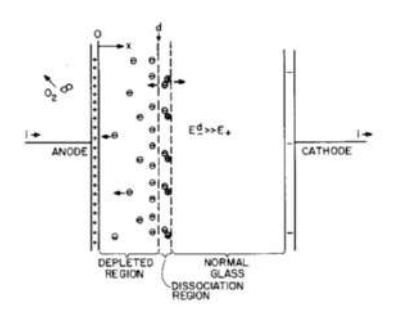
Thermally poled glasses



During the last century...



Poling Mechanisms



D. E. Carlson

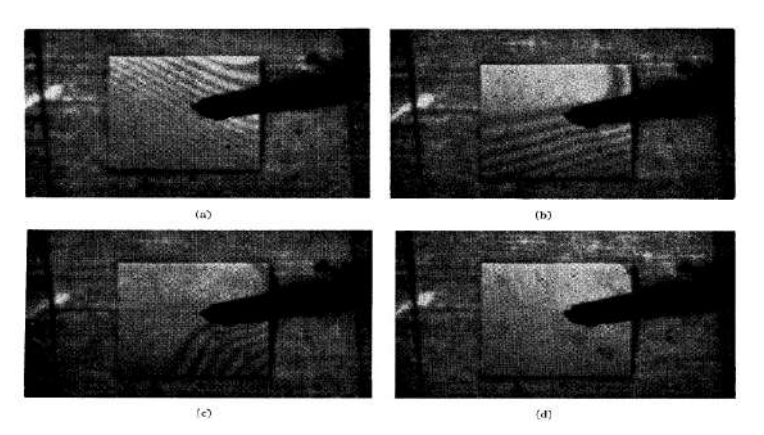
J. Amer. Ceram. Soc. 55-337-1972

J. Amer. Ceram. Soc. 57-291-1974

J. Amer. Ceram. Soc. 57-295-1974

J. Amer. Ceram. Soc. 57-461-1974

Anodic Bonding



G. Wallis, D. I. Pomerantz JAP 40-10 1969

Large second-order nonlinearity in poled fused silica

R. A. Myers, N. Mukherjee, and S. R. J. Brueck Center for High Technology Materials, University of New Mexico, Albuquerque, New Mexico 87131 Received July 15, 1991

Opt. Lett., 16 1732-1734 (1991).

Large second-order nonlinearity in poled fused silica

R. A. Myers, N. Mukherjee, and S. R. J. Brueck

Center for High Technology Materials, University of New Mexico, Albuquerque, New Mexico 87131

Received July 15, 1991

A large second-order nonlinearity [$\chi^{(2)}\sim 1$ pm/V $\sim 0.2~\chi_{22}^{(2)}$ for LiNbO₃] is induced in the near-surface ($\sim 4~\mu$ m) region of commercial fused-silica optical flats by a temperature (250–325°C) and electric-field ($E\sim 5\times 10^4$ V/cm) poling process. Once formed, the nonlinearity, which is roughly 10^3-10^4 times larger than that found in fiber second-harmonic experiments, is extremely stable at room temperature and laboratory ambient. The nonlinearity can be cycled by repeated depoling (temperature only) and repoling (temperature and electric field) processes without history effects. Possible mechanisms, including nonlinear moieties and electric-field-induced second-order nonlinearities, are discussed.

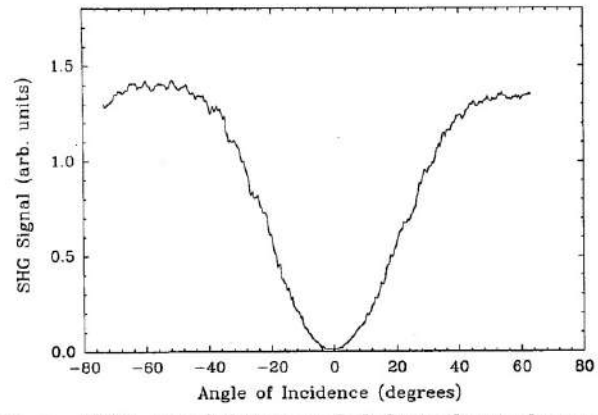


Fig. 1. SHG signal from a poled Optosil sample versus the angle of incidence for a TM-polarized fundamental beam at 1.06 μ m.

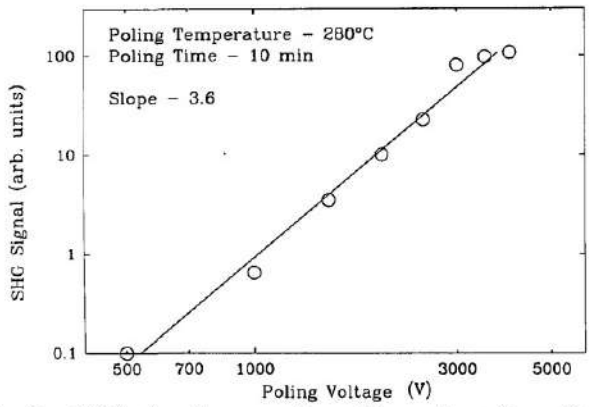


Fig. 2. SHG signal versus the poling voltage for a fixed temperature and poling time. The signal was obtained on a single sample with successive polings at higher poling voltages.

Thermally poled glass: frozen-in electric field or oriented dipoles?

P.G. Kazansky, P.St.J. Russel

Optoelectronics Research Centre, University of Southampton, Southampton S09 5NH, UK

Received 25 February 1994; revised manuscript received 24 May 1994

Abstract

Evidence that a frozen-in space charge field causes the appearance of high quadratic nonlinearities in thermally poled glass is obtained from experimental tests of the ratio of nonlinear tensor components and the spatial distribution of the induced $\chi^{(2)}$. A mechanism to explain the fixation of the $\chi^{(2)}$ near the anodic surface is proposed.

$$\chi^{(2)} \approx 3\chi^{(3)}.E_{dc} + \frac{Np\beta}{5k_bT}.E_{loc}$$

PHYSICAL REVIEW A, VOLUME 65, 043816

Model of charge migration during thermal poling in silica glasses: Evidence of a voltage threshold for the onset of a second-order nonlinearity

Yves Quiquempois*

Université des Sciences et Technologies de Lille, Laboratoire de Physique des Lasers, Atomes et Molécules, Bâtiment P5, 59655 Villeneuve d'Ascq Cedex, France

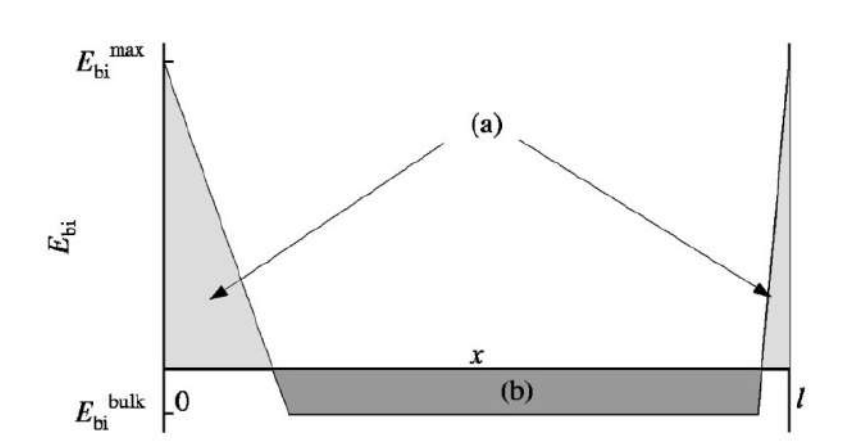
Nicolas Godbout

ITF Optical Technologies, 45, Montpellier, Saint-Laurent (Québec), Canada H4N 2G3

Suzanne Lacroix

Laboratoire des Fibres Optiques, Département de Génie Physique, École Polytechnique de Montréal, Code Postal 6079, Succursale Centreville, Montréal (Québec), Canada H3C 3A7 (Received 16 November 2001; published 4 April 2002)

T. M. Proctor and P. M. Sutton, "Static Space-Charge Distributions With a Single Mobile Charge Carrier," *J. Chem. Phys.*, 30 212 (1959).

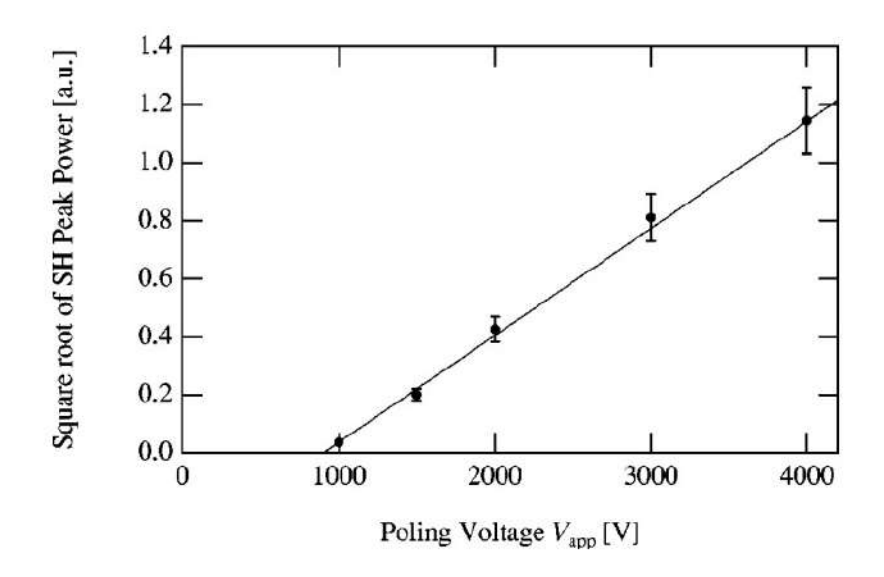


$$\frac{\partial p}{\partial t} = D \frac{\partial^2 p}{\partial x^2} - \mu \frac{\partial (Ep)}{\partial x} + q - a,$$

$$\frac{\partial n}{\partial t} = q - a,$$

$$\frac{\partial E}{\partial x} = \frac{e}{\epsilon} (p - n),$$

$$E(x) = \sqrt{\frac{2c_0e}{\epsilon}(V_{\text{app}} - V_t) + (E_t)^2 - \frac{c_0e}{\epsilon}x}.$$



September 15, 2002 / Vol. 27, No. 18 / OPTICS LETTERS

643

Integrated fiber Mach-Zehnder interferometer for electro-optic switching

M. Fokine, L. E. Nilsson, Å. Claesson, D. Berlemont, L. Kjellberg, L. Krummenacher, and W. Margulis

Acreo, Electrum 236, SE-164 40 Kista, Sweden

Received February 19, 2002

Molten alloys under high pressure were used to obtain fibers with long internal electrodes that are solid at room temperature. An integrated Mach–Zehnder interferometer was constructed from a twin-core twin-hole fiber that permitted application of an electric field preferentially to one of the cores. Good stability and a switching voltage of 1.4 kV were measured with a 1-m-long fiber device with a quadratic voltage dependence. © 2002 Optical Society of America

OCIS codes: 060.4370, 190.4360.

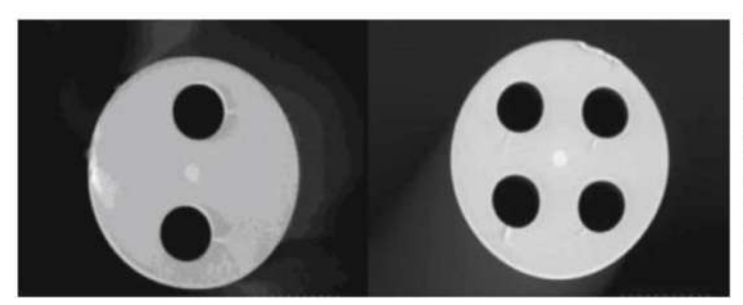


Fig. 6.21
Example of a microstructured optical fiber designed for electrical poling. In black: the holes for electrode insertion; in white the core of the fiber. Reprinted from [6.128]

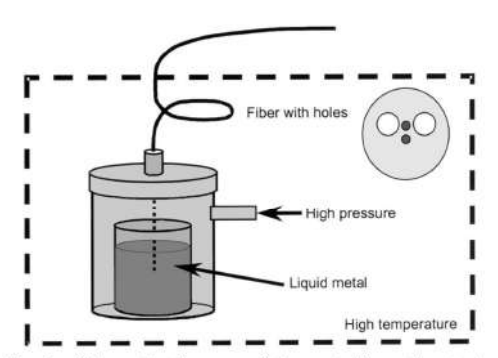
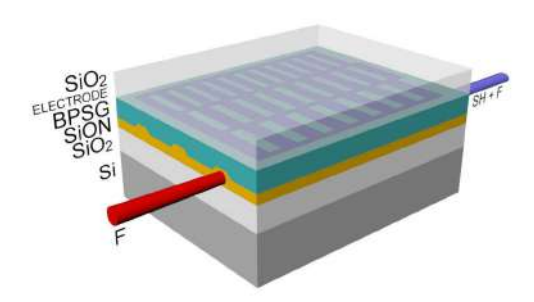


Fig. 1. Schematic diagram of the metal-insertion technique. The fiber cross section is also shown.

Planar glass devices for efficient periodic poling

Jacob Fage-Pedersen, Rune Jacobsen, and *Martin Kristensen

Research Center COM, Technical University of Denmark, building 345V,
DK-2800 Kgs. Lyngby, Denmark
*Present address: Department of Physics and Astronomy, University of Aarhus,
DK-8000 Århus C, Denmark
fage@com.dtu.dk



2005 / Vol. 13, No. 21 / OPTICS EXPRESS 8514

Second order optical properties in niobate amorphous thin films

Electric field induced second order optical response

$$\chi^{(2)} = 3\chi^{(3)}E$$

OPTICS LETTERS / Vol. 16, No. 22 / November 15, 1991

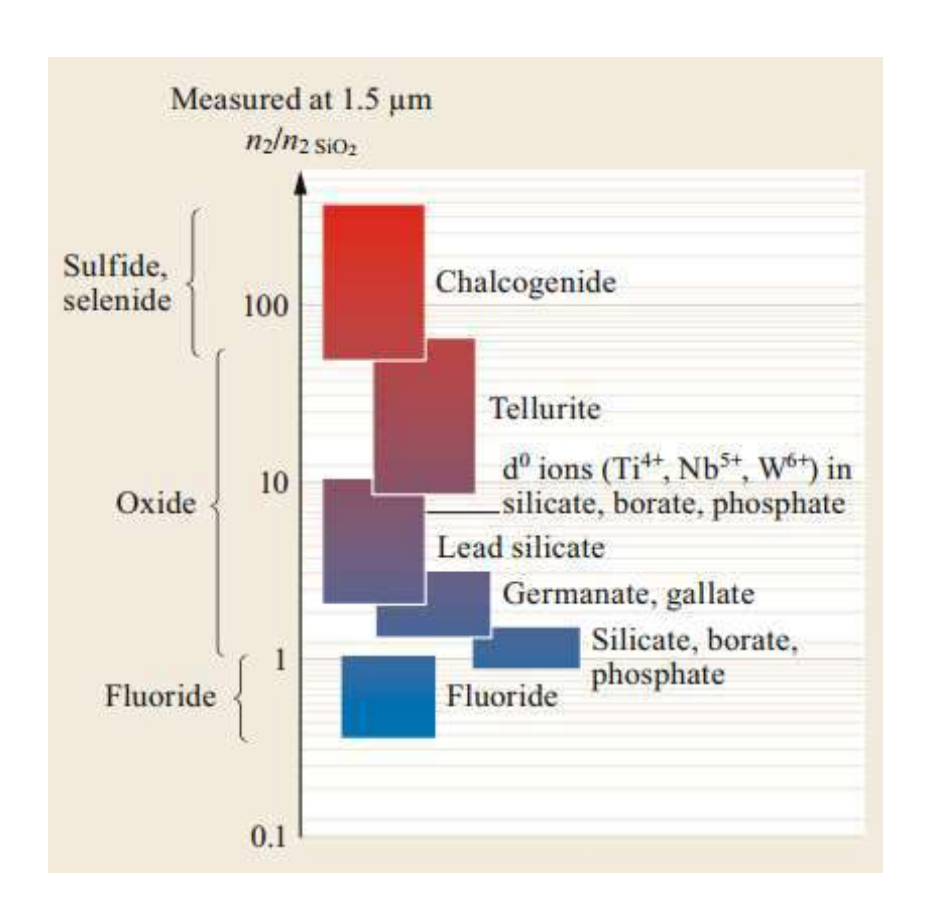
Large second-order nonlinearity in poled fused silica

R. A. Myers, N. Mukherjee, and S. R. J. Brueck

Center for High Technology Materials, University of New Mexico, Albuquerque, New Mexico 87131

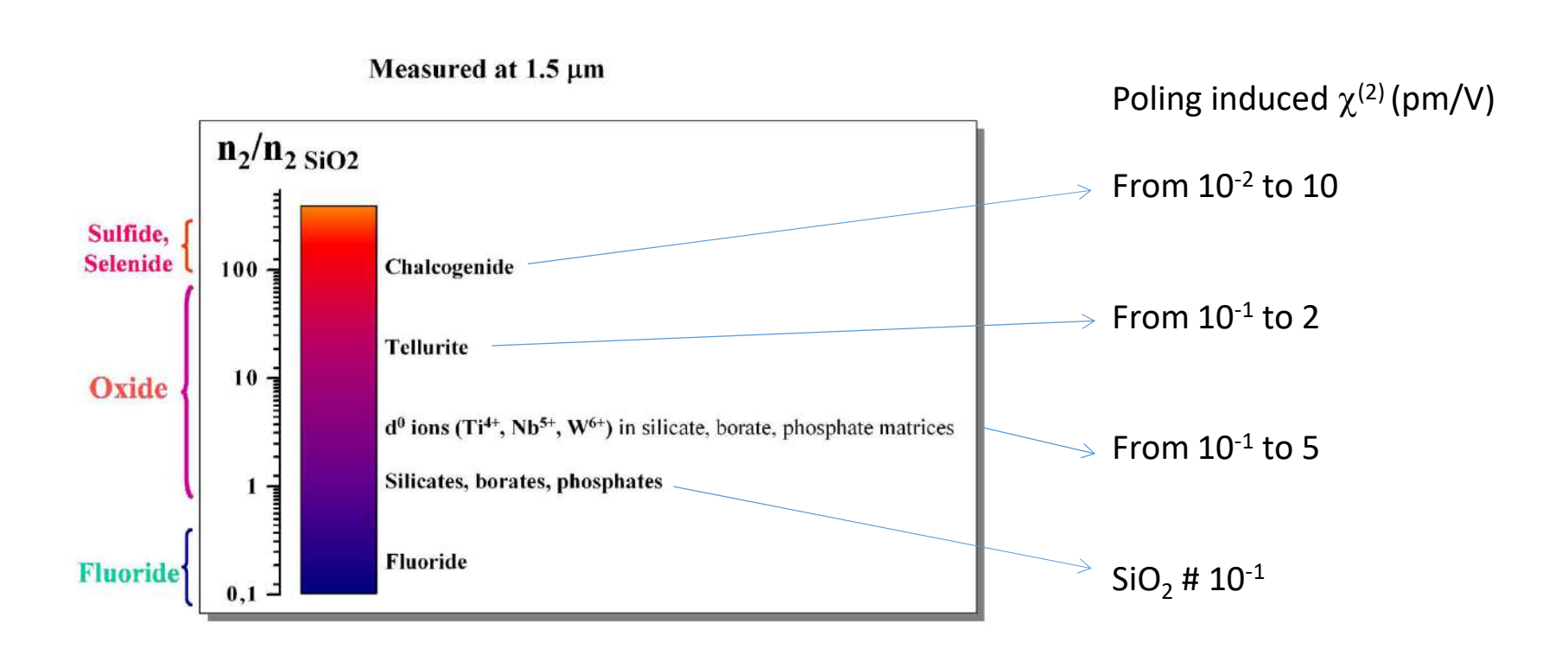
$$\chi^{(2)} = 0.1 \text{ pm/V}$$

Recall, LiNbO₃: $\chi^{(2)} \approx 60 \text{ pm/V}$

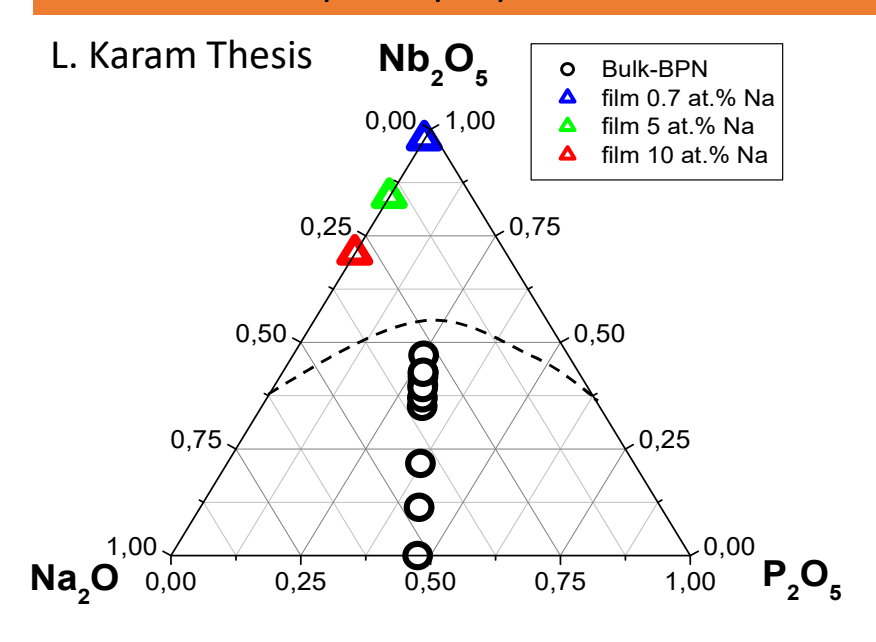


M. Dussauze, T. Cardinal, Springer Handbook. Glass 2019

Which family of Thermally poled glasses?



Second order optical properties in niobate amorphous thin films



bpn45
bpn45
bpn45
bpn45
bpn45
bpn45
bpn47-bpn35
bpn43-bpn35
-O-bpn40-bpn35

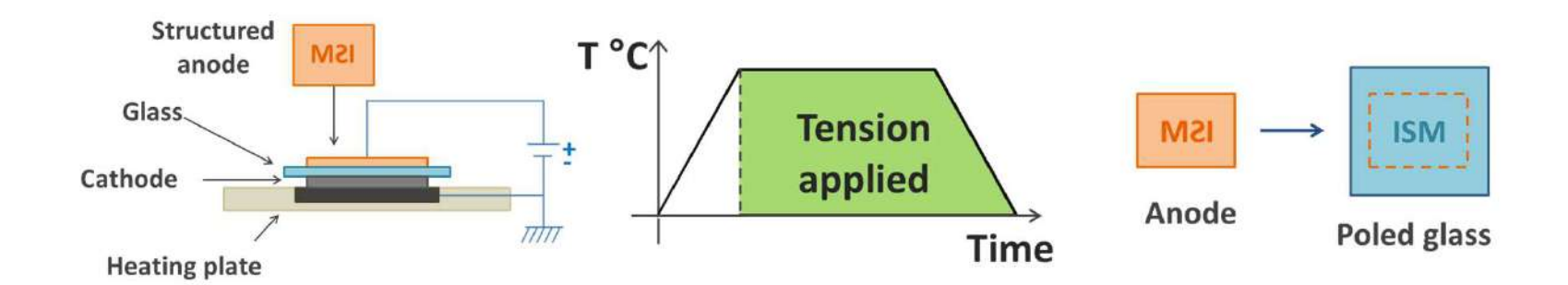
500 600 700 800 900 1000110012001300
cm⁻¹

Table 1
Results obtained from best fits to experimental data for bpn glasses

	$n_{ m 1064nm} \\ \pm 0.01$	$n_{532\mathrm{nm}} \pm 0.01$	$\langle \chi^{(2)} \rangle$ (pm/V) ± 0.1	$L~(\mu{ m m}) \ \pm 0.1$
Bpn35	1.73	1.82	0.16	3.2
Bpn40	1.76	1.84	1.3	4.2
Bpn45	1.86	1.93	2.8	4.3
Bpn47	1.91	1.99	3.6	3.7
Bpn48	1.93	2.02	4.2	3.2

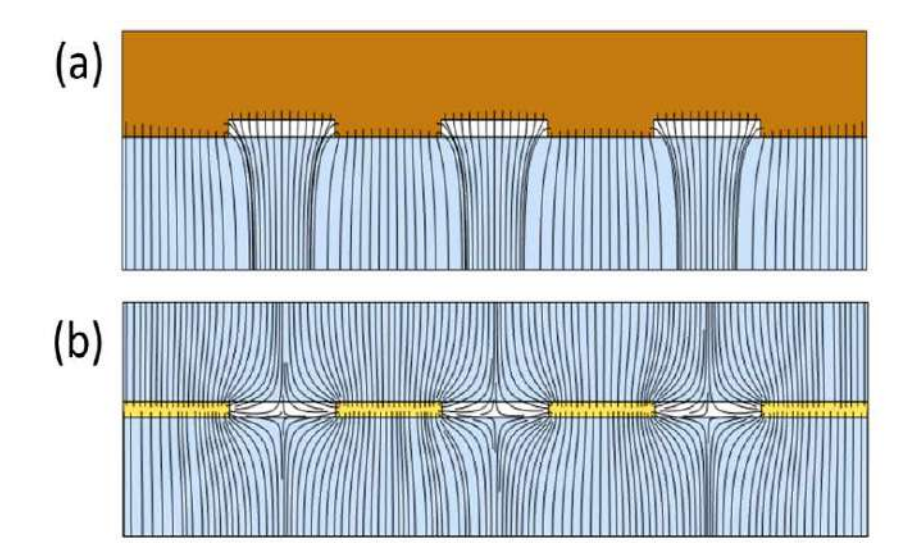
Opt. Materials 2006

Micro-imprinting by thermal poling



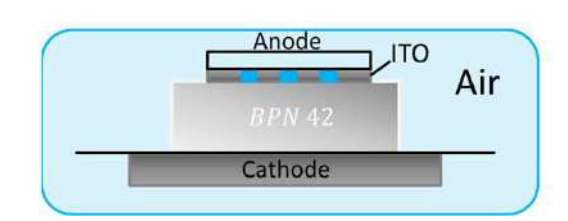


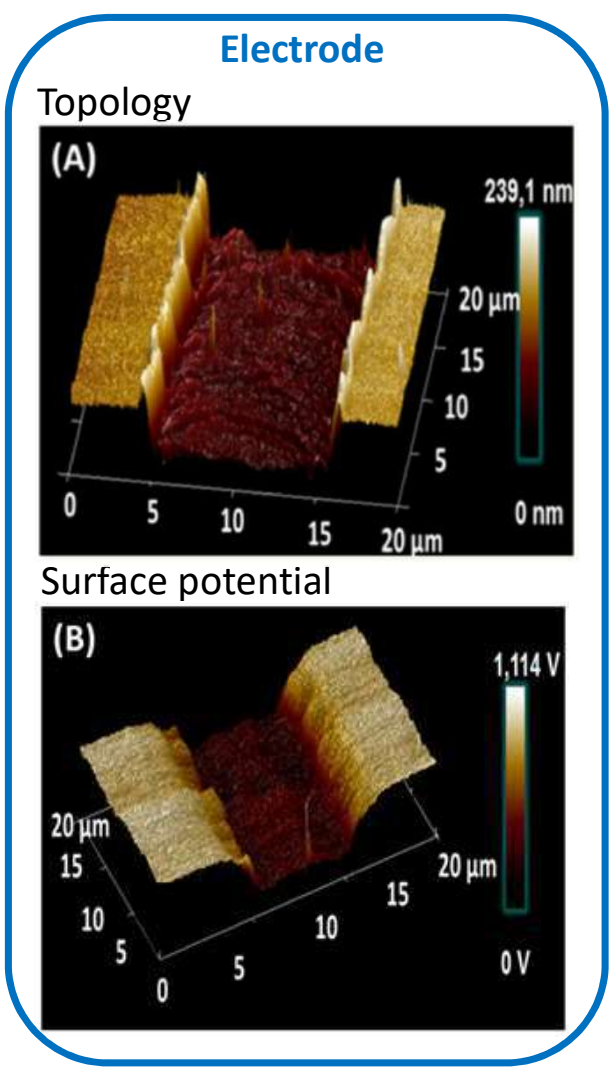


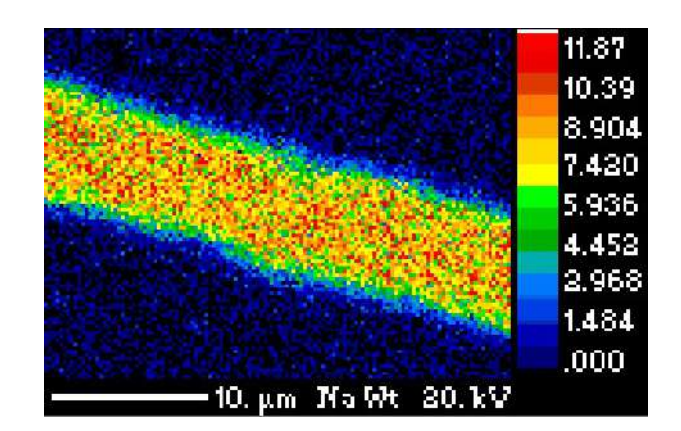


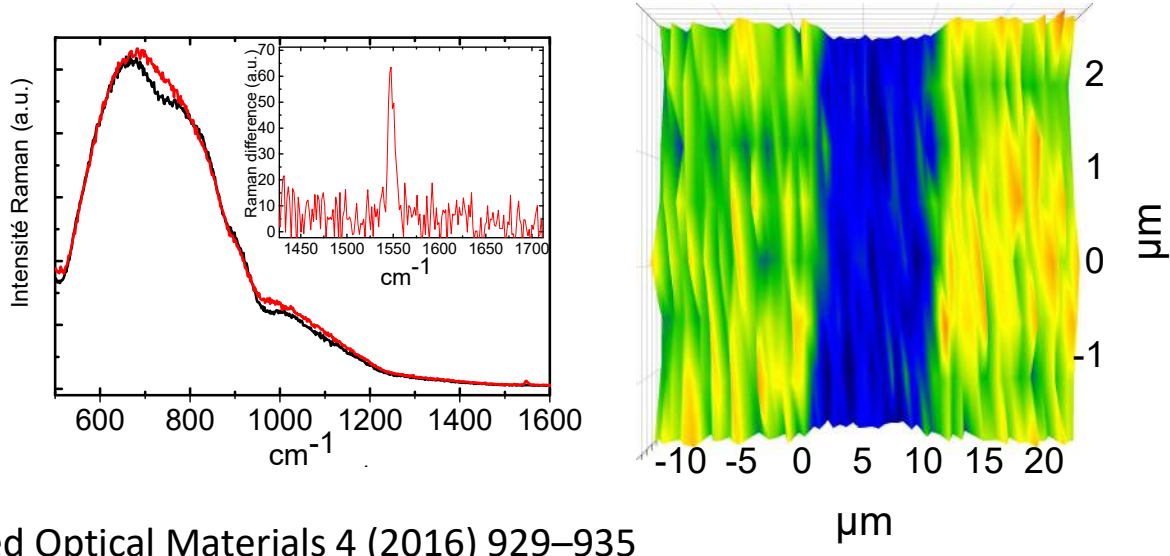
Micro-imprinting by thermal poling

 \rightarrow 0,58 (0,95 NaPO₃ + 0,05 Na₂B₄O₇) + 0,42Nb₂O₅



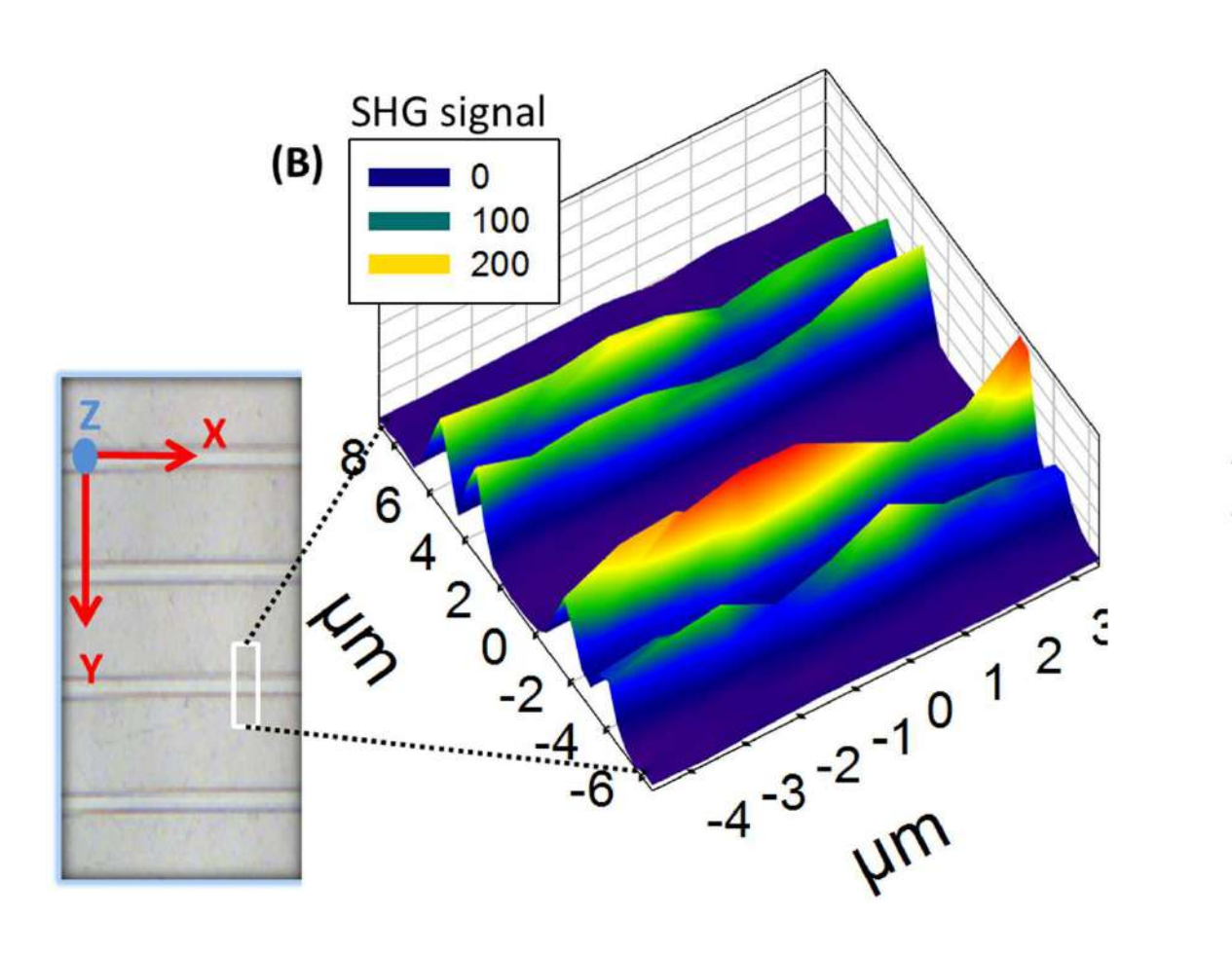


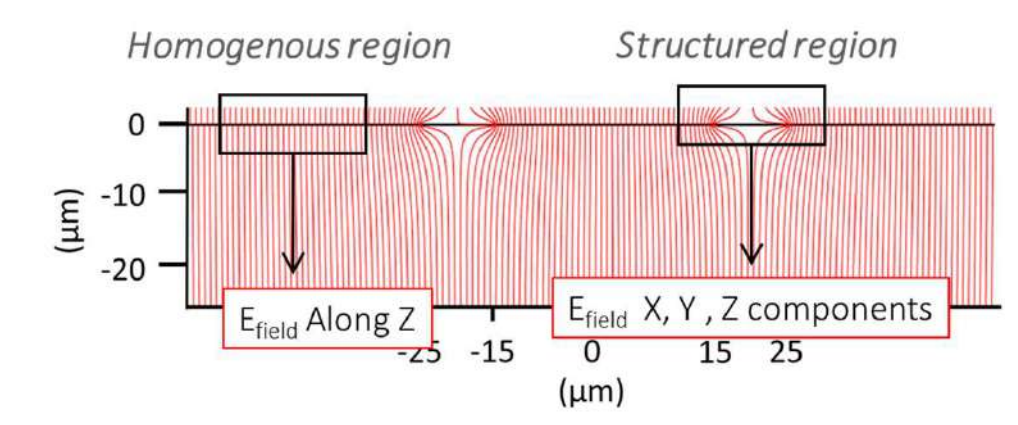




Advanced Optical Materials 4 (2016) 929–935

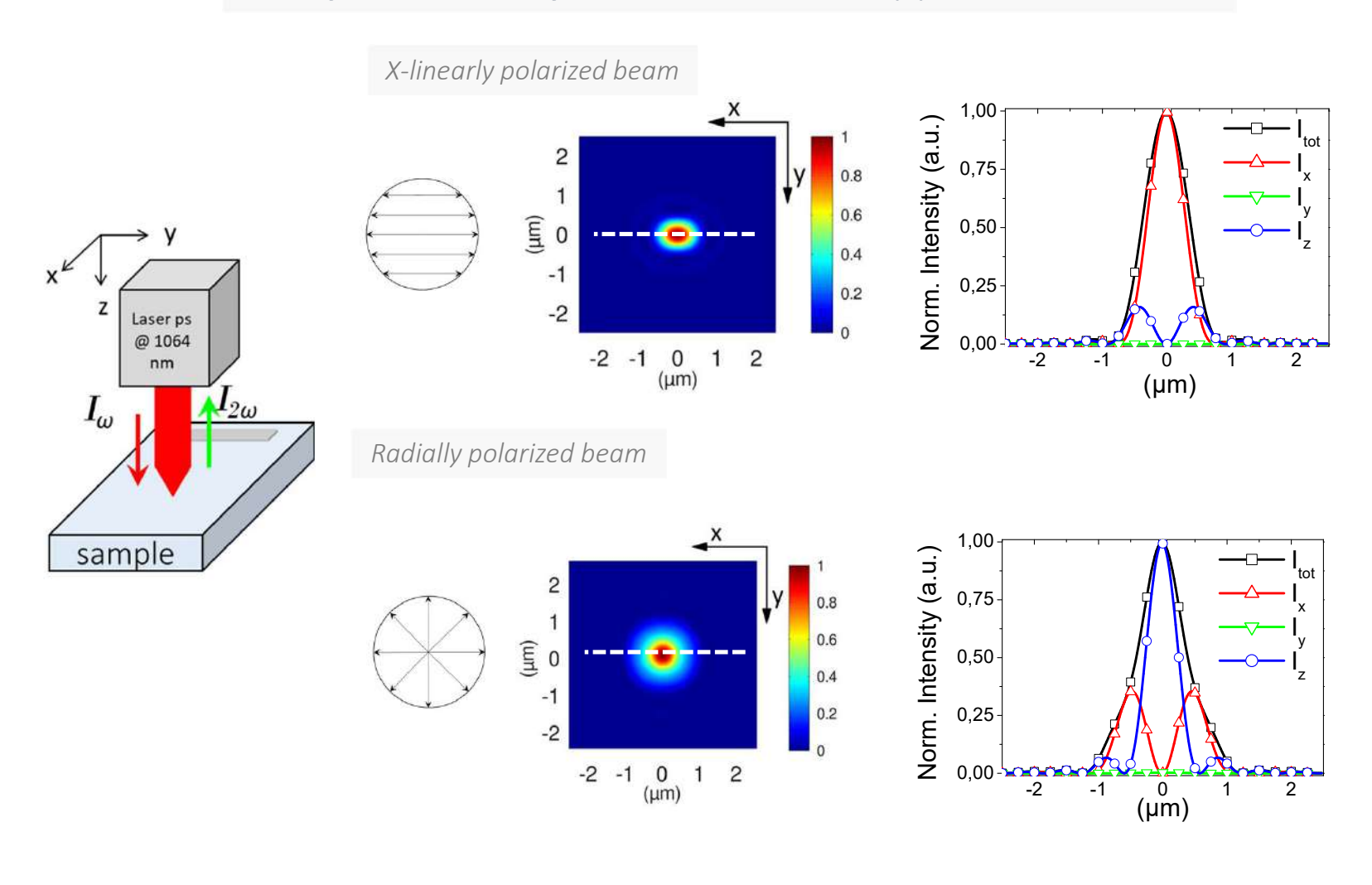
Micro-imprinting by thermal poling

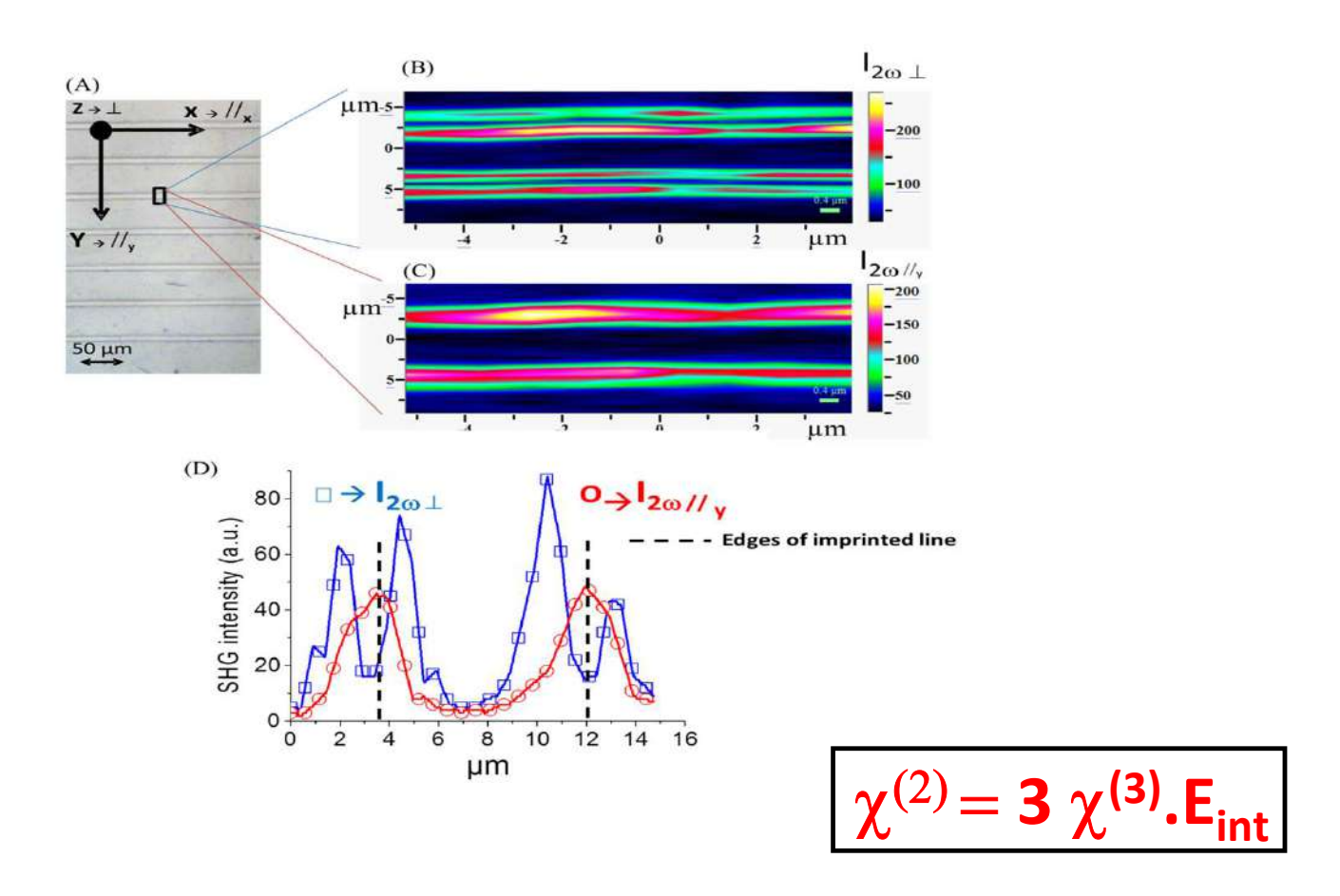




Advanced Optical Materials 4 (2016) 929–935

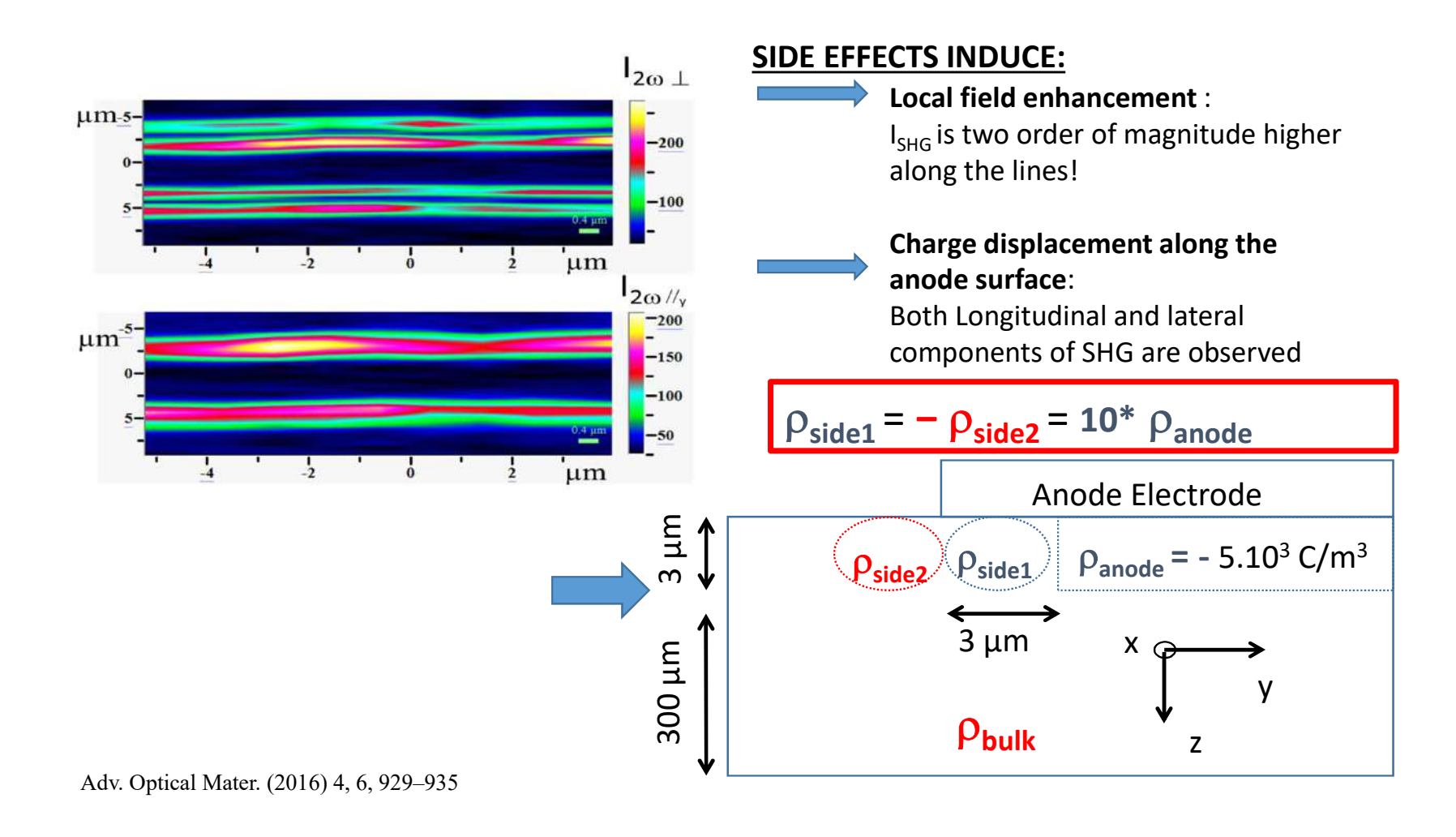
Confocal SHG reflectance microscopy, 100X NA=0.9

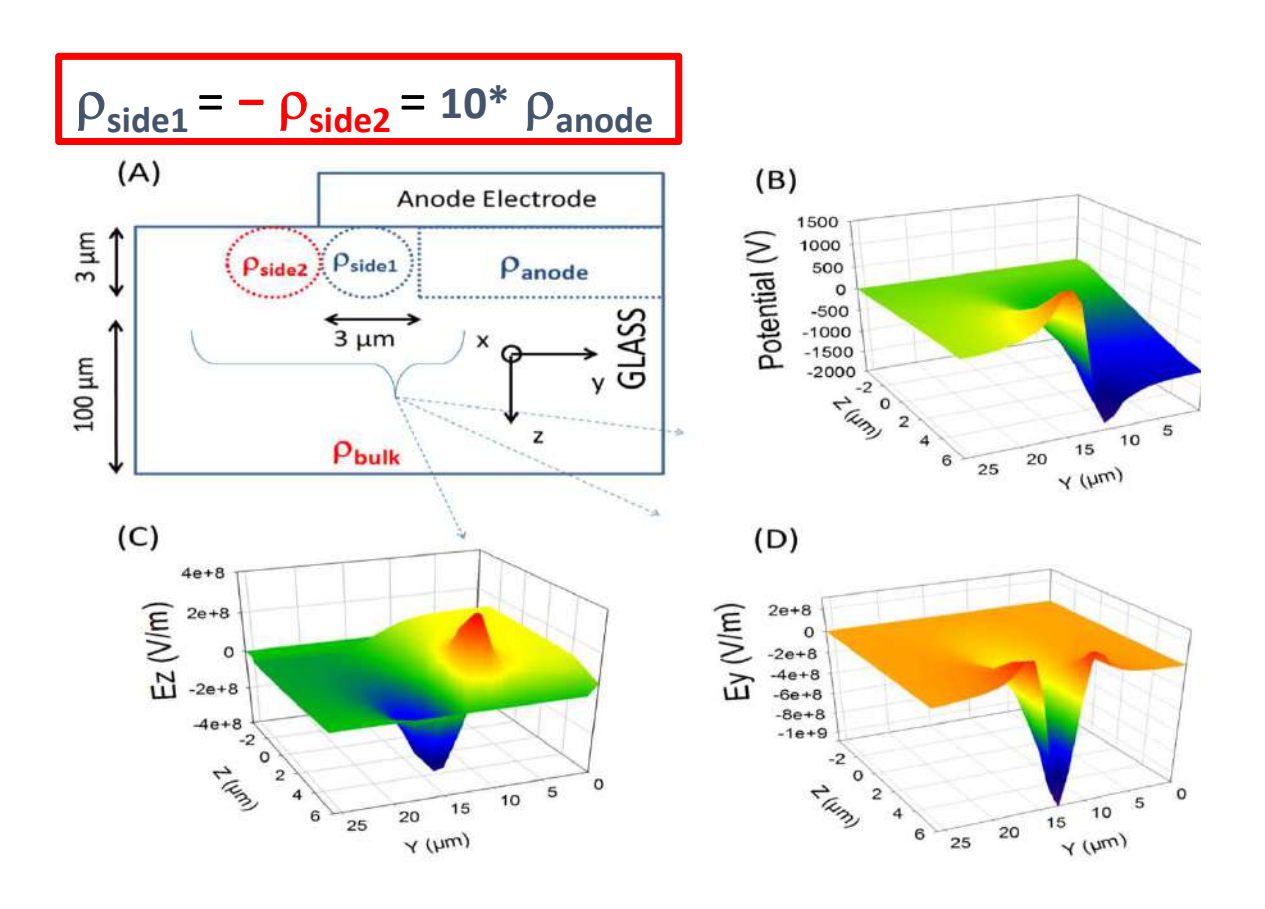




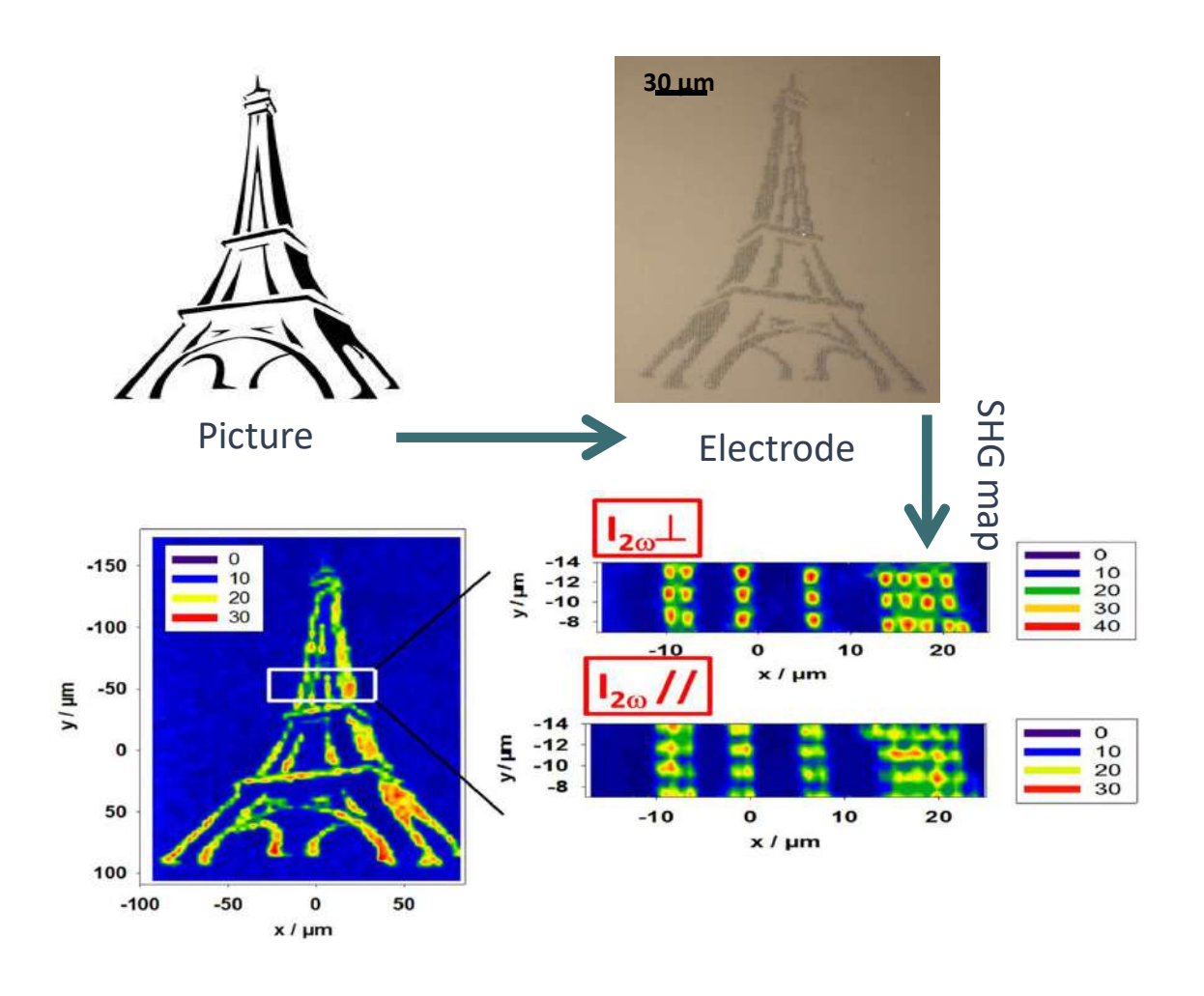
→ Geometry control and Micrometric localization of the SHG response

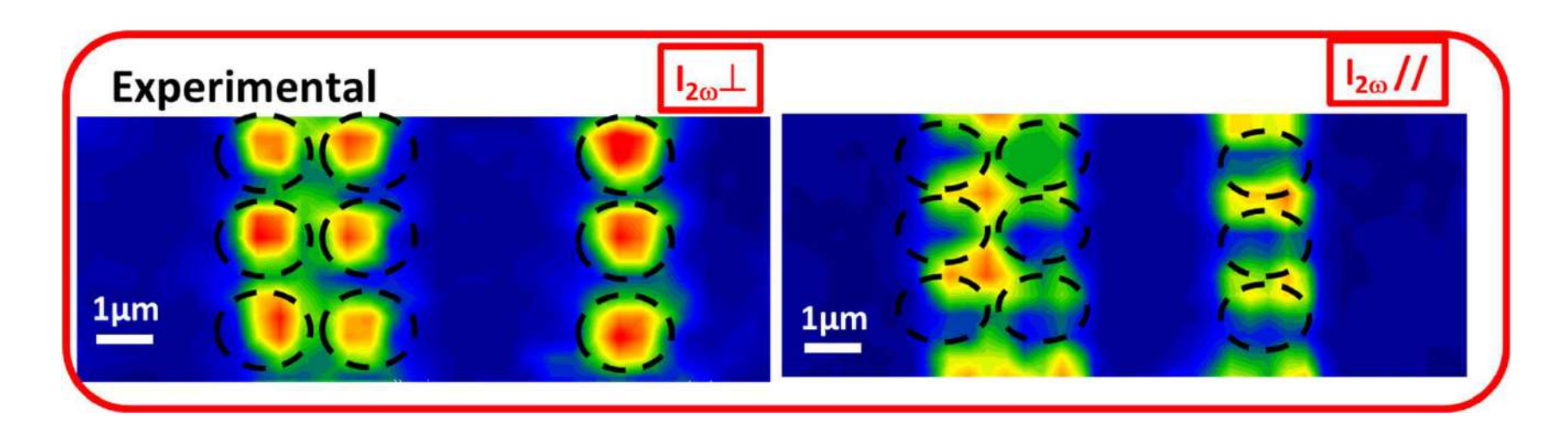
Adv. Optical Mater. (2016) 4, 6, 929-935

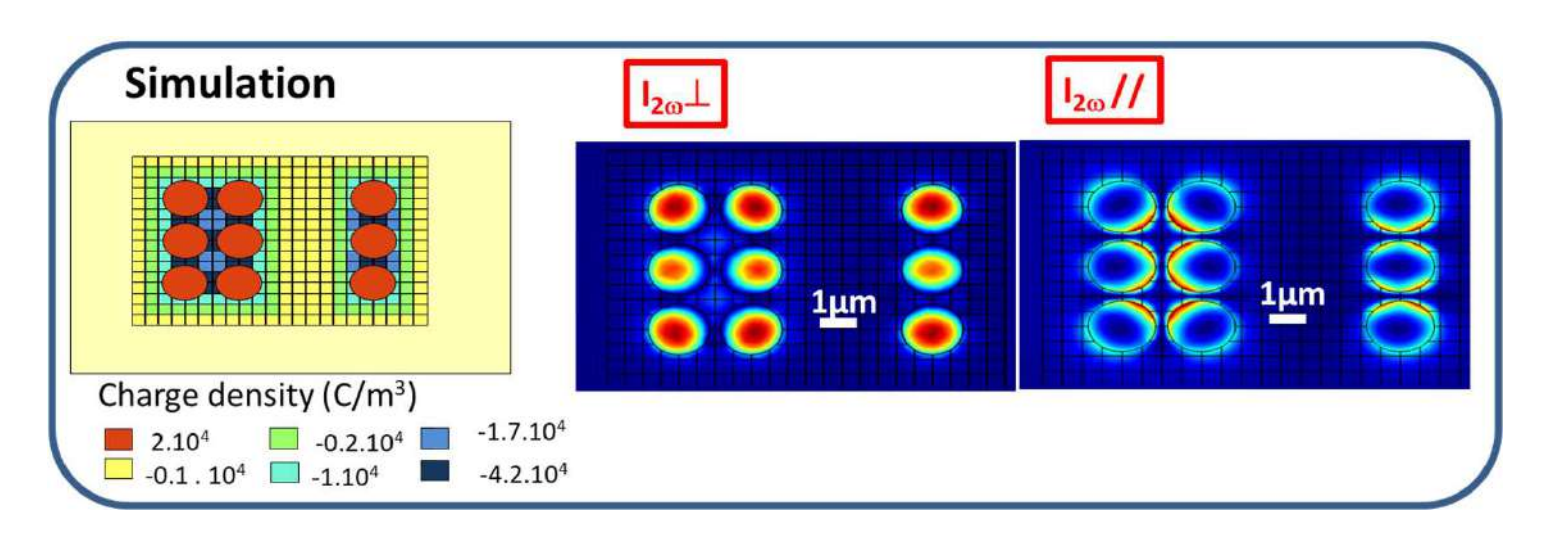




Adv. Optical Mater. (2016) 4, 6, 929-935

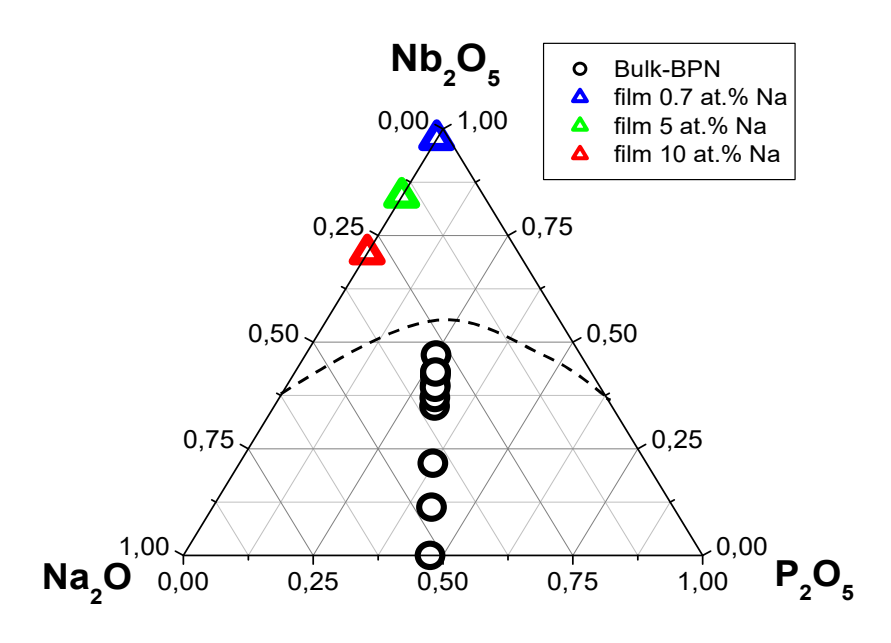






Second order optical properties in niobate **amorphous** thin films

L. Karam Thesis





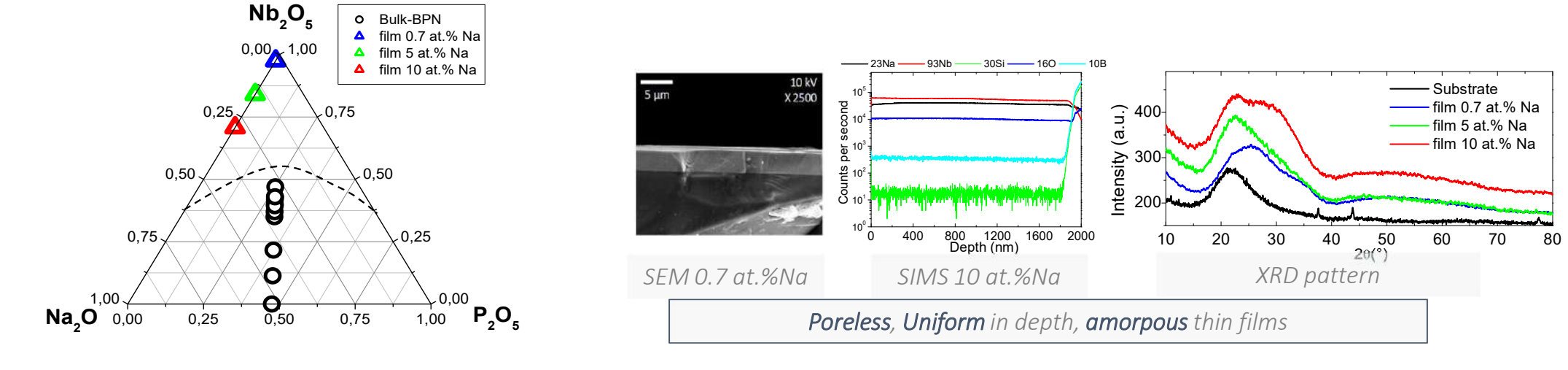
Bulk glass synthesis Liquid to solid in few seconds ~1000 °C to ~20 °C

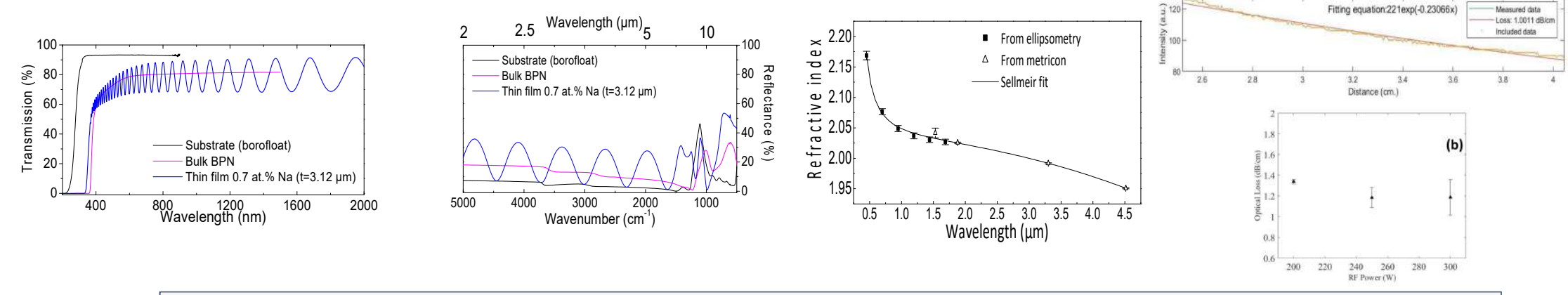


Sputtered film Plasma to solid ~10¹⁶ °C/s

Second order optical properties in niobate amorphous thin films

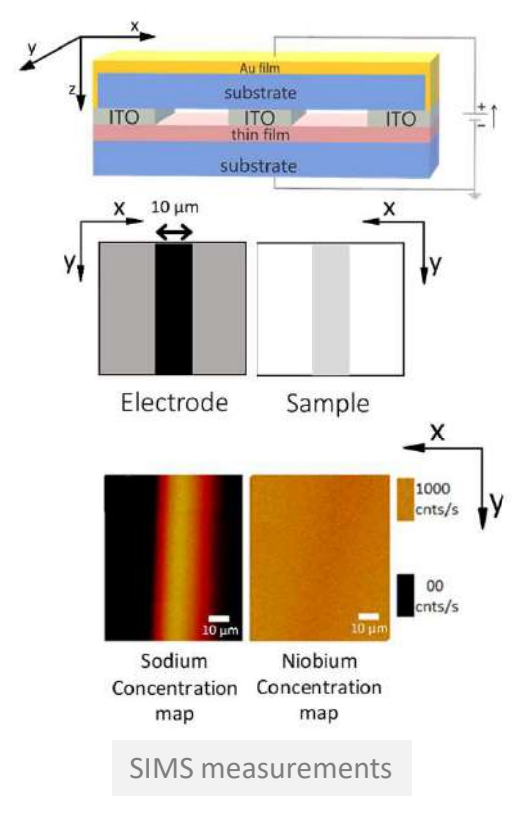
L. Karam Thesis

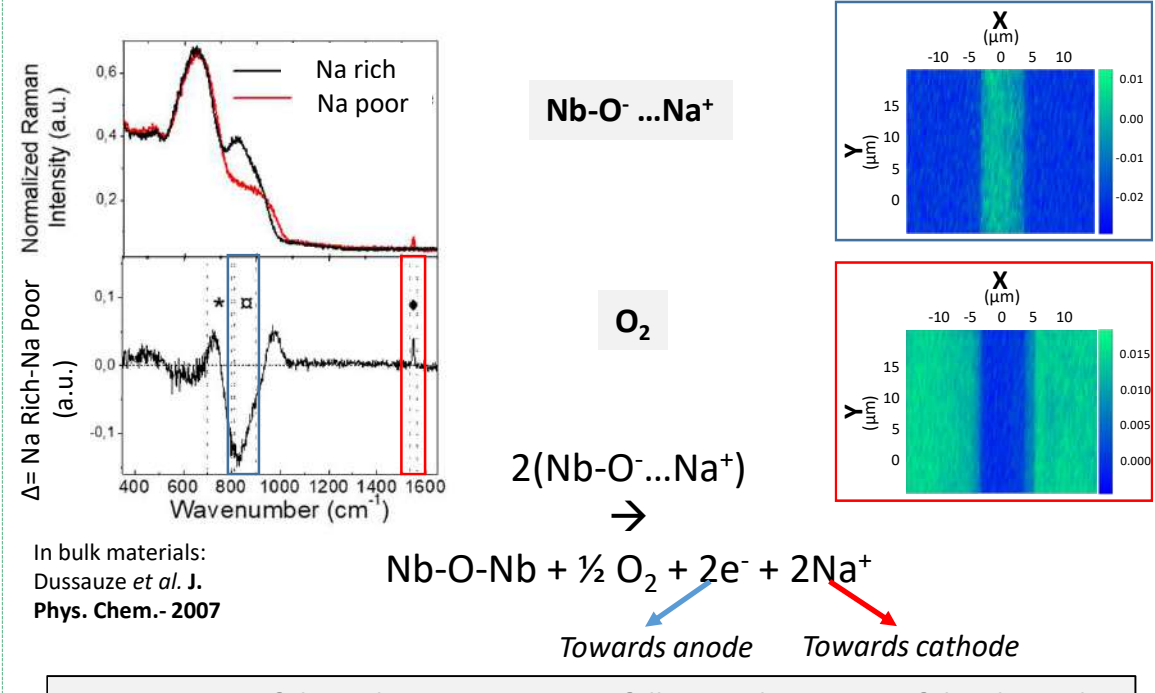




Tranparent from visible to midIR (0.35~6 μm), high refractive index (2.03-2.19 @1550 nm), Guiding Losses 1dB/cm @1550nm)

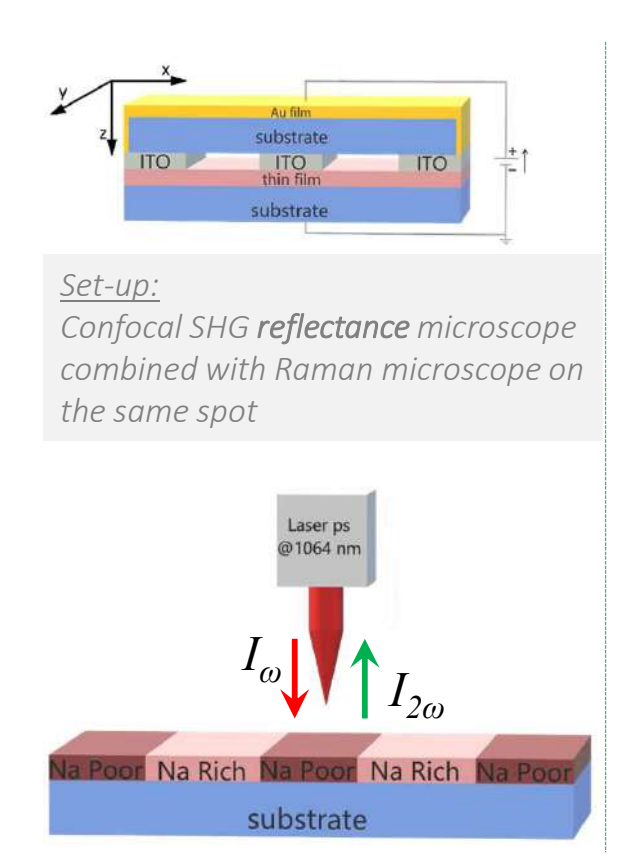
Second order optical properties in niobate thin films

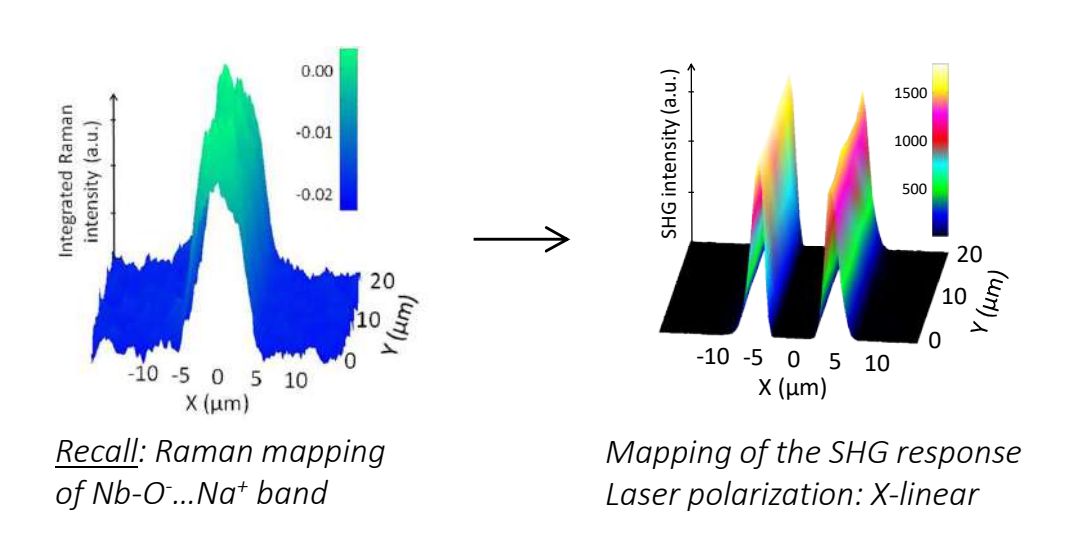




- o Structuring of the sodium concentration following the pattern of the electrode
- o Spatial homogeneity of the structural rearrangements
- o Polarization mechanisms similar to those observed in bulk materials

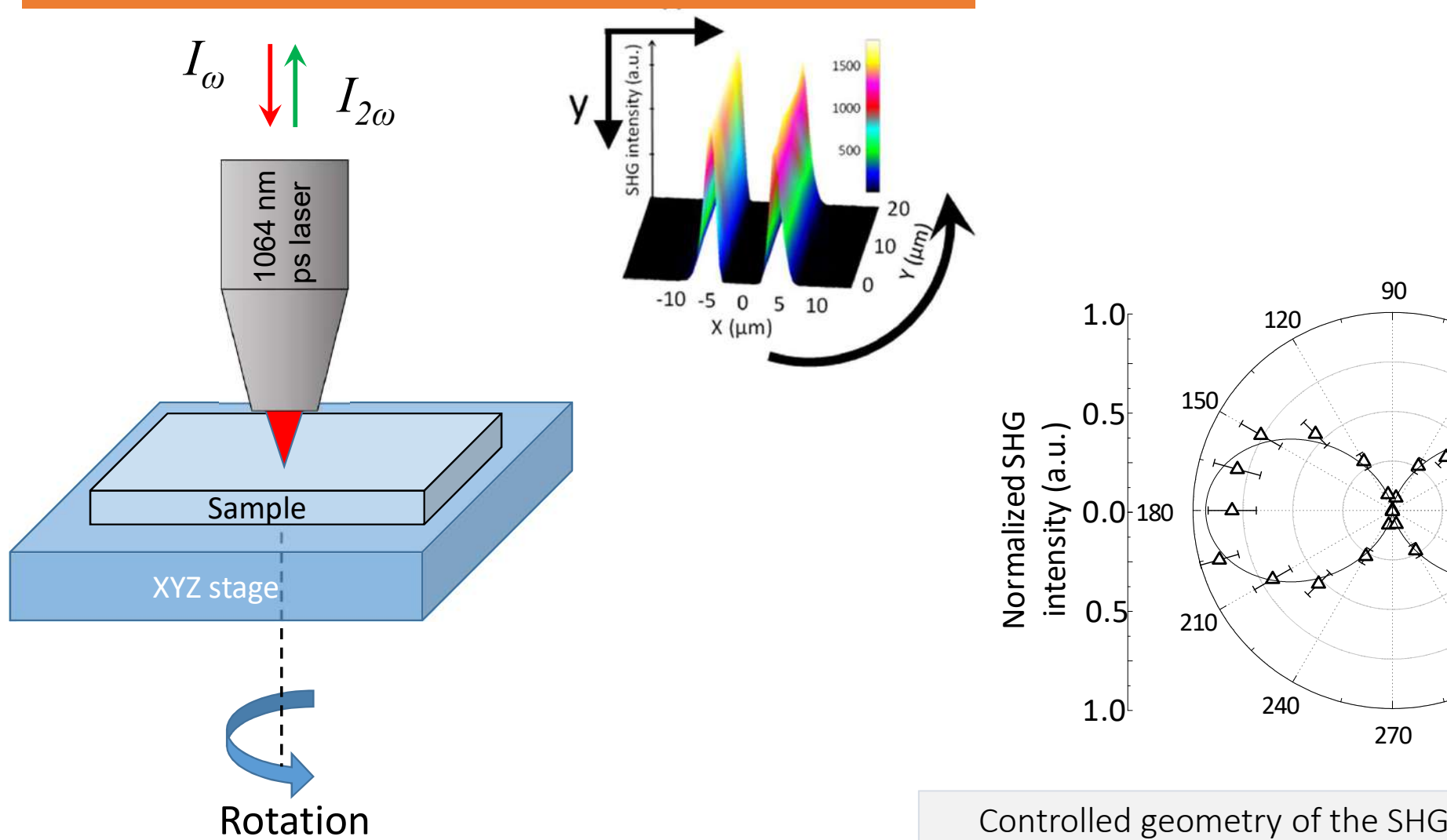
Second order optical properties in niobate thin films





Response **localized** on a **few microns** at the Na Rich / Na Poor **frontier**

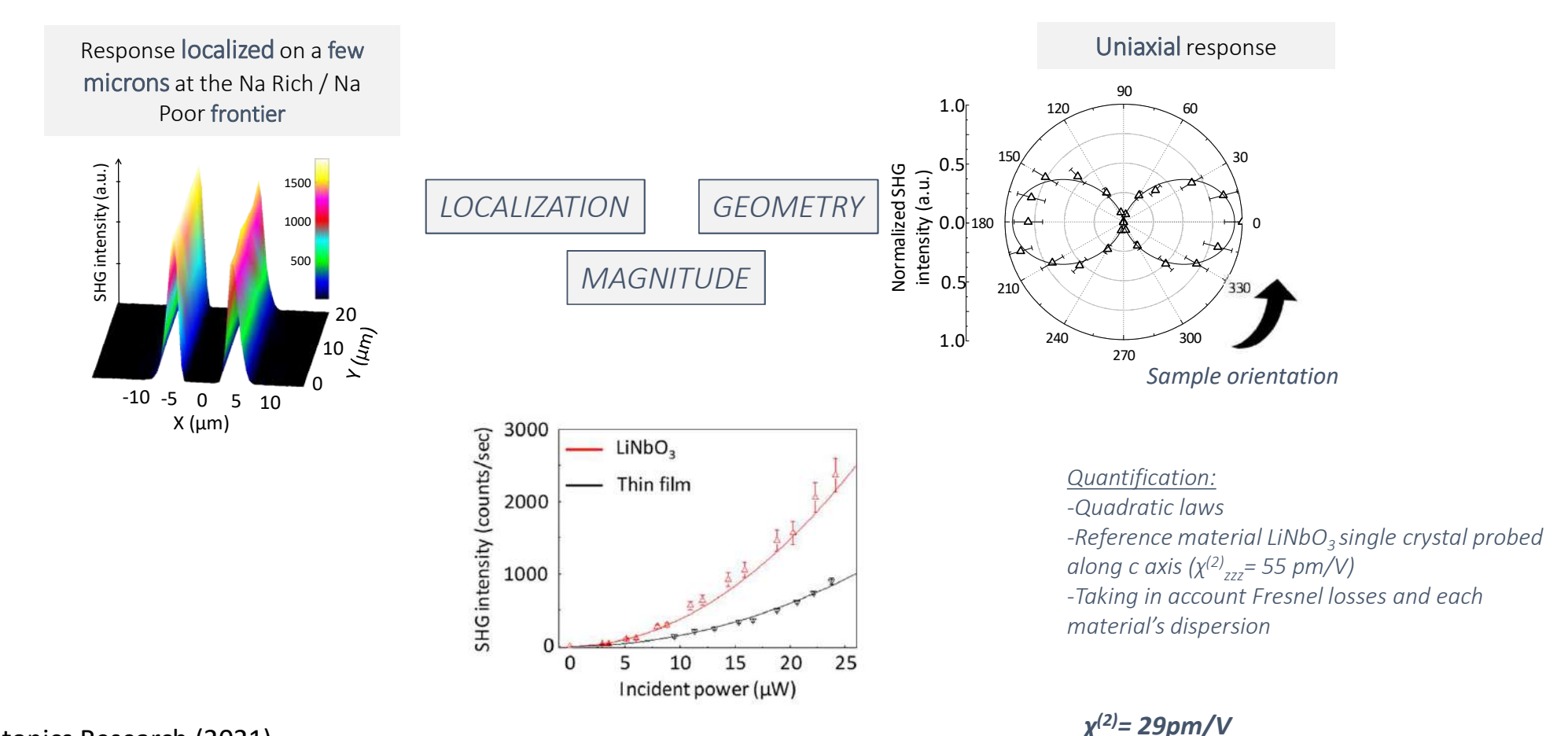
Second order optical properties in niobate amorphous thin films



Controlled geometry of the SHG response: uniaxial response

Second order optical properties in niobate thin films

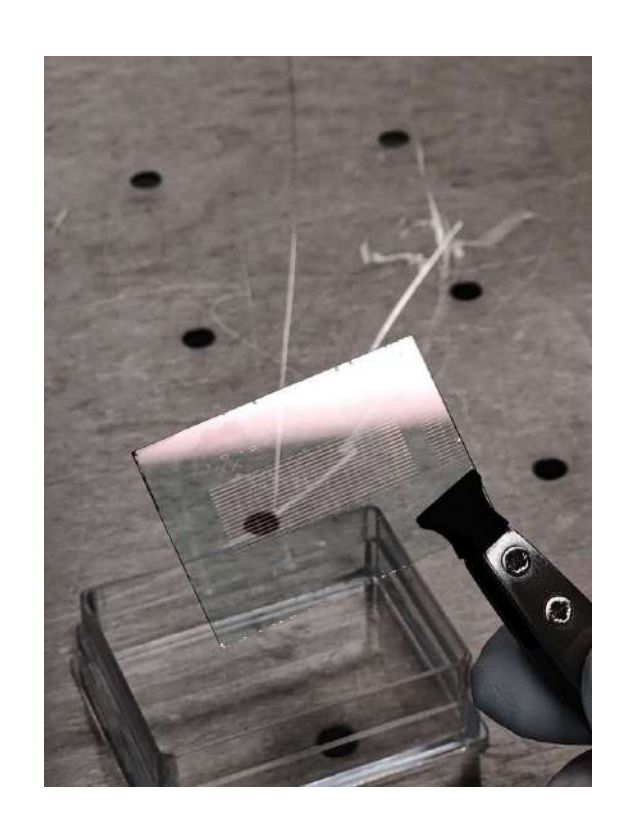
L. Karam Thesis

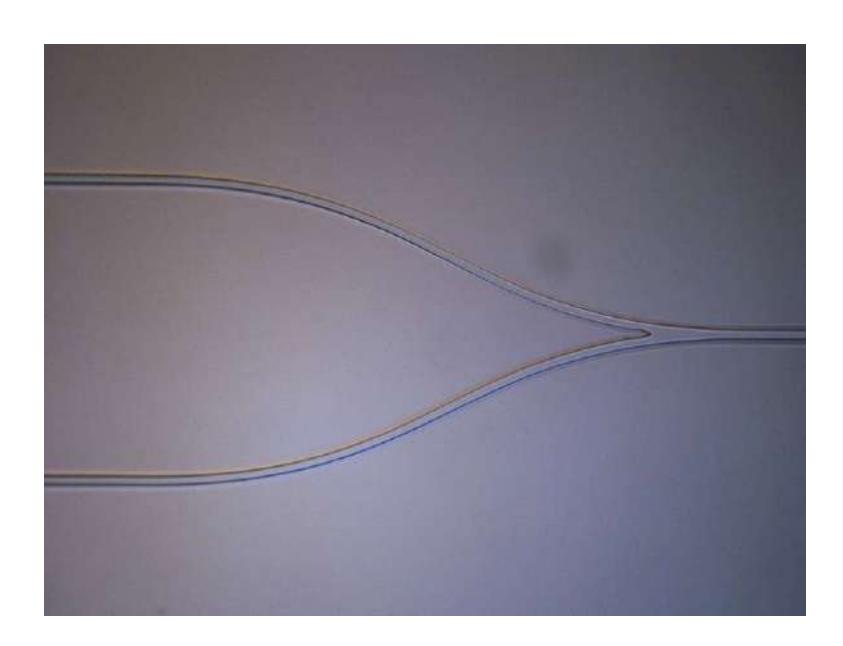


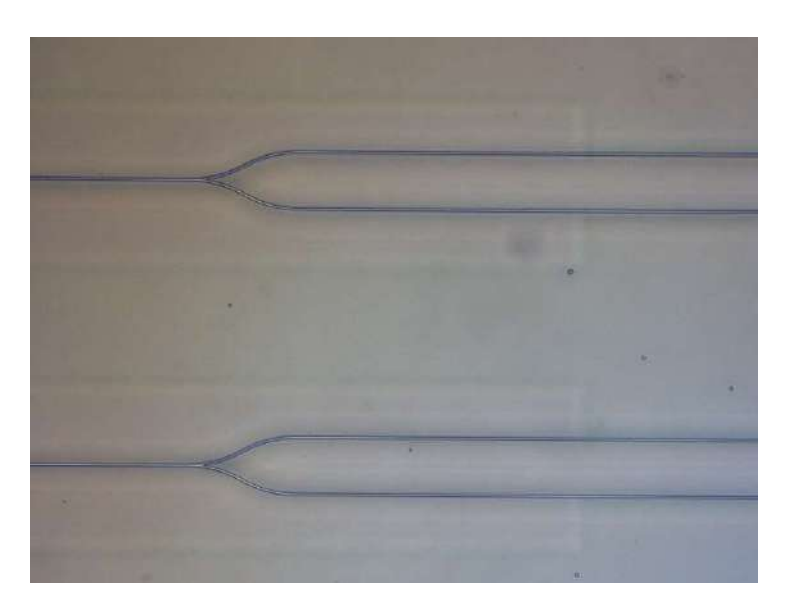
Highest value ever obtained on amorphous material

Advanced Photonics Research (2021) Advanced Optical Materials (2020)









Marc Dussauze, Thierry Cardinal

Numerous innovations in photonics have been realized on the basis of nonlinear optical properties, notably in information technologies. To take advantage of the nonlinear optical properties of glass, multidisciplinary research efforts were necessary, combining optics, glass chemistry, material science, as well as development of optical or electrical polarizations processes. This chapter addresses both fundamental aspects of nonlinear optical responses and also the exploitation of nonlinear optical phenomena in glassy material. It starts by a general introduction to nonlinear optical phenomena and concepts. Then, the specific cases of second and third optical responses in glasses are treated separately and described in detail as a function of the corresponding optical phenomena, the various glass families, and their applications.

Polarization at the Microscopic Scale	194
Polarization at the Macroscopic Scale	195
Nonlinear Optical Susceptibility	196
Third-Order Nonlinearity in Glass	197
Transparent Media (Out of Resonance)	197
Absorbing Medium (Resonance)	197
Kerr Effect in Glass	198
	201
Generation	204
Second-Order Optical Properties	
in Glasses	206
Second-Order Optical Response	
by Optical Poling	207
3-D Optical Poling by fs Laser Irradiation	207
Second-Order Optical Response	
in Glasses by Thermal Electrical Poling	209
Conclusion	219
ences	219
	Polarization at the Macroscopic Scale Nonlinear Optical Susceptibility

Part A | 6